Dipl.Ing. Martin Hajnsek

Sensor for Monitoring Glucose in Interstitial Fluid

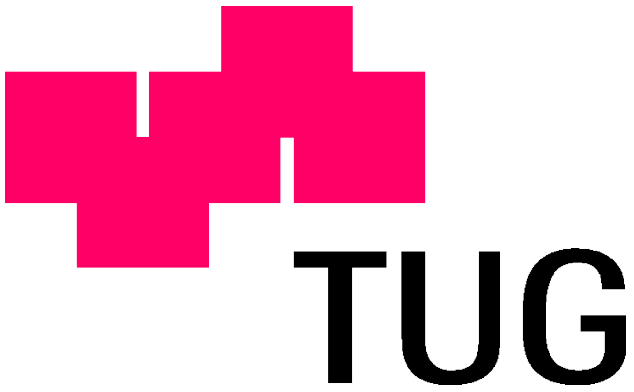

DISSERTATION

zur Erlangung des akademischen Grades
eines Doktors der technischen Wissenschaften

erreicht an der

Technischen Universität Graz

Institut für chemische Technologie von Materialien
Ao.Univ.-Prof. Dipl.-Chem. Dr.rer.nat. Jörg Albering

April 2010

This work was supported by

Roche Diagnostics Graz GmbH
Kratkystr.2
A-8020 Graz

and

Roche Diagnostics GmbH Mannheim
Sandhoferstr. 116
D-68305 Mannheim

STATUTORY DECLARATION

I declare that I have authored this thesis independently, that I have not used other than the declared sources / resources, and that I have explicitly marked all material which has been quoted either literally or by content from the used sources.

Graz, ...
date signature

TO MY DAUGHTER HELENA

Abstract

Diabetes is a worldwide disease which affects about 8% of the world´s population and estimates for the next decades predict that this number will further increase dramatically. Due to this huge number of people suffering from this disease, many companies are searching for new and better solutions for the diagnosis and therapy of diabetes. The development of systems for online glucose monitoring is a part of these efforts. The aim of monitoring systems is to provide actual blood sugar information to diabetes patients 24 hours a day, in contrast to the measurement with test strips, where diabetes patients must prick their fingers four times a day on an average, without receiving any information about the period between two individual measurements. Despite more than a decade of efforts to develop non-invasive blood glucose measurement techniques in the 1990´s, no adequate system could be launched successfully to the market. Instead, transcutaneously measuring systems were the first to enter the monitoring market with mobile and wearable systems. Two different basic techniques were established: the in vivo measurement with needle type sensors, and the ex vivo measurement where a sampling probe is implanted and the glucose sensor is placed outside the body. Both techniques measure glucose concentrations in the interstitial fluid which correlates sufficiently to blood glucose [51, 52]. This work deals with the development of a glucose sensor for an ex vivo online monitoring system using the microdialysis technique as sampling method.

Zusammenfassung

Diabetes ist eine weltweite Krankheit, die ca. 8% der Weltbevölkerung betrifft, wobei Schätzungen für die nächsten Jahrzehnte davon ausgehen, dass diese Zahl weiter dramatisch ansteigen wird. Auf Grund dieser hohen Zahl an betroffenen Menschen forschen viele Firmen an neuen und besseren Lösungen zur Diagnose und Therapie von Diabetes. Die Entwicklung von Systemen zum Online Glukose Monitoring sind ein Teil dieser Anstrengungen. Das Ziel dieser Monitoring Geräte ist, Diabetes Patienten 24 Stunden am Tag mit aktuellster Information über ihren Blutzuckerspiegel zu versorgen. Bei Messungen mit handelsüblichen Teststreifen, wobei Diabetes Patienten sich im Durchschnitt 4 Mal am Tag für die Blutzuckermessung in den Finger stechen, erhalten sie keine Information darüber, welchen Verlauf der Glukosespiegel im Blut zwischen zwei Messungen genommen hat. In den 1990-ern wurde intensiv nach nicht-invasiven Glukose Testmethoden geforscht, jedoch konnte bis heute kein System erfolgreich auf den Markt gebracht werden. Transkutane Messsysteme waren die ersten tragbaren Monitoring Geräte auf dem Markt. Dabei haben sich zwei Basistechnologien etabliert: Die in-vivo Messung mit Nadelsensoren, und die ex-vivo Messung, wobei nur die Probenahme implantiert wird und der Sensor außerhalb des Körpers getragen wird. Beide Techniken messen in interstitieller Flüssigkeit deren Glukose Konzentration ausreichend mit der von Blut korreliert [51, 52]. In dieser Arbeit wird die Entwicklung eines Glukose Sensors beschrieben, der in einem ex-vivo Messgerät mit Mikrodialyse-Katheter zum Einsatz kam.

Contents

1 Introduction

1.1 Diabetes

Diabetes is a disease which occurs as a result of problems with the production and supply of insulin in the body. Most of the food we eat is turned into glucose. We use glucose as a source of energy to provide power for our muscles and other tissues, and therefore, it is distributed throughout the body by the blood. A healthy person´s blood sugar is usually between 70 and 110 mg/dL or 3,9 and 6,1 mmol/L. To absorb glucose from the blood, muscles and other tissues need the hormone insulin. Without insulin, our bodies cannot obtain the necessary energy from our food. Insulin is produced in the beta cells of the pancreas. When a person has diabetes, either the pancreas produces less insulin than needed, or the body cannot use the produced insulin effectively. As a result, people with diabetes cannot use enough of the glucose in the food they eat, which leads to increasing glucose concentrations in the blood. They are called “high blood sugar” or hyperglycaemia. High levels of glucose in the blood can lead to medical complications which are explained in section 1.2 [33]. There are different types of Diabetes which differ in the cause and the severity of the disease.

1.1.1 Type 1 Diabetes

Type 1 diabetes is sometimes called insulin-dependent, immune-mediated or juvenile-onset diabetes. People with type 1 diabetes are usually unable to produce any insulin at all. The condition can affect people of any age, but usually occurs in children or young adults. The predominant cause of type 1 diabetes is the autoimmune destruction of the beta cells which leads to absolute dependence on insulin treatment. People with this disease need to have injections of insulin every day in order to control the levels of glucose in their blood. People with type 1 diabetes will die, if they do not have access to insulin.

1.1.2 Type 2 Diabetes

Type 2 diabetes is sometimes called non-insulin dependent diabetes or adult-onset diabetes. It is characterized by insulin resistance and relative insulin deficiency. The specific reasons for the development of these abnormalities are not known yet. People with type 2 diabetes usually do not require injections of insulin. They can control the blood glucose levels by watching their diet, taking regular exercise and in some cases by taking medications. Type 2 diabetes is most common in people older than 45 who are overweight. However, as a consequence of increased obesity among the young, it is becoming more common in children and young adults. Type 2 diabetes is the most common type of diabetes and accounts for 90 - 95% of all people with diabetes. If people with type 2 diabetes are not diagnosed and treated, they can develop serious complications which may even result in their death. Worldwide, many millions of people have type 2 diabetes without even knowing it or without access to adequate medical care.

1.1.3 Gestational Diabetes

Gestational diabetes is a temporary form of diabetes that sometimes occurs in pregnant women. It develops in 2-5% of all pregnancies, but usually disappears when the pregnancy is over. However, women who have had gestational diabetes or who have given birth to a large baby (4 kg or greater) are at a greater risk of developing Type 2 diabetes at a later stage in their lives.

Diabetes is a chronic, life-long condition that requires careful control. Without proper management it can lead to various complications such as cardiovascular disease, kidney failure, blindness and nerve damage.

1.2 Medical complications caused by Diabetes

1.2.1 Short-term complications

Low blood sugar (hypoglycaemia)

Persons who need to take insulin are going to face the problem of their blood sugar falling too low at some point (because they have overestimated the insulin they need, have exercised more than anticipated or have not eaten enough). Hypoglycaemia can be corrected rapidly by eating some sugar. If it is not corrected it can lead to unconsciousness and subsequently to death.

Ketoacidosis

When the body breaks down fats, acidic waste products called ketones are produced. The body cannot tolerate large amounts of ketones and will try to get rid of them through the excretion of urine. However, if the body cannot release all the ketones,

they will build up in the blood. Ketoacidosis, a severe condition caused by lack of insulin that mainly affects people with type 1 diabetes, can form.

Lactic acidosis

Lactic acidosis is the build up of lactic acid in the body. Cells produce lactic acid when they use glucose for energy. If too much lactic acid stays in the body, the balance tips and the person begins to feel ill. Lactic acidosis is rare but mainly affects people with type 2 diabetes.

Bacterial/fungal infections

People with diabetes are more prone to bacterial and fungal infections. Bacterial infections include sties and boils. Fungal infections include athlete's foot, ringworm and vaginal infections.

1.2.2 Long-term complications

Eye disease

Eye disease, or retinopathy, is the leading cause of blindness and visual impairment in adults in developed societies. About 2% of all people who have had diabetes for 15 years become blind, while about 10% develop a severe visual impairment.

Kidney disease

Diabetes is the leading cause of kidney disease (nephropathy). About one third of all people with diabetes develop kidney disease and approximately 20% of people with type 1 diabetes develop kidney failure.

Nerve disease

Diabetic nerve disease, or neuropathy, affects at least half of all people with diabetes. There are different types of nerve diseases which can result in a loss of sensation in the feet or in some cases the hands, pain in the feet and problems with the functioning of different parts of the body including the heart, the eyes, the stomach, the bladder and others. A lack of sensation in the feet can lead to people with diabetes injuring their feet without realising it. These injuries can lead to ulcers and possibly amputation.

Disease of the circulatory system

Disease of the circulatory system, or cardiovascular disease, accounts for 75% of all deaths among people with diabetes of European origin. In the USA, coronary heart disease is present between 8% and 20% of the people with diabetes over 45 years of age. Their risk of heart disease is 2-4 times higher than in those who do not have diabetes, and it is the main cause of disability and death of people with type 2 diabetes in industrialized countries.

Amputation

Diabetes is the most common cause non accident related amputations. People with diabetes are 15 to 40 times more likely to require lower-limb amputation compared to the general population.

1.3 Treatment of diabetes

Today, there is no cure for diabetes, but effective treatment exists. If you have access to the appropriate medication, quality of care and good medical advice, you should be able to lead an active and healthy life and reduce the risk of developing complications. Good diabetes control means keeping your blood sugar levels as close to normal as possible. This can be achieved by a combination of the following:

Controlled diet

Food raises blood sugar levels. People with diabetes have the same nutritional needs as anyone else, that is to say, a well-balanced diet.

Physical exercise

Exercise lowers blood sugar. Like insulin, it also supports the body to use its blood sugar efficiently. It may also help insulin work more effectively, and it will also help to lose weight.

Medication

Insulin lowers blood sugar levels. People with type 1 diabetes require multiple daily insulin injections for survival. People with type 2 diabetes may require oral hypoglycaemic drugs to lower their blood sugar and some may also need insulin injections.

It is important to achieve the right balance of the above elements. Too much or too little of either can impact upon how the patient feels. Achieving this balance is a lifelong commitment on the part of the person with diabetes. Studies undertaken in the United Kingdom by the Diabetes Control and Complications Trial Research Group (DCCT) [9] [10] and the UK Prospective Diabetes Study Group (UKPDS) [35] have

shown conclusively that effective control of blood glucose in an effort to keep blood sugar levels as close to normal as possible is beneficial in preventing and delaying the progression of the complications of diabetes. The results showed that appropriate control of blood sugar and blood pressure led to massive reductions in developing complications:

- Up to a 76% reduction in the risk of developing eye disease.
- Up to a 50% reduction in the risk of developing kidney disease.
- Up to a 60% reduction in the risk of developing nerve disease.
- More than a 33% reduction in strokes.
- Up to a 33% reduction in death from long-term complications.

1.4 Prevalence of diabetes

Estimates of the prevalence of diabetes are available for 212 countries and territories, which have been allocated into one of the seven regions by the International Diabetes Federation (IDF) [31]: Africa (AFR), Eastern Mediterranean and Middle East (EMME), Europe (EUR), North America (NA), South and Central America (SACA), South-East Asia (SEA) and Western Pacific (WP). Rates for each country have not been age-standardized, but are presented as the crude rates for the specific country and region according to the number of persons aged 20-79 years for that national or geographical entity. Furthermore, because the emphasis is on numbers of people with diabetes for each country, prevalence rates are markedly affected by the population age distribution so that those countries with older age distributions will inevitably have higher crude prevalences for the 20-79 year age group. The consequence of applying current age and gender specific prevalence rates to the projected prevalence

rates of the year 2025 is that only changes in the age and urban/rural distribution of the population will affect the estimates. Since it is likely that the age specific prevalence rates (the prevalence at any given age) will rise due to increasing obesity, the figures are probably underestimates.

	WP	SEA	EUR	AFR	EMME	NA	SACA
total population [in mio]	1900	1200	820	541	461	422	405
adult population [in mio]	1200	658	580	225	221	274	235
adults with diabetes [in mio]	46	49	32	2,5	14	21	11
estimated diabetes prevalence	3.8%	7.5%	5.5%	1.1%	6.4%	7.8%	4.8%
type 1 Diabetes [in 1000]	627	922	1600	108	490	1000	445
estimated type1 Diabetes	0.03%	0.08%	0.19%	0.02%	0.11%	0.25%	0.11%

Table 1.1: Diabetes prevalence in the world

1.5 Economic impact of diabetes

Diabetes is expected to cause 3.8 million deaths worldwide in 2007, accounting for about 6% of total global mortality, which is about the same as HIV/AIDS. Using World Health Organization (WHO) figures on years of life lost per diabetic case, it is observed that more than 25 million years of life are lost each year. Global health expenditures to treat and prevent diabetes and its complications totalled at least USD 232 billion in 2007. By 2025, this number will exceed USD 302 billion. Expressed in international dollars (ID), which correct for differences in purchasing power, at least ID 286 billion of goods and services was consumed by diabetes in 2007, and at least ID 381 billion will be in 2025 [32]. WHO estimates that mortality from diabetes, heart disease and stroke cost about 250 billion international dollars (ID) in China, ID 225 billion in the Russian Federation, and ID 210 billion in India in 2005. Much of

the heart disease and stroke in these estimates was linked to diabetes. Between 2005 and 2015 WHO estimates that diabetes, heart disease and stroke together will lead to losses in national income of:

- ID 555.7 billion in lost national income in China over the next 10 years
- ID 303.2 billion in the Russian Federation
- ID 333.6 billion in India
- ID 49.2 billion in Brazil
- ID 2.5 billion even in a developing country like Tanzania

These estimates are based on lost productivity resulting primarily from premature death. Accounting for disability might double or triple these figures. Diabetes is costly even before it is diagnosed. This is true both in industrialized and developing countries. In 2007, the world is estimated to spend at least US$ 232 billion to treat and prevent diabetes and its complications. By 2025, this lower-bound estimate will exceed US$ 302.5 billion.

In industrialised countries, about 25% of medical expenditures for diabetes go to treating elevated blood sugar; 25% are spent to treat long-term complications, largely cardiovascular disease, and 50% is consumed by the additional general medical care that is associated with diabetes. The cost, for example, of a person with diabetes who has end-stage kidney disease is 3 to 4 times higher than the cost of a person with diabetes and no complications. In the USA, acute hospitalization consumes 44% of diabetes-attributable costs; followed by:

- 22% for outpatient care
- 19% for drugs and supplies

- 15% for nursing care

Similar proportions are reported for other high-income countries such as Finland. In middle-income countries, half of diabetes medical expenditures are used for blood sugar control which is essential for the prevention of acute life-threatening hyperglycaemia. The remainder is split between general medical care and chronic complications. In Latin America and the Caribbean, for example, drugs to reduce blood sugar levels are believed to account for about 50% of all spending. It is believed that in low-income countries almost all expenditure for diabetes is directed towards drugs to prevent death from high blood sugar. The following table shows data on the healthcare-costs caused by diabetes in Western Europe.

Country	**General healthcare costs per patient (US$)**	**Additional costs due to diabetes (US$)**	**Annual cost per patient with type 2 diabetes (US$)**
Belgium	1495	1647	3142
France	1979	1009	2988
Germany	2146	1330	3476
Italy	1259	1611	2870
Netherlands	1634	180	1814
Spain	1046	241	1287
Sweden	1710	855	2565
UK	1144	881	2025

Table 1.2: Healthcare costs due to Diabetes in selected European countries

2 Biosensors

A biosensor can be defined as a self-contained integrated device which is capable of providing specific quantitative or semi-quantitative analytical information using a biological recognition element, which is in direct spatial contact with a transducer element. The biochemical receptor may be an enzyme, antibodies, nucleic acids, cell receptors, organelles, microorganisms and even tissues, but also biologically derived material or biomimics. A biosensor should be clearly distinguished from a bioanalytical system, which requires additional processing steps, such as reagent addition. Furthermore, a biosensor should be distinguished from a bioprobe which is either disposable after one measurement, e.g. single use test strips, or unable to continuously monitor the analyte concentration [28]. The general scheme of a biosensor configuration is shown in Figure 2.1.

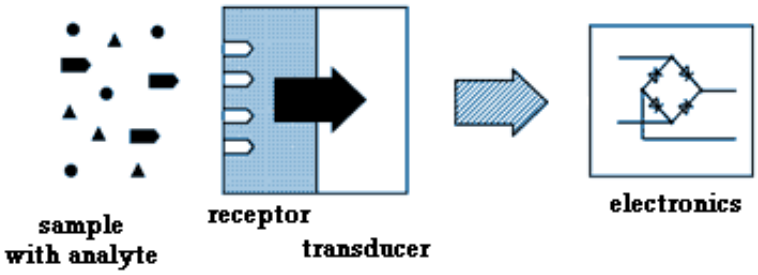

Figure 2.1: Scheme of a biosensor

Biosensors incorporate a recognition element of biological nature, or a biological

derived material (biomimic) that allows the selective recognition of an analyte in the course of a biochemical reaction and also an energy transducer that transforms the chemical information about the analyte into an electrical signal for data acquisition and interpretation. In general, biosensors are classified either by their biological recognition element or the transducer used:

Sensor classification by recognition element

- **Biocatalytic** sensors, also known as metabolism sensors, rely on enzymatically catalyzed reactions. The recognition element can be of biological nature, such as an isolated enzyme, a living cell or a tissue slice, or of synthetic origin such as molecularly imprinted polymers (MIPs).
- **Bioaffinity** sensors, based on ligand-binding interactions between a target molecule and the receptor, for instance ion sensitive sensors, antigen-antibody assays or DNA sensors.

Sensor classification by transducer

- **electrochemical** transducers are often used in amperometrical enzyme sensors, potentiometrical affinity sensors or as ion sensinsitve electrodes.
- **optical** transducers are used for fluorescence measurements, surface plasmon resonance sensors (SPR) or electrochemiluminescence.
- **thermometrical** transducers are suitable for biocatalytic sensors but are not as often used as electrochemical transducers.
- **piezoelectric** transducers demonstrate their strengh in detecting analytes by affinity reactions of antigen and antibody or DNA without label where tiny masses as small as single molecule detection is possible.

Biosensors usually yield an electronic signal which is proportional to the concentration of a specific analyte or group of analytes. Biosensors have been applied to a wide variety of analytical devices in medicine, drug discovery, food and process industries, environment, security and defence.

The first biosensor was built by Cark and Lyons in 1962 [7]. They combined an oxygen electrode with the enzyme glucose oxidase in order to measure glucose concentrations. The decay of oxygen caused by the enzyme reaction, which consumes oxygen to oxidate glucose, was detected by the oxygen electrode and allowed to calculate the glucose levels.

The combination of highly specific biological reactions with an appropriate transducer gives biosensors a number of advantages such as high sensitivity and specivity. The recognition of analytes by biological receptors is far superior to most chemical recognition systems. Some enzymes even distinguish between the stereoisomers of the same analyte. Biosensors also provide short response times which allow for real-time measurements. The nature of biosensors also allows miniaturisation which is a prerequisite for the integration into portable instruments. In many cases, they are made using mass production techniques such as screen printing, thin film technique, dye coating, microstructuring processes, etc. [48] and can therefore be produced very cheaply.

The application of biosensors in the medical market has been highly successful and biosensors are of growing importance in the environmental and foodstuff analysis. Stricter legislation in the United States and European Union requires improved and fast analysis of a growing number of analytes, especially in the environmental sector. Due to the high specivity, biosensors can operate in complex matrix samples and directly monitor toxic analytes.

The clinical market for biosensors is dominated by the glucose sensor. The reason

for the outstanding success of this single biosensor is not that it is so much better than other sensors, but simply the huge demand due to diabetic patients needing to check their glucose levels several times per day.

2.1 Amperometric biosensors

Amperometric biosensors are based on the measurement of a steady state current produced when a constant potential is applied. This current can be related to an electrochemical active species that is consumed or produced by the recognition element. Amperometric sensors can be realised with relatively simple instrumentation. The electrochemical setup frequently consists of three electrodes: a working electrode made of gold, platinum, graphite or carbon paste, a reference electrode such as Ag/AgCl, and an auxiliary– or counter electrode, often made from platinum or carbon [6]. The constant potential is applied to the working electrode by a potentiostat. The best-known example for an enzyme based biosensor is the detection of glucose with glucose oxidase (GOx). More recent biosensors use mediators for the electron transfer or enzymes with a direct electron transfer from the active center to the electrode. In case of affinity biosensors such as immunosensors or DNA based sensors, the biological element is frequently labelled with an enzyme that produces or consumes an electroactive species. Again glucose oxidase or horseradish peroxidase can be used. The label can also consist of redox-active substances like ferrocene, but unlike the enzyme label, no signal amplification occurs.

2.1.1 Diffusion

The rate of an electrode reaction is mainly determined by two factors, namely electrode kinetics and mass transport. Electrode kinetics can be described with a rate

constant for the oxidation at the electrode and a rate constant for the reduction at the electrode. The conditions during amperometry can be chosen so that the electrode kinetics are sufficiently fast and the control of the electrode process is determined by mass transport. This can be achieved by applying a suitable potential. In this work, a potential of +350 mV (vs. Ag/AgCl) guarantees sufficiently fast oxidation of hydrogen peroxide at the electrode surface (see section 4.4 Voltammetry). Mass transport occurs by migration, convection and diffusion. Migration can be neglected when a sufficiently high concentration of inert electrolyte is used. This leaves diffusion, which is the movement of species due to concentration gradients, convection, which is movement due to thermal gradients, and forced convection such as stirring or pumping, as causes for mass transport.

Diffusion of the analyte to the electrode surface is described in Fick´s first law:

$$J = -D\frac{\delta c}{\delta x} \tag{2.1}$$

J is the flux of species, D is the diffusion coefficient of the analyte in the medium and $\frac{\delta c}{\delta x}$ is the concentration gradient in direction x. Because the electrode consumes the analyte, the substrate concentration in the bulk solution will decrease over time. In that case Fick´s second law is applicable, which describes the variation of concentration in time due to diffusion:

$$\frac{\delta c}{\delta t} = D\frac{\delta^2 c}{\delta x^2} \tag{2.2}$$

$\frac{\delta c}{\delta t}$ is the time dependence of the concentration, D is again the diffusion coefficient and $\frac{\delta^2 c}{\delta x^2}$ is the second derivative of the concentration c with respect to the distance x.

In the system described in this work, forced convection occurs as the pump continuously delivers fresh dialysate from the microdialysis catheter to the sensor, so there is no depletion of the analyte. Therefore the substrate concentration in the bulk solution c_∞ can be assumed constant. In that case the electrode process is controlled by diffusion and the sensor signal is proportional to the analyte concentration.

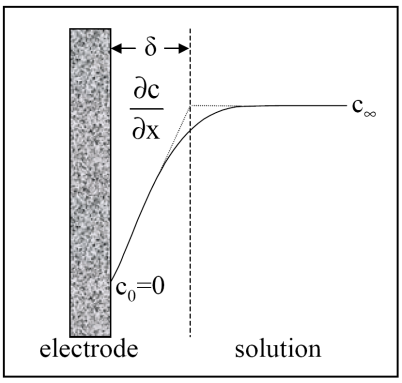

Figure 2.2: general scheme of the diffusion layer on the surface of the electrode

2.1.2 Enzyme kinetics

Enzymes play an important role in the measurement of organic and especially biologic analytes. Enzymes rise the reaction-rates to factors of 10^6 to 10^{12} compared to uncatalysed reactions and therefore they are more effective by orders of magnitude than chemical catalytic converters. Reactions catalysed by enzymes take place at mild conditions and are highly specific. To a great extent an enzymatic reaction gives defined products and not mixtures of different products.

$$\text{Substrate} \xrightarrow{\text{Enzyme}} \text{Product} \tag{2.3}$$

For the use of enzymes in technical applications it is important to know the kinetics of the used enzyme. The Michaelis-Menten equation is the basic theory to the kinectics of enzymatic reactions. [11]

Leonor Michaelis and Maude Menten realised that the reaction rate of an enzymatic reaction depends on the concentration of the substrate. At this point they postulated that the reaction is split in two parts. In the first step the substrate S and the enzyme E form a complex ES which will decompose in the second step by regenerating the enzyme and releasing the product P.

$$\mathrm{E} + \mathrm{S} \underset{\mathrm{k}-1}{\overset{\mathrm{k}_1}{\rightleftharpoons}} \mathrm{ES} \xrightarrow{\mathrm{k}_2} \mathrm{E} + \mathrm{P} \tag{2.4}$$

The final Michaelis Menten equation can be specified by two presumptions:

1. A preexisting equilibrium of enzyme and substrate is presumed: The constant of the decay of the complex [ES] k_{-1} is supposed to be much higher than the constant of the second reaction, which forms the product. This results in a equilibrium state of enzyme, substrate and complex. The constant of the dissociation of the complex is therefore given as K_s.

$$K_s = \frac{k_1}{k_{-1}} = \frac{[E][S]}{[ES]} \tag{2.5}$$

2. Presumption of a steady state: The enzyme will be transformed to the enzyme-substrate complex when the concentration of the substrate is much higher then the concentration of the enzyme, because each free enzyme molecule will immediately be occupied by the next substrate molecule. The rate of the emerging of the ES-complex is quite the same as the rate of the decomposition of the complex and therefore the amount of ES-complex stays constant.

$$\frac{d[ES]}{dt} = 0 \tag{2.6}$$

Both presumptions lead to the final Michaelis-Menten equation (equation 2.7), which describes the speed of reaction only depending on the substrate concentration.

$$v_0 = \frac{v_{max}[S]}{K_M + [S]} \tag{2.7}$$

$$K_M = \frac{k_{-1} + k_2}{k_1} \tag{2.8}$$

$$v_{max} = k_2[E]_t \tag{2.9}$$

The Michaelis constant K_M is given by the sum of the reaction-rates of the ES complex decay divided by the reaction-rate of the forming of the complex (equation 2.8). The maximum speed of the whole enzyme reaction is proportional to the total enzyme concentration $[E]_t$ (equation 2.9).

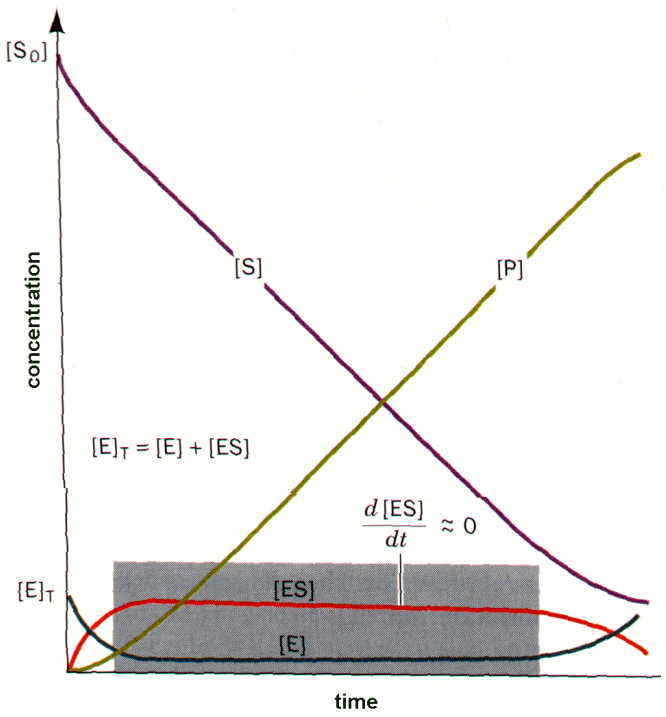

Figure 2.3: changes in concentrations during an enzyme-catalysed reaction

2.1.3 Glucose Oxidase

The enzyme used in this work is glucose oxidase (EC 1.1.3.4) from aspergillus niger expressed in recombinant microorgansims and was obtained from Roche. The holoenzyme is a dimer and is made up of two identical subunits of 79 kDa each. The protein has a high activity of more than 250 U/mg lyophilizate and is acidic, having an isoelectric point (pI) of 4.3 [54]. The Michaelis Constant K_M in 200 mM potassium phosphate buffer at a pH of 7.5 and a temperature of 25 °C is 48 mM, the molecular activity (turnover number) = $2.28 \cdot 10^4$.

2.2 The glucose sensor

The electrochemical glucose sensor developed in this work uses the enzyme Glucose-Oxidase (GOx) as the receptor of the sensing electrode.

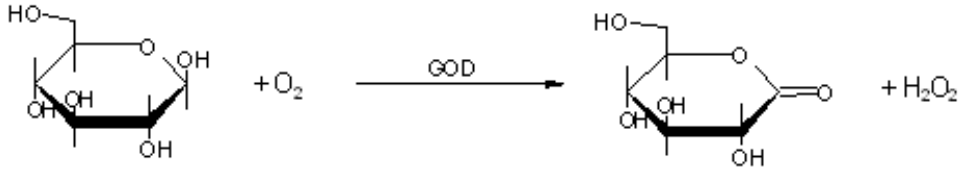

(2.10)

The oxidation of glucose to gluconolactone is a wide-spread reaction which allows 4 different ways to detect glucose concentrations:

1. The oxidation of glucose is accompanied by an oxygen consumption which can be detected by an oxygen sensor. The disadvantage of this method is that the variation of the oxygen levels in biological samples makes a second electrode necessary in order to get the initial oxygen concentration of the sample. The determination of the glucsoe levels is achieved by substracting the oxygen level of the glucose electrode from the oxygen level of the reference electrode.

2. The second method is to detect the decrease of pH due to the hydrolysation of the gluconolactone. This is even more difficult because the changes in pH depend on the puffer capacity of the sample. Additionally, the initial pH-value has to be detected analogously to the oxygen consumption method.

3. Due to the exothermic reaction of glucose and oxygen, the glucose concentration can also be estimated by the amount of heat generated by the reaction. This is a demanding task due to the tiny changes in temperature and the massive effort for thermal isolation of the measuring system.

4. The last method is to detect the hydrogen-peroxide. It is the product of the enzyme reaction and can be detected easily by oxidation on suitable transducers like Pt-electrodes. Hydrogen peroxide does not occur in human body fluids and is therefore the best choice for a glucose sensor for diagnostic use.

The sensor is built up as a 3-electrode system with a working electrode for analyte detection, a counter electrode to allow a current flow between working- and counter elctrode, and a reference electrode to keep the polarisation voltage of the working electrode constant.

2.2.1 The electrodes

Reference electrode

Electrodes are electrochemical half-cells, which consist of a liquid phase (the electrolyte) and a solid phase (the metal), which are essential for building up a potential. Electrodes with a solid phase made of a metal salt of low solubility are called electrodes of the 2. kind. The potential of such a half-cell is primarily determined by the concentration of metal ions. The metal ion concentration is strictly connected to the concentration of the corresponding anion by the solubility product of the salt. The potential of an electrode of the 2. kind is consequently determined by the concentration of the anion, which is variable within a certain range, and can be described with the Nernst Equation and the solubility product.

$$E = E^0 + \frac{RT}{zF} \cdot ln[M^+] \tag{2.11}$$

E	electrode potential [V]
E^0	standard electrode potential [V]
R	universal gas constant = 8.3145 [J·K^{-1}·mol^{-1}]
T	absolute temperature [K]
F	Faraday constant = 96485.34 [C·mol^{-1}]
z	number of electrons transferred in the half-cell reaction

The reference electrode used in the glucose sensor is made of silver and silver-chloride flakes which are bound to the sensor by the screen-printing ink. When this electrode is in contact with a fluid of constant concentration of chloride ions, the potential of this half-cell at a temperature of 25°C is given by the following Nernst-equation:

$$E(AgCl) = E^0(Ag/Ag^+) + \frac{RT}{F} \cdot ln[Ag^+] \tag{2.12}$$

Due to the low solubility of AgCl, the concentration of silver ions is determined by the concentration of chloride ions following the solubility product of AgCl.

$$K_L = [Ag^+] \cdot [Cl^-] \tag{2.13}$$

The combination of the Nernst equation and the solubility product gives the following description of the electrode potential:

$$E(AgCl) = E^0(Ag/Ag^+) + \frac{RT}{F} \cdot ln\frac{K_L}{[Cl^-]} \tag{2.14}$$

$$E(AgCl) = E^0(Ag/Ag^+) + \frac{RT}{F} \cdot ln(K_L) - \frac{RT}{F} \cdot ln[Cl^-] \tag{2.15}$$

The first two members of the equation are constant at a certain temperature, therefore they can be combined to the standard-potential of the AgCl electrode:

$$E^0(AgCl) = E^0(Ag/Ag^+) + \frac{RT}{F} \cdot ln(K_L) = +0.222V \tag{2.16}$$

Which gives the final equation for the AgCl-elektrode:

$$E(AgCl) = E^0(AgCl) - \frac{RT}{F} \cdot ln[Cl^-] \tag{2.17}$$

In humans, the concentration of chloride can be assumed constant within the physiological range at room tmperature (25°C) and is about 117 mM in interstitial fluid [55]. In that case, the potential of the reference electrode will be 277 mV against the standard hydrogen electrode, as calculated in the following equation.

$$E(AgCl) = 0.222V - \frac{8.31447Jmol^{-1}K^{-1} \cdot 298K}{96485C \cdot mol^{-1}} \cdot ln(0.117) = 277mV \tag{2.18}$$

Working electrode

The working electrode is polarised with 350mV against the Ag/AgCl reference electrode, which is sufficient to oxidise hydrogen peroxide on the surface of the manganese dioxide particles of the transducer (see results of cyclic voltammetry in section 4.4).

The detection of the analyte results from two different reaction steps on the working electrode. In the first step, the enzyme reaction, glucose is oxidised to gluconolactone by the enzyme glucose oxidase which generates equimolar amounts of hydrogen peroxide. In the second step, the electrode reaction, the hydrogen peroxide is oxidised to oxygen by the transducer which delivers two electrones to the working electrode. Assuming 100% conversion in both reaction steps, 2 electrones per glucose molecule were received by the electrode as the sensor signal. The current is proportional to the amount of glucose present.

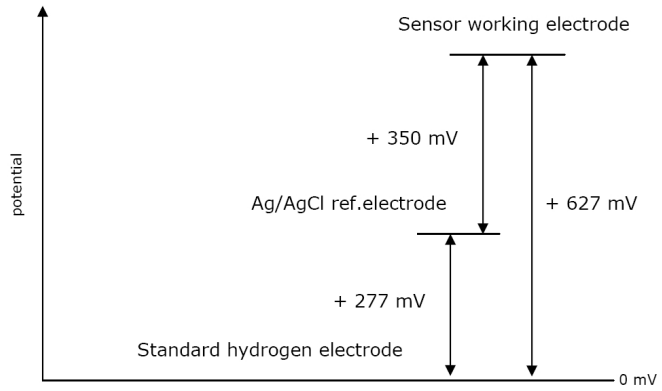

Figure 2.4: working potential of the sensing electrode

Enzyme reaction:

$$\text{Glucose} + O_2 \xrightarrow{\text{GOx}} \text{Gluconolactone} + H_2O_2 \tag{2.19}$$

Electrode reaction:

$$H_2O_2 \xrightarrow{350\,\text{mV}} 2\,H^+ + O_2 + 2\,e^- \tag{2.20}$$

As depicted in figure 2.5, the working electrode comprises a carbon track as conducting layer onto which the transducer consisiting of manganese dioxide powder mixed into the cabon screen printing ink is applied, thus forming a porous structure [47]. The enzyme solution is dispensed onto the transducer, filling the porous structure and leaving the enzyme in close vicinty to the transducer which strenghtens the effect of oxygen recycling in the electrode. The top layer is a dispensed aliphatic polyurethane polymer, which prevents protein adhesion due to its biocompatible properties. The loss of enzyme by washing off the electrode is prevented by enzyme inclusion.

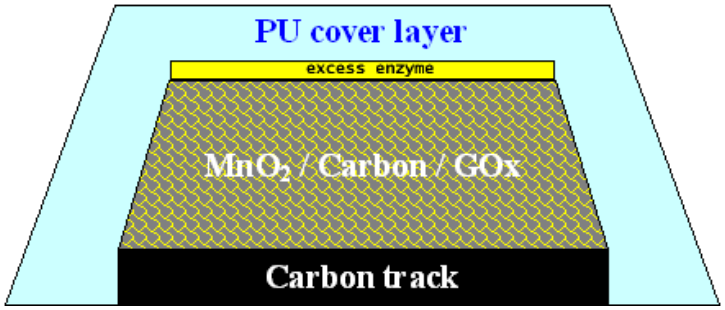

Figure 2.5: schematic illustration of the different layers of the working electrode

Oxygen recycling

The use of manganese dioxide as transducer of the glucose sensor bears three advantages compared to state-of-the-art platinum electrodes.

1. Manganese dioxide is able to promote the oxidation of hydrogen peroxide at lower potentials than platinum electrodes. A potential of 350 mV against Ag/AgCl is sufficient for a manganese dioxide electrode. Platinum electrodes have to be polarised with at least 600 mV to ensure hydrogen peroxide oxidation. The lower polarisation potential also decreases the effect of electrochemical interfering substances, thus leading to more accurate measurements in biological matrices.

2. Printed in the mixture with carbon ink, the manganese dioxide particles form a porous electrode with a large active surface area. The enzyme can deeply penetrate the electrode and cover the surface of the pores all over the electrode volume. The intimate contact of enzyme and transducer leads to a high hydrogen peroxide efficiency due to the short diffusion paths within the electrode.

3. Furthermore, the oxidation of hydrogen peroxide occurs within the electrode nearest to the site of oxidation of glucose by the enzyme. So the oxygen consumed by the enzyme reaction can be recycled by the electrode reaction, the

oxidation of the hydrogen peroxide, which produces oxygen for the oxidation of the next glucose molecule.

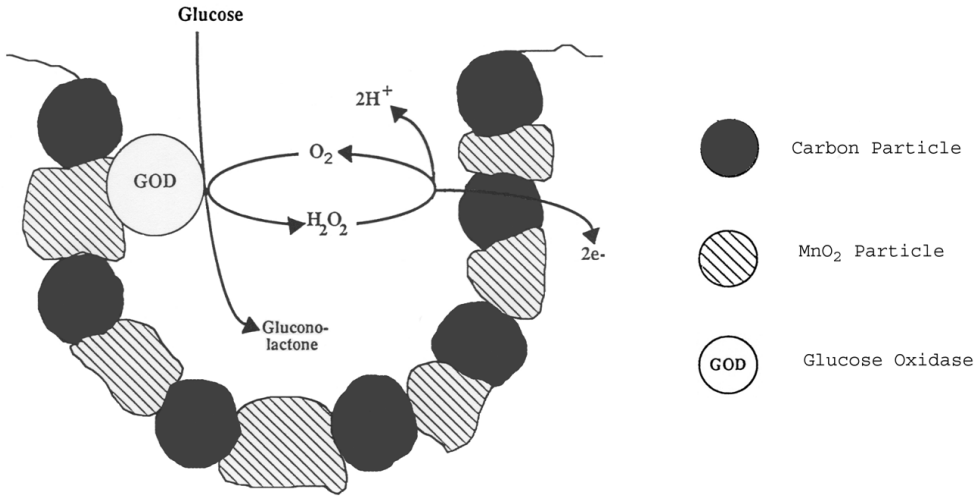

Figure 2.6: schematic illustration of the oxygen recycling process within the porous working electrode

Counter electrode

The counter electrode is used to allow sensor current flow between working and counter electrode, thus leaving the reference electrode virtually without any current flow. This is necessary, because a current flow over the reference electrode would alter the reference potential of the Ag/AgCl electrode.

Measuring cell

The measuring chamber is formed by combining the screen-printed sensor substrate with the top cover, which includes the measuring channel. Its length is 8 mm, the width is 0.9 mm and the depth is 0.3 mm respectively which results in a measuring channel volume of 2.16 μL. A sealing gasket is used to guarantee a water-tight connection of both parts.

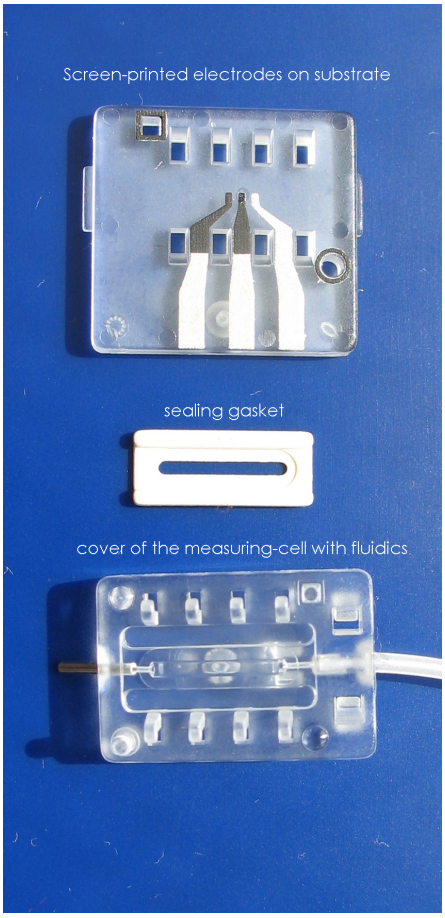

Figure 2.7: glucose sensor: substrate, gasket, measuring chamber

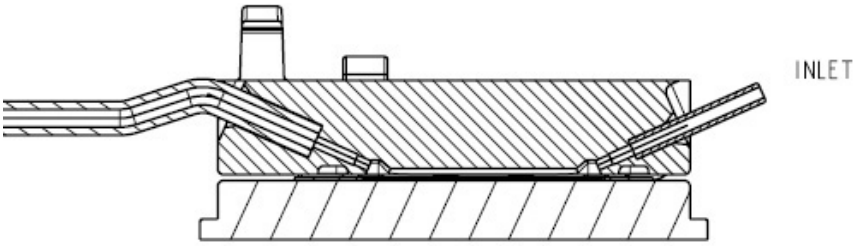

Figure 2.8: section through the measuring channel of the sensor

3 Methods

3.1 Thick film technology

Screen printing is a technique first used by the Chinese almost 2000 years ago. They used human hair stretched across a wooden frame to form the screen. In 1907, it was Samuel Simon near Manchester who patented the first ever industrial screen printing process. The substrates or surfaces on which screen printing can be carried out are manifold. Any surface the ink adheres to is a surface for screen printing. E.g. CD covers, t-shirts, signs, watch dials and even electronics can be screen printed. The screen is a finely woven fabric called mesh that is stretched over a frame, to which a stencil has been applied. It is placed atop a substrate, then ink is placed on top of the screen, and a floodbar is used to fill the mesh openings with ink. Then a squeegee (a rubber blade) is moved down the screen and it pushes the ink, located in the mesh openings, to the substrate. This happens in a controlled and prescribed way, so that the wet ink deposit is proportional to the thickness of the mesh and/or the stencil. As the squeegee moves toward the rear of the screen, the tension of the mesh pulls the mesh up away from the substrate (called snap-off) leaving the ink upon the substrate surface which is illustrated in figure 3.1. The stencil openings determine the image that will thus be imprinted.

Screen printing is widely used in the field of sensor production because it is a cost-effective technology which allows for high volume production. A big advantage of

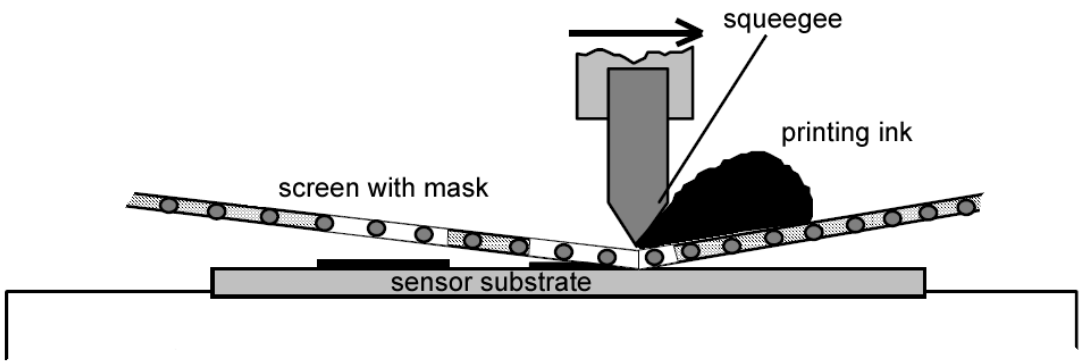

Figure 3.1: principle of screen-printing technique

the thick film technology is (as the name promises) that the applied layers of active substances are relatively thick (in the range of about 10 μm), and therefore reasonable lifetimes of the produced sensors can be achieved [25].

The substrate, used as support for the electrode system, is an injection molded polycarbonate tile, equipped with two ”noses” to fix the substrate in a magazine. The magazines hold 14 sensor substrates which allow the simultaneous processing of 28 sensors in one screen printing step when two magazines are used. The tiles also have 8 holes where the hooks of the cover are snapped in to combine the sensor substrate and the sensor cover, which forms the measuring channnel. A square in the left top corner and a circle in the right bottom are used for proper alignment of stencil and substrate during the screen printing process (see figure 3.2).

The whole electrode system is produced in 3 screen printing steps:

1. Ag/AgCl ink is printed to form the reference– and counter electrode, and the conductive tracks for the electrical connection of the electrodes to the potentiostate.

2. Carbon ink is used to cover the Ag/AgCl track of the counter electrode and as the conductive base of the working electrode.

3. the transducer is applied from a mixture of carbon ink and manganese dioxide to form a small rectangle of 300 μm length and 400 μm width (see figure 3.2).

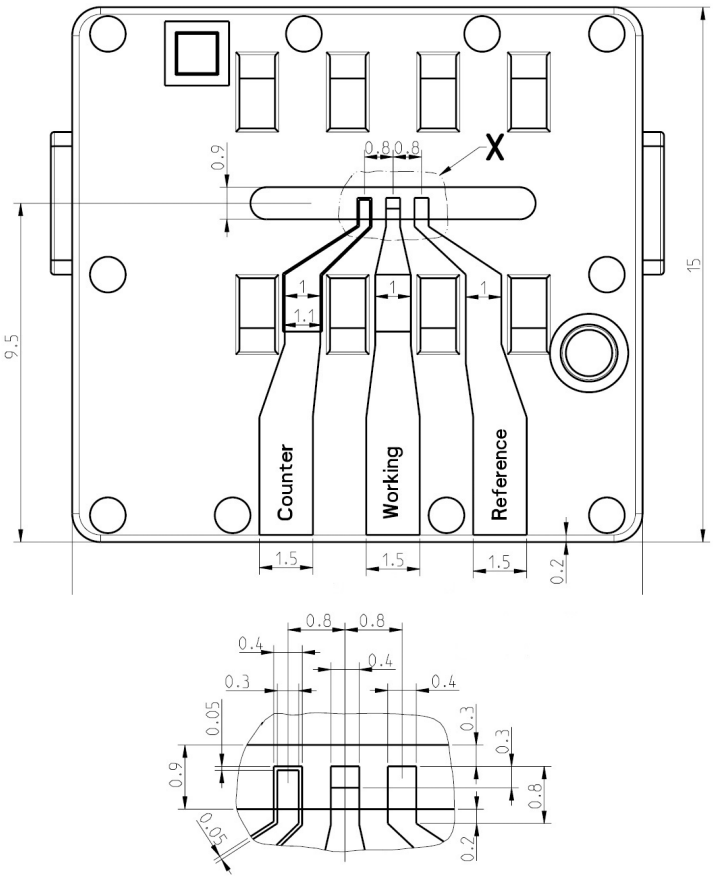

Figure 3.2: substrate and electrodes of the glucose sensor

3.2 Dispensing

Dispensing is a technique that allows for the application of single droplets of dissolved reagents onto a substrate. It is widely used in immuno-assays where labels and reagents are spotted into microtiter plates and measured by automated plate readers. Dispensing, as used for sensor production, is a bit different, because tiny volumes of about 16 nl have to be applicated onto the small active surface of the working electrode (which has a size of 300 x 400 μm). This requires a very precise positioning of the dispensing nozzle to the working electrode area.

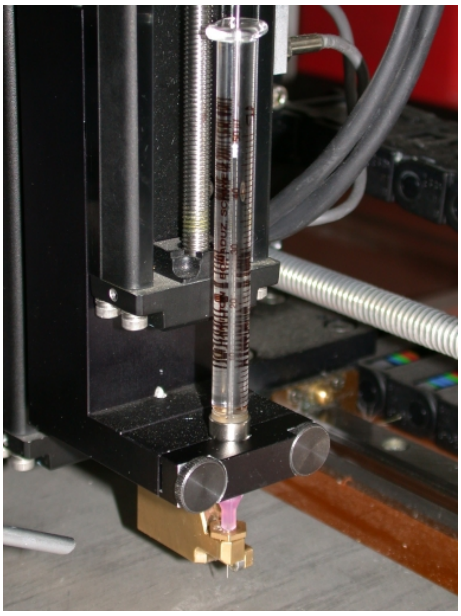

Figure 3.3: automated dispensing machine with installed Hamilton syringe

An in-house built automated dispensing machine was used to apply the enzyme solution onto the screen printed working electrode. It comprised a rigid baseplate where 2 spindles are mounted at right angles for movement in x- and y-directions, two brackets to clamp a Hamilton syringe and the piston of the syringe, and a screw with a drilled hole which exactly fits the dispensing needle for fixation. 4 stepper motors are used for the positioning the dispensing needle to the electrode. 2 motors

are used for movement in x- and y-directions, 1 is used to lift the syringe during movement and one to move the piston of the syringe, thus controlling the volume of liquid dispensed.

3.3 Microdialysis

Clinical microdialysis has been shown to be a safe, reproducible and relatively inexpensive technique for studying tissue biochemistry and drug distribution in humans. Today microdialysis is becoming an established clinical technology that can be applied to most organs in appropriate clinical situations. Microdialysis data is mostly derived from 4 different fields: intensive care research, clinical pharmacology and drug development, dermatology, and metabolic and endocrinological research. The technique involves the implantation of a small probe into a specific region of a tissue or fluid-filled space. Semipermeable membrane materials used in probe construction range from low– to high molecular weight cutoff. During microdialysis, a physiologically compatible perfusion fluid (perfusate) is delivered through the probe at a low and constant flow rate (typically ranging between 0.1 and 5.0$\mu L/$min). Exchange of solutes occurs in both directions across the semipermeable membrane of the probe (see figure 3.4) depending on the orientation of the solute concentration gradients [20].

Microdialysis models examine the relationship between the concentration of analyte measured in the dialysate sample collected at the probe outlet C_{out} and that of the external medium surrounding the probe $C_{E,\infty}$ where the infinity symbol denotes that the external concentration is far enough from the probe to be unperturbed by the dialysis process [59]. On occasion, analyte is added to the perfusion buffer, in which case, the concentration at the probe inlet is referred to as C_{in}. There are two parameters that describe the probe performance: The proportion of a substance removed

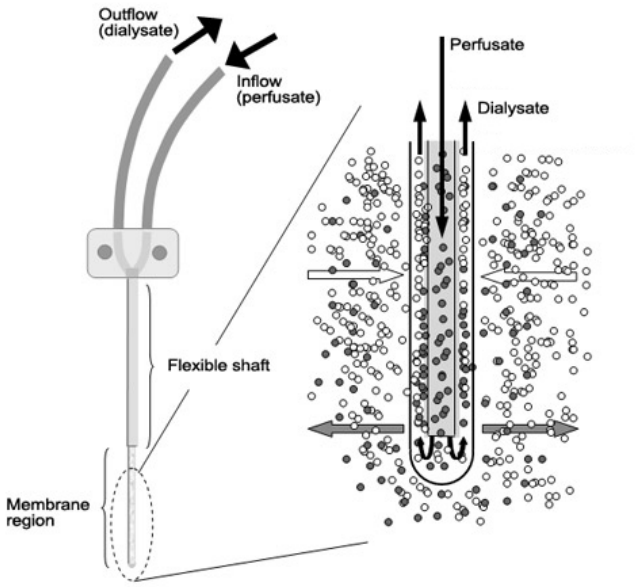

Figure 3.4: scheme of a microdialysis probe

from the tissue by the microdialysis probe is expressed as the extraction fraction E (see equation 3.1).

$$E = \frac{C_{in} - C_{out}}{C_{in} - C_{E,\infty}} \tag{3.1}$$

The second parameter is the relative recovery R (see equation 3.2) which describes the ratio of the analyte concentration in the dialysate to the analyte concentration outside the catheter and is expressed in percent.

$$R = \frac{C_{out}}{C_{E,\infty}} \cdot 100 \tag{3.2}$$

Many experimental conditions affect the relative recovery, including flow rate (perfusion), temperature, probe membrane composition, surface area and other factors that influence molecular diffusion characteristics [17]. In general, the higher the perfusion flow rate, the lower the relative recovery. Higher temperatures and larger probe membrane areas usually result in increased recoveries [16].

Probe implantation trauma

Insertion of microdialysis probes has been shown to cause tissue trauma, which could influence the results of microdialysis experiments [30]. To allow "tissue equilibration" (to provide time for the initial trauma to subside), probe perfusion for about one hour has shown to be sufficient before starting probe calibration, although longer recovery times (12-24 hours) may be required [19]. This is based on the finding that several markers of tissue trauma (eg thromboxane B2, adenosine triphosphate, adenosine, K^+, glucose, lactate, lactate/pyruvate ratio) are elevated after probe insertion and reach baseline or become undetectable within this time range. Furthermore, changes in local skin circulation after insertion of microdialysis probes have been investigated with laser Doppler perfusion imaging and were found to return to baseline within 60 minutes. Histological studies have shown that the implantation of small-diameter dialysis tubing does not induce foreign-body reactions if implantation times are kept below 24 hours. Also, bleeding at the site of insertion is usually not a problem [41].

3.4 E-beam sterilisation

For a terminally sterilised medical device to be labelled sterile, the theoretical probability of there being a viable microorganism present on the device shall be equal or less than 10^{-6} (EN 556 Sterilisation of medical devices) [58]. The principal technologies used for sterilising medical devices are ethylene oxide (52%), gamma radiation (39%), electron beam (7%) and steam (2%).

Heat sterilisation is commonly carried out in the well-proven autoclave. It is a simple to use method with short processing times. The drawback of this method is that it is not suitable for temperature sensitive molecules like enzymes and proteins, and process temperatures also exceed the glass transition temperature of most plastics,

and it is also difficult to carry out on a large scale [27].

Ethylene oxide sterilisation is cost-effective, provides high levels of sterilty assurance and does not damage most materials. But the total processing times typically range from two to five days as the sterilisation is a batch process and needs a degassing step which is required in order to remove residuals of the sterilising agent from the product after sterilisation.

Gamma radiation is cost-effective, especially for large volumes, provides high levels of sterilty assurance and is also nondamaging to most materials. It is a continuous process with fast processing times. The disadvantages of the method include damage to certain plastic materials and also the inability to penetrate dense materials which leaves shadowed areas unsterilised [1].

Electron beam sterilisation (e-beam sterilisation) is a commercially successful technology for sterilising a variety of disposable medical devices with a wide range of densities. The e-beam inactivates microorganisms by causing either microbial death as a direct effect of the destruction of a vital molecule or by an indirect chemical reaction. This is the same mechanism as in gamma irradiation and the dose required is the same. For many materials, e-beam processing results in less material degradation than with gamma irradiation. The extremely rapid treatment times of electron beam sterilisation greatly reduce effects on materials. This is especially noticeable with products made of non-wovens and polypropylenes. High energy electrons offer good depth penetration for the sterilization of medical devices in their final shipping boxes.

The disposables of the Clinical Research Tool, used to perform the glucose monitoring experiments in a clinical trial, had to be sterilised prior to the use with diabetic patients. The disposables, including the glucose sensor, were sterilised using e-beam radiation with an energy of 4.5 MeV. The applied dose of radiation was 25 kGy.

3.5 In vitro characterisation

3.5.1 Test rig

The development and the in-vitro characterisation of the glucose sensor was performed on a custom built test rig. It used HEPES buffered saline solutions with 7 different concentration levels of glucose. The different solutions were selected by an adapted Roche OMNI "Turn-and-Dock" system which filled the actual glucose solution into a barrel. From this barrel, up to 9 sensors could be supplied by a pump (from Watson Marlow) which allowed low flowrates of 300 nl/min. The sensors were controlled by a custom built 10-channel potentiostat which allowed the aquisition of data from 9 sensors simultaneously and, additionally, it logged the data from a PT100 temperature probe.

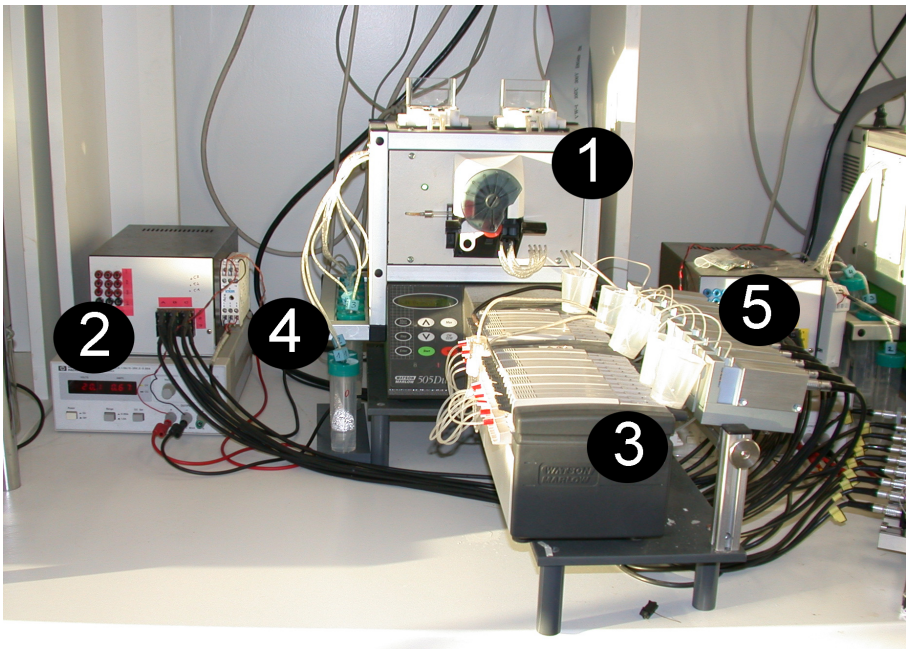

Figure 3.5: Picture of the test rig used for sensor characterisation: 1 - "Turn-and-Dock" system for automatic exchange of test solutions, 2 - potentiostat with electric power supply, 3 - peristaltic pump, 4 - test solutions containing different glucose concentrations, 5 - sensor supports with spring contacts for electrical connection to the potentiostat

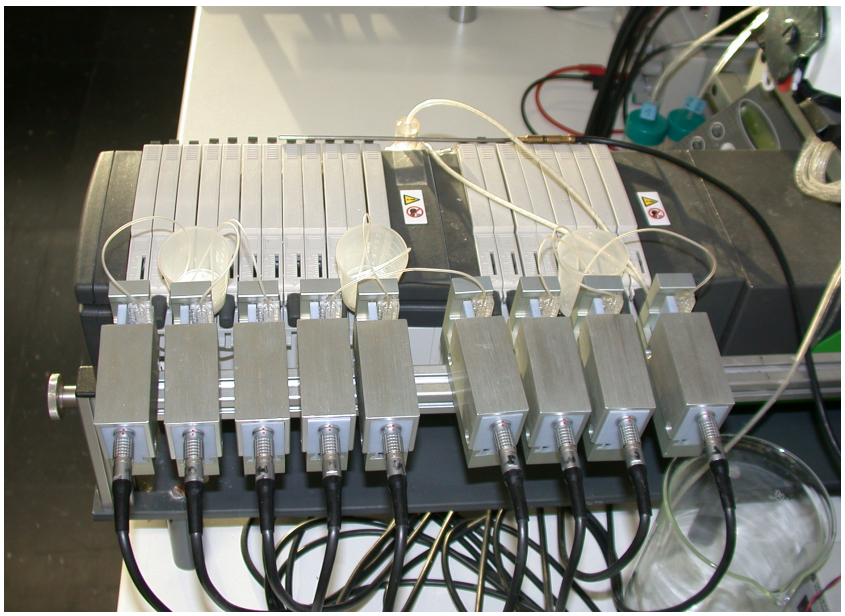

Figure 3.6: 9 supports holding the sensors for simultaneous measurement

Due to the fact that the reaction rates of enzyme reactions are temperature dependend, it was necessary to compensate for variations in temperature. This was achieved by normalising the measured sensor signal I_{meas} from the measured temperature T_{meas} to a fixed reference temperature T_{ref} of 30 °C with a temperature coefficient α of 4.5 %/°C (see equation 3.3).

$$I_{korr} = I_{meas} \cdot (1 + \frac{\alpha}{100}(T_{meas} - T_{ref})) \tag{3.3}$$

3.5.2 Reagents

Interstitial Fluid is found in the intercellular spaces where it bathes and surrounds the cells of the body, providing a means of delivering materials to the cells, intercellular communication, and removal of metabolic waste. It is composed of water, amino acids, sugars, fatty acids, coenzymes, hormones, neurotransmitters, salts and cellular products. The main electrolytes in interstitial fluid are listed in table 3.1 [55].

Kations	conc. [mval/L] ([mmol/L])	Anions	conc. [mval/L] ([mmol/L])
Na^+	145	Cl^-	117
K^+	4.4	HCO_3^-	27
Ca^{2+}	3.0 (1.5)	phosphate	2.3
Mg^{2+}	0.9 (0.45)	proteins	0.4
		others	6.2
Sum	153		153

Table 3.1: Ion concentrations in interstitial fluid

The glucose solutions are similar to the electrolyte composition of interstitial fluid, additionally, HEPES puffer is added to keep pH constant at a physiological level of 7.4 and sodium azide is added for preservation (see table 3.2). Different glucose concentrations in the range of 0 - 25 mM were made by addition of different amounts of a 1M glucose stock solution.

HEPES free acid	9,54 g
HEPES sodium salt	10,42 g
NaCl	4,38 g
KCl	0,228 g
Sodium azide	0,95 g
distilled water	1000 mL

Table 3.2: Puffer for glucose solutions

3.5.3 Measurements

In vitro characterisation was performed by a defined sequence of different glucose concentrations which took a time of 24 hours (see figure 3.7). This glucose concen-

tration profile was repeated five times to obtain information on in-use stability of the sensor (drift). Some measurements where carried out longer than the standardised 5 days, to see, when the sensor will finally decay..

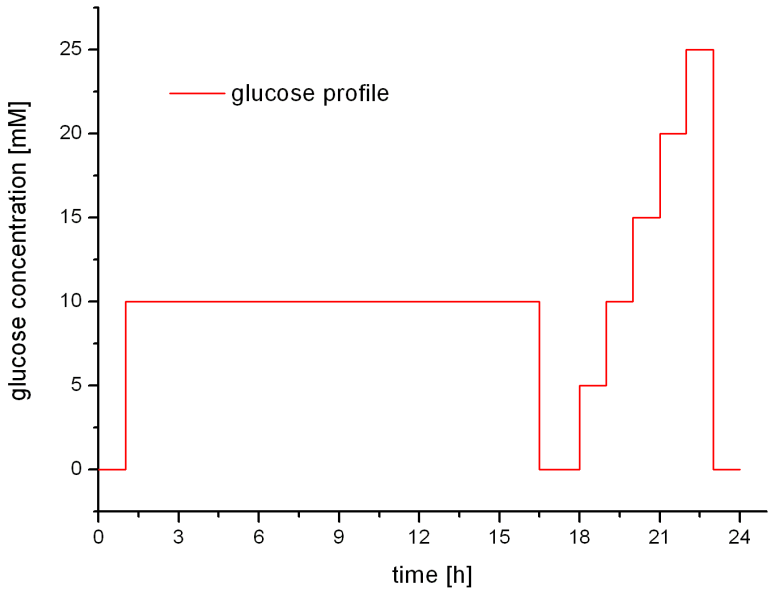

Figure 3.7: Profile of glucose concentrations for in-vitro characterisation

From this measuring sequence three parameters were calculated to benchmark the sensor performance:

- The **slope** is given as the quotient of sensor current I in [nA] and the corresponding glucose concentration in [mM] (equation 3.4). In this work the slope is always calculated with a glucose concentration of 5 mM for comparability reasons.

$$slope[nA/mM] = \frac{I_{(5mM)}}{5mM} \tag{3.4}$$

- **Linearity** is the slope at 25 mM glucose compared to the slope at 5 mM glucose. The quotient is given as percent value (equation 3.5).

$$Lin[\%] = \frac{slope_{(25mM)}}{slope_{(5mM)}} \cdot 100 \tag{3.5}$$

- **Drift** compares the 5mM slope values of different days as an index of change in sensor characteristics over time (equation 3.6).

$$drift[\%/d] = \frac{slope_{(day\,n)} - slope_{(day\,1)}}{slope_{(day\,1)} \cdot (n-1)} \tag{3.6}$$

4 Sensor development

A glucose sensor can be easily built by adsorbing glucose oxidase onto the transducer of a hydrogen peroxide sensor as described in a previous work [46]. Due to the weak adhesion of the enzyme to the surface, the bulk enzyme will be washed off within a short time and only exiguous enzyme activity will remain on the electrode. This will result in a strong decrease of the sensor slope especially in the first hours of operation.

4.1 Enzyme application by screen printing

As the electrodes are formed by screen printing, it is obvious, that screenprinting the biological receptor in a suitable matrix would offer the advantages of easy mass production and good reproducibility. But the enzyme is the most fragile part of the biosensor, and the high shear stress during printing and heat stress during the drying process could be detrimental to the sensor performance. Three inks with varying amounts of enzyme, MnO_2 and solvent were tested (see table 4.1). All inks were processed identically and cured at 80°C for 30 minutes.

Results

Ink 1 was very hard to process by screen printing because of the high amount of lyophilisate. The enzyme drew high amounts of solvent from the ink, so it became highly viscous. This resulted in the poor slope of the sensors, which was less than

	ink 1	ink 2	ink 3
carbon ink	20.0 g	20.0 g	20.0 g
GOx	2.0 g	2.0 g	3.5 g
MnO_2	7.0 g	4.0 g	3.5 g
solvent	0.6 g	0.6 g	0.9 g

Table 4.1: different compositions for screen printing the working electrode

0.5 nA/mM without any linearity at glucose concentrations higher than 10 mM. The second day the slope of the sensor was near zero.

Ink 2, with a reduced amount of MnO_2, was more printable and yielded more stable sensors. The slope was higher than that of ink 1 and the sensors had a mean linearity of 58 % (n=8). The sensor slope decreased at a mean rate of 8.7 %/d.

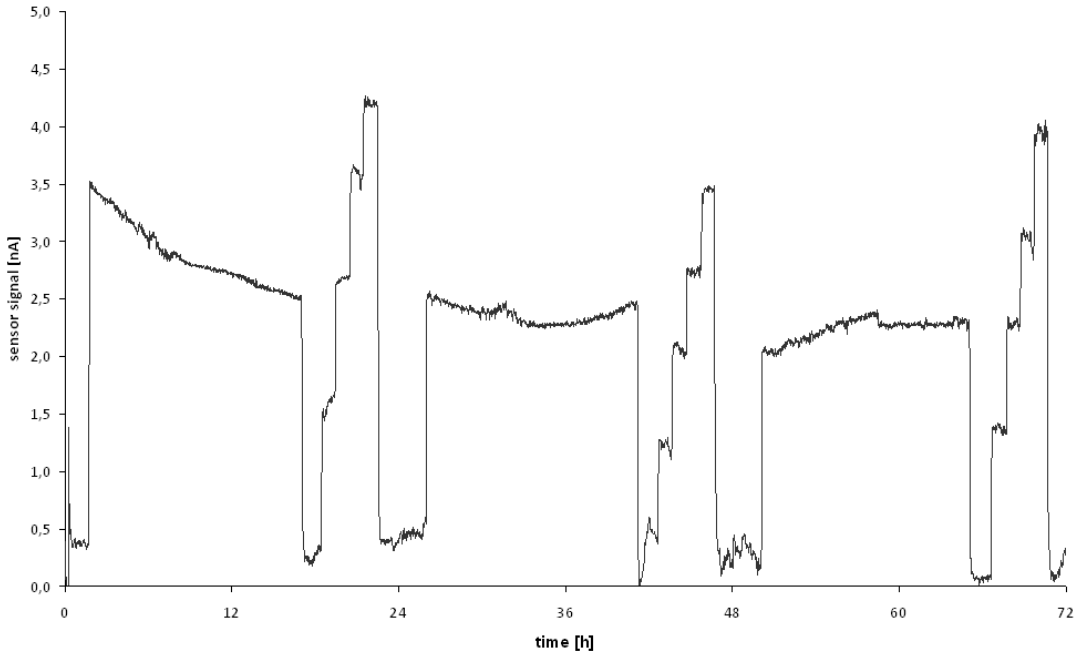

Figure 4.1: glucose sensor profile with screen printed enzyme using ink 2

Ink 3 was mixed with further decreased amount of MnO_2, even more enzyme and an also increased quantity of solvent. The higher enzyme load improved the slope of the sensors to a value of 1.20 nA/mM (n=7) but did not result better linearity and the sensor drift even deteriorated. The results are summarized in table 4.2.

sensor design	slope [nA/mM]	lin [%]	drift [%/d]
ink 1	0.48	-	-
ink 2	0.70	58	-8.7
ink 3	1.20	56	-14.2

Table 4.2: sensor results of screen-printed enzyme inks

4.2 Enzyme application by dispensing

Dispensing is a more gentle method for applying the enzyme on the transducer. The enzyme is dissolved in a suitable solvent and small volumes of the solution are dropped onto the electrode. There are many different methods for dispensing small volumes, e.g. piezo actuators, microvalves, etc. In this work the automated dispensing machine described in section 3.2 on page 31 was used.

4.2.1 GOx dispensed in aqueous solutions

Similar to the adsorption of enzyme from a solution passing the working electrode of a hydrogen peroxide sensor (described in [46]), the enzyme can be adhered to the electrode by dispensing the enzyme solution directly on top of the transducer. After the electrode has been gently dried at room temperature for one hour, the sensor was ready to perform the first measurements. Due to the fact, that both sensors are based on weak adhesion of enzyme to the transducer surface, the characteristics do not differ much from each other.

Because the working electrode had hydrophobic properties due to the carbon ink used, the enzyme was dispensed from two different solutions. 50 mg of glucose oxidase was dissolved in 1000 μL of distilled water and another 50 mg of enzyme was dissolved in 1000 μL of detergent solution containing 10% Tween20 in water. The use of detergent should improve the wetting characteristics of the dispensing solution and hence the enzyme could be detained better to the electrode surface [4].

Results

There was a significant difference between the two dispensing solutions used: The detergent containing solution demonstrated a more than ten times higher slope than the sensors made from pure water enzyme solution. The values of linearity and drift are also improved by the detergent.

sensor design	slope [nA/mM]	lin [%]	drift [%/d]
H_2O	0.76	38	-13.3
Tween20	13.48	45	-10.3

Table 4.3: sensor results for enzyme solutions with– and without detergent

An explanation may be that the detergent enhanced the interaction of enzyme and the transducer. As the transducer is built from manganese dioxide powder mixed into a carbon screen printing ink, it forms a porous electrode with a large electrochemical active surface. Dispensed in pure water the enzyme can hardly penetrate the porous structure because of the high hydrophobicity of the carbon. The detergent allows a deeper immersion of the enzyme into the electrode structure. When the enzyme and MnO_2 are in intimate contact over the whole volume of the porous structure of the electrode, diffusion lengths within the electrode become very short and the hydrogen peroxide generated by the enzyme is decomposed immediatly by the manganese

dioxide. The loss of H_2O_2 is minimized because it is produced within the electrode in contrast to enzyme layers on top of an electrode.

In all following sensor designs the enzyme was dispensed in a detergent solution containing 10% Tween20 in water.

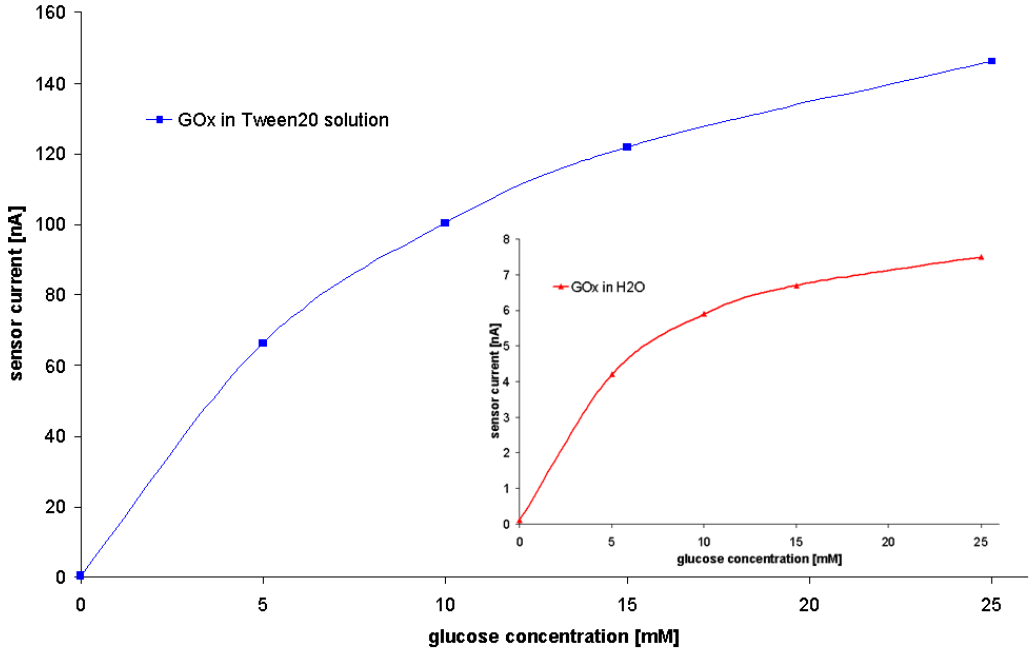

Figure 4.2: sensor characteristics: enzyme dispensed in pure water or 10% Tween20 solution respectively

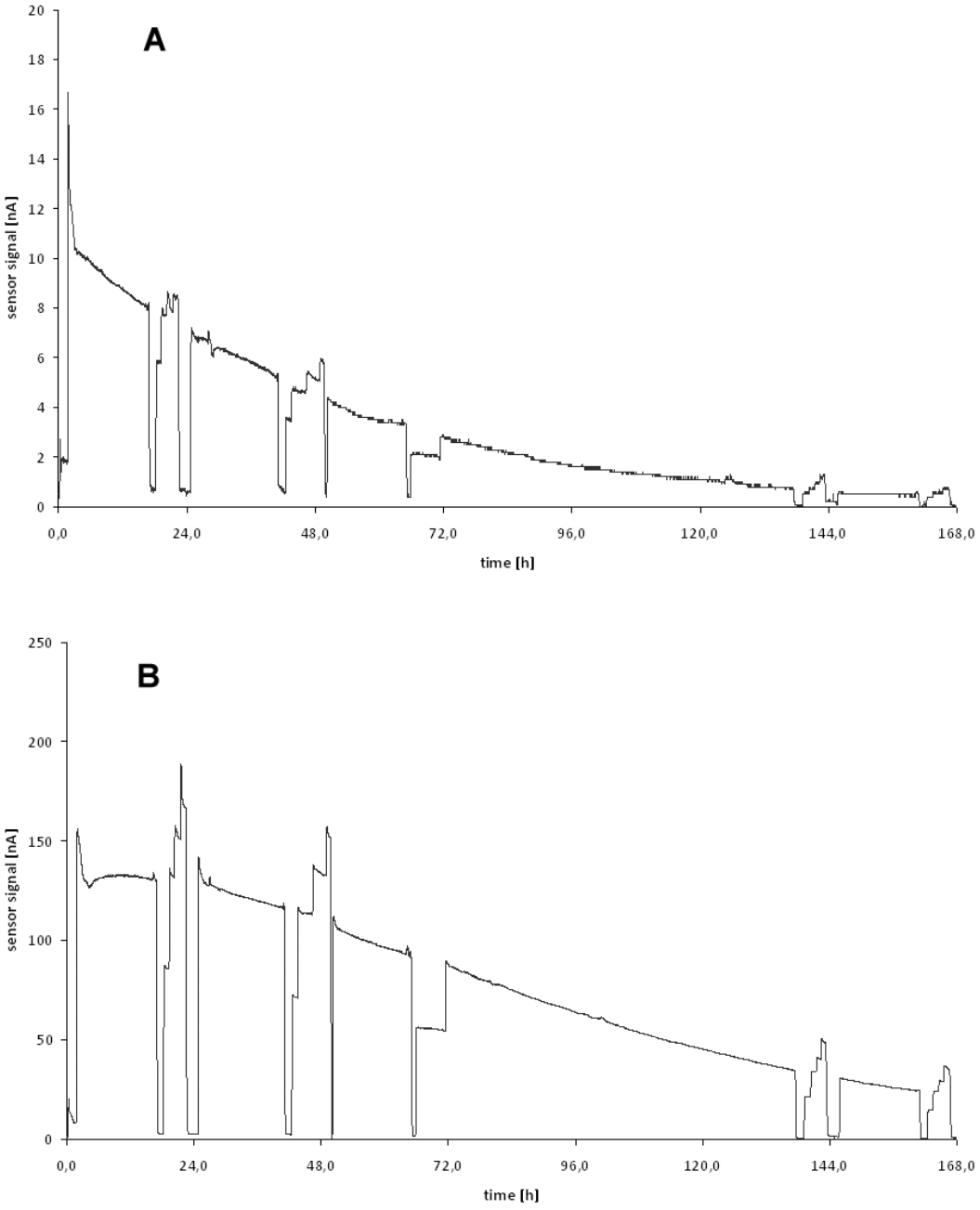

Figure 4.3: example of the sensor results, A: enzyme is dissolved in pure water, B: enzyme dissolved in 10% Tween20 solution

4.2.2 Enzyme stabilisation kit

To improve the in-use stability of the sensors an ”enzyme stabilisation kit” was purchased from Applied Enzyme Technology Ltd (UK). The kit consisted of 23 different solutions containing different combinations of polyalcohols and polyelectrolytes.

The polyalcohols including sugars, sugar alcohols and other species with many hydroxyl-groups modify the water environment surrounding a protein, competing for and replacing the free water, thus modifying the hydration shell of the protein. This modified hydration shell confers protection to the protein while maintaining 3D structure and biological activity.

The polyelectrolytes include numerous polymers of varying size, charge and structure. The interactions between proteins and polymers are electrostatic and form large protein-polyelectrolyte complexes which retain full biological activity.

The combination of polyalcohols and polyelectrolytes leads to a synergistic stabilisation effect. Polyelectrolyte molecules bind multiple protein molecules depending on the size of the polyelectrolyte involved. The addition of polyelectrolytes to solutions of proteins promotes the formation of soluble protein - polyelectrolyte complexes by electrostatic interaction. Polyhydroxyl compounds are then able to penetrate the structure more effectively leading to stabilisation.

The enzyme stabilisation solutions were double concentrated, so they could be used in a 1:1 mixture with the enzyme solution (which was also made double concentrated).

substance	amount
GOx	500 mg
Tween20 sol. 20%	2.5 mL

Table 4.4: preparation of the double concentrated enzyme solution

100 μL enzyme solution was added to 100 μL of each solution from the enzyme stabilisation kit and mixed thouroughly. As a control, 100 μL of enzyme solution was added to 100 μL of distilled water. These 24 solutions were dispensed onto the working electrode and dried at room temperature. The next day the electrodes were covered with the PVC based membrane described in section 4.3.1. Four sensors from each group were measured using the standard measuring protocol.

Results

The effects of the different stabilisation solutions vary to a great extent, the results of this series of measurements are given in table 4.5. Compared to the control group, the sensor slope could be halved or doubled, depending on the stabilizing agent used, and linearity was mostly improved. The drift, which is the target of the stabilisation kit, varies from an inferior -15.2 to an excellent -2.6 %/d respectively. The best drift value was achieved with AET sol. 17, but it also resulted in a poor linearity as a drawback. The best overall performance was achieved using AET sol. 14 which resulted in good linearity of 71 % and a low drift of -3.8 %/d. An exemplary glucose profile is depicted in figure 4.4.

solution	slope [nA/mM]	linearity [%]	drift [%/d]
control sol.	11.6	58	-8.3
AET sol. 01	10.5	68	-7.8
AET sol. 02	10.4	74	-7.3
AET sol. 03	12.9	72	-12.9
AET sol. 04	9.7	73	-10.9
AET sol. 05	6.6	75	-8.2
AET sol. 06	11.0	69	-11.8
AET sol. 07	5.8	76	-10.3
AET sol. 08	6.2	62	-10.9
AET sol. 09	5.2	54	-10.4
AET sol. 10	6.4	50	-10.8
AET sol. 11	6.6	54	-9.5
AET sol. 12	20.2	47	-5,4
AET sol. 13	15.2	61	-7.3
AET sol. 14	11.8	71	-3.8
AET sol. 15	14.7	71	-7.2
AET sol. 16	15.4	69	-9.7
AET sol. 17	27.1	45	-2.6
AET sol. 18	15.3	62	-15.2
AET sol. 19	9.5	58	-13.0
AET sol. 20	9.6	63	-12.2
AET sol. 21	12.5	68	-5.7
AET sol. 22	12.0	69	-5.3
AET sol. 23	10.2	70	-5.8

Table 4.5: sensor results derived from AET´s enzyme stabilisation kit

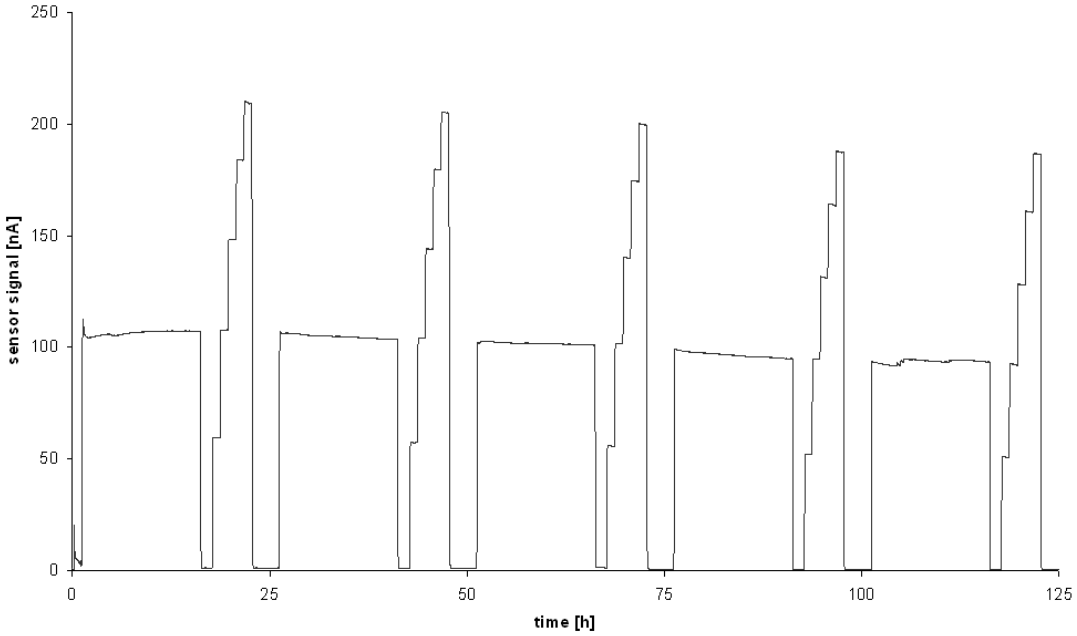

Figure 4.4: exemplary measurement with a sensor derived from AET solution 14

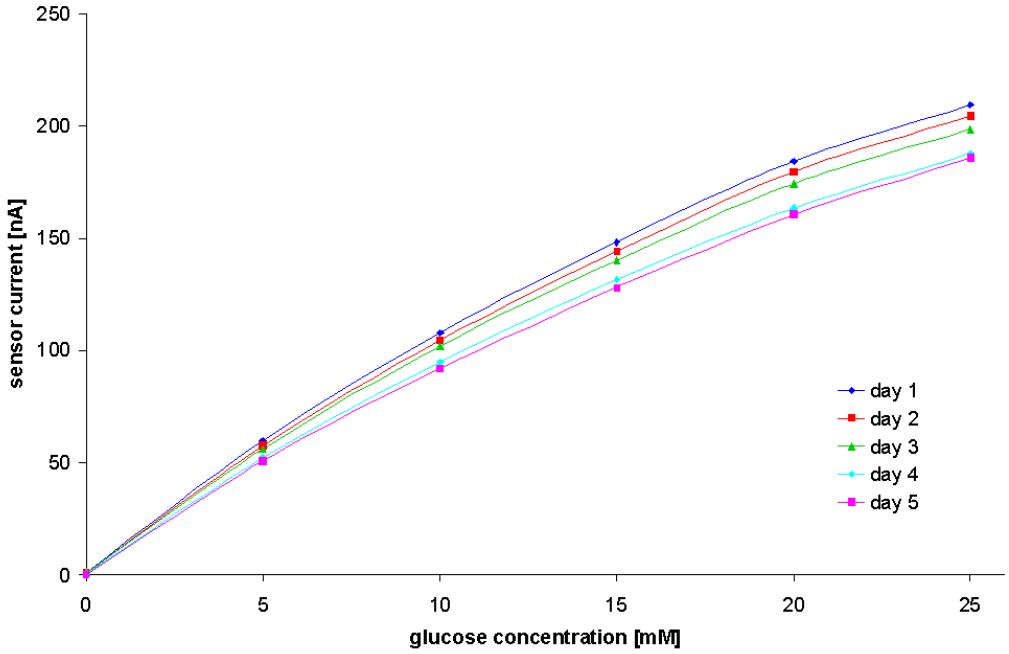

Figure 4.5: sensor characteristics of sensors derived from AET solution 14

4.3 Application of different cover membranes

As it is obvious that the slope of the sensors presented in the preceding sections 4.1 and 4.2 decay very fast, it can be assumed that the enzyme is washed off the electrode in a short time. There are several ways to treat this issue:

- The enzyme could be covalently bound to the electrode surface which would lead to a great loss of enzyme activity and would also prevent the benefit of the detergent effect.
- Crosslinking the individual enzyme molecules would raise the molecular weight and therefore reduce solubility.
- Enzyme retention could be achieved by a suitable cover membrane which is applied on top of the enzyme electrode. An additional benefit of this method is that membranes also restrict the diffusion of analyte to the electrode and therefore increase the measureable range to higher glucose concentration. Proteins in the dialysate cannot pass suitable membranes and so the electrode is protected from fouling. On the other hand, it is necessary that the membrane is permeable to oxygen, which is essential for the sensor performance as it is the co-substrate for the enzyme.

Covalent binding and crosslinking are processes which can significantly reduce the activity of the enzyme, therefore, the way of employing different cover membranes was chosen.

4.3.1 PVC based membrane

The first material tested is poly(vinyl chloride-co-vinyl acetate-co-maleic acid), referred to as PVC. The material has good oxygen permeability and is a strict diffusion

barrier for glucose. To avoid too small sensor currents 3 mg of glycerol was added to the dispensing solution as a plasticiser. The PVC material is tested on both sensor types presented in section 4.2 which were produced with and without detergent in the enzyme solution.

Glycerol	3 mg
PVC	200 mg
2-Butoxyethanol	5000 mg

Table 4.6: formulation of the dispensing solution of the PVC cover membrane

Results

As well as the sensors without a membrane the sensors with enzyme dispensed in Tween20 solution yielded much higher slopes with a linearity of 53 % (n=7) and a loss of slope of 8.4 %/d. Comparing the results of sensors with and without membrane, there was only a small improvement of the sensor performance due to the additional membrane for the detergent group of sensors. Sensors without detergent seemed even to get worse by the addition of the membrane.

sensor design	slope [nA/mM]	lin [%]	drift [%/d]
H_2O	0.76	38	13.3
H_2O and PVC membrane	0.94	34	13.4
Tween20	13.48	45	10.3
Tween20 and PVC membrane	12.80	53	8.4

Table 4.7: sensor results with and without PVC membrane

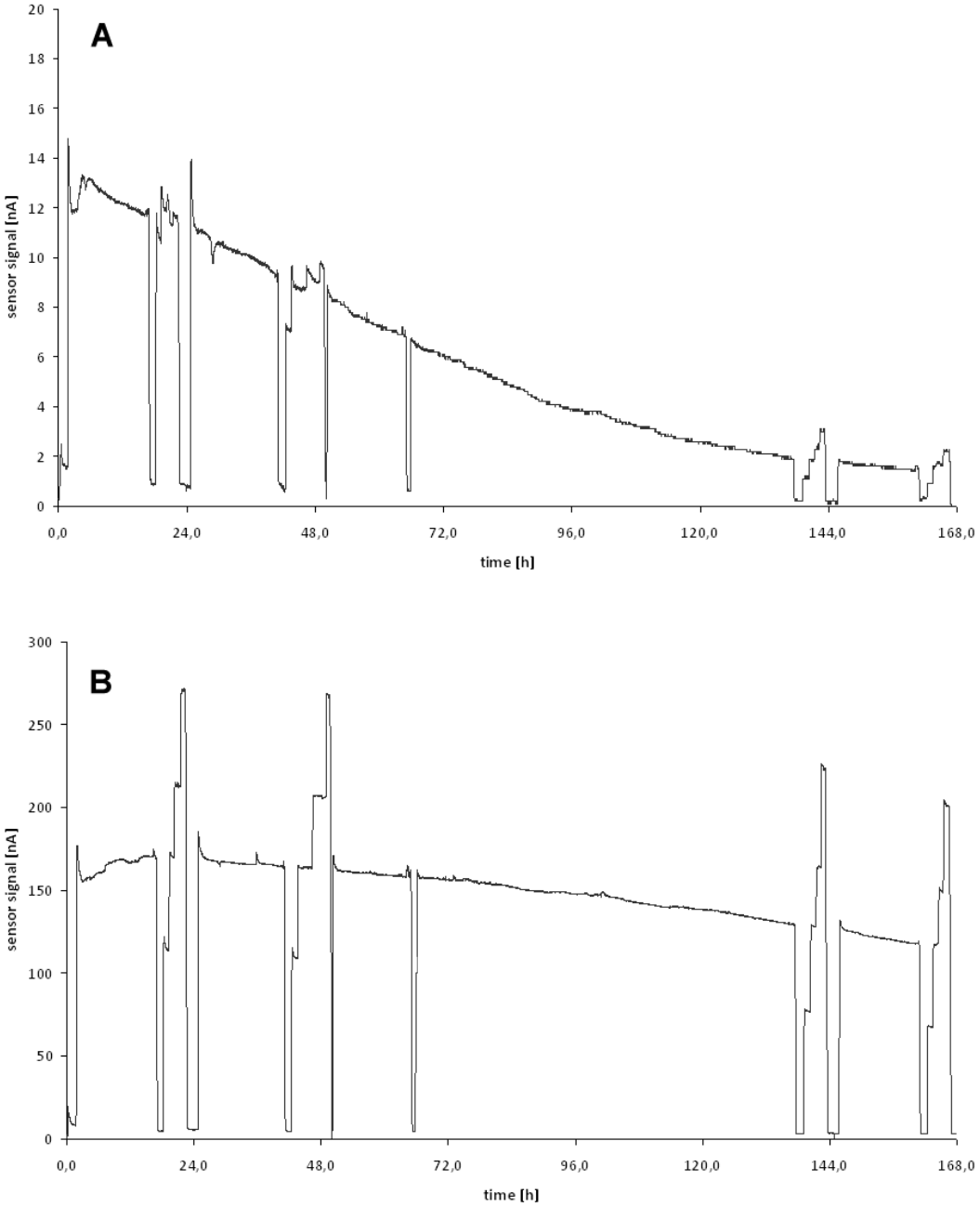

Figure 4.6: example of the sensor results, A: enzyme is dissolved in pure water, additional PVC membrane is applied, B: enzyme dissolved in 10% Tween20 solution, additional PVC membrane is applied

4.3.2 Poly-HEMA membranes

Poly(2-hydroxyethyl methacrylate) (poly-HEMA) is known as a biocompatible hydrogel [49], it is soft and flexible and is therefore often used in contact lenses. The sensors were produced with two different HEMA solutions, E2W and F1/2W respectively which differed in the ratio of HEMA to methyl-methacrylate. Acrifix 190 was used as the source of methyl-methacrylate in the formulations of table 4.8. The HEMA solutions were dispensed onto the working electrodes and were then cured with UV radiation for 5 minutes. During the curing process, the curing box was flushed with argon gas to prevent the disruptive influence of oxygen to the polymerisation reaction.

p-HEMA E2W		p-HEMA F1/2W
10.0 g	Acrifix 190	10.0 g
12.0 g	HEMA	16.0 g
1.2 g	TEGDM	0.75 g
4.5 g	H_2O	5.4 g
0.2 g	UV-initiator	0.3 g

Table 4.8: HEMA solutions E2W and F1/2W membranes

Results

sensor design	slope [nA/mM]	lin [%]	drift [%/d]
p-HEMA E2W	0.5	54	-6.2
p-HEMA E2W dil. 1:1	4.1	39	-12.4
p-HEMA F1/2W	1.9	50	-9.3
p-HEMA F1/2W dil. 1:1	3.4	39	-10.7

Table 4.9: sensor results with different poly-HEMA membranes

The poly-HEMA membrane derived from solution E2W yielded sensors with small slopes, linearity of 54 % and low drift values of -6.2 %/d (n=5). The sensor character-

istics of sensors made with solution F1/2W were quite similar. The slope was higher, but linearity and drift results were slightly worse. Due to the small sensor currents a second group of sensors was dispensed with HEMA solutions diluted 1:1 with 2-propanol and the curing process unchanged. The sensor slopes raised as expected, but the drawbacks were decreasing linearities and increasing drift values.

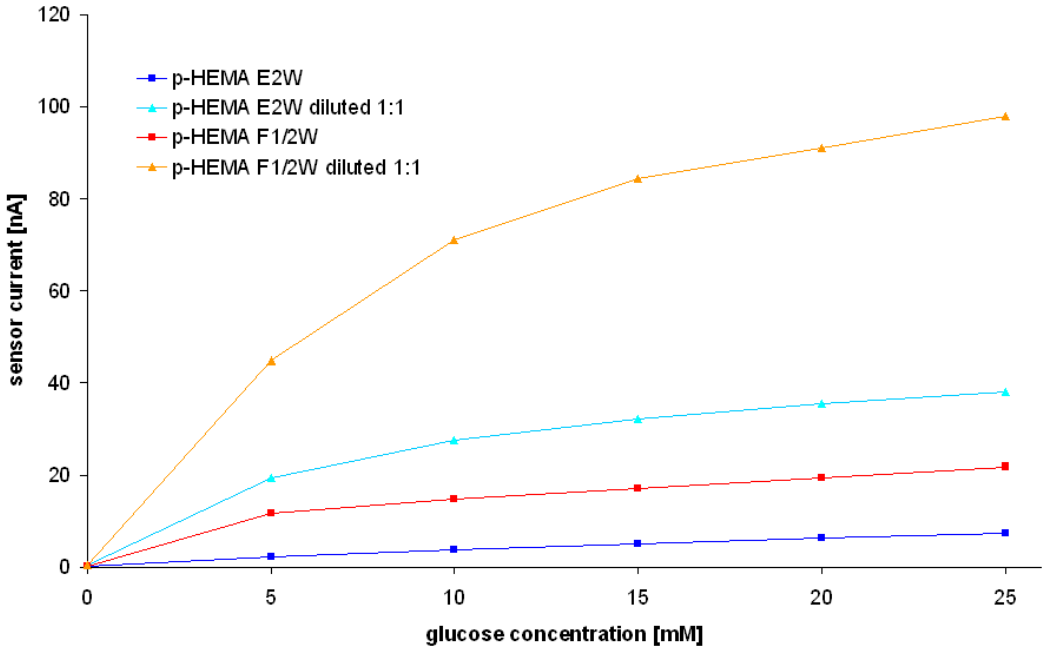

Figure 4.7: characteristics of sensors with various p-HEMA membranes

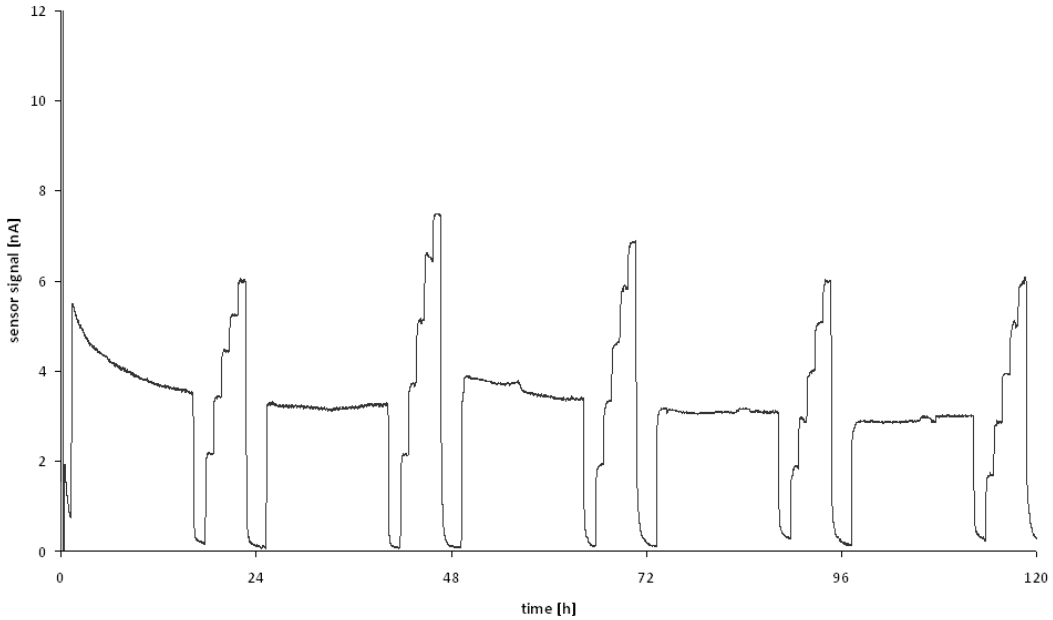

Figure 4.8: exemplary measuring result from a sensor with a p-HEMA E2W membrane

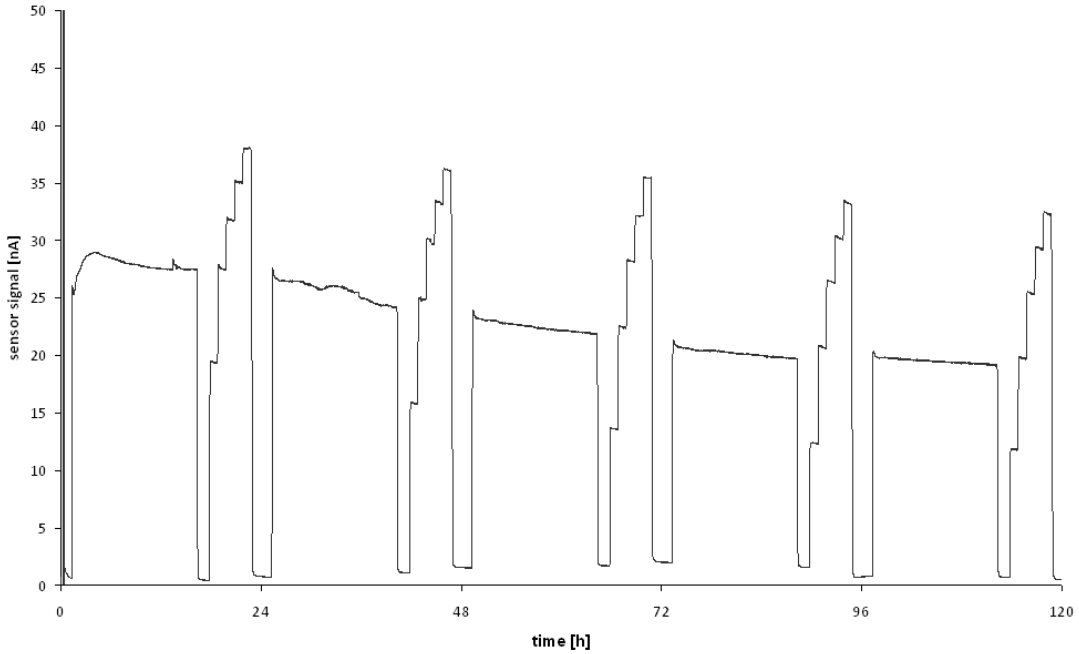

Figure 4.9: exemplary measuring result from a sensor with a p-HEMA E2W membrane diluted 1:1 with 2-propanol

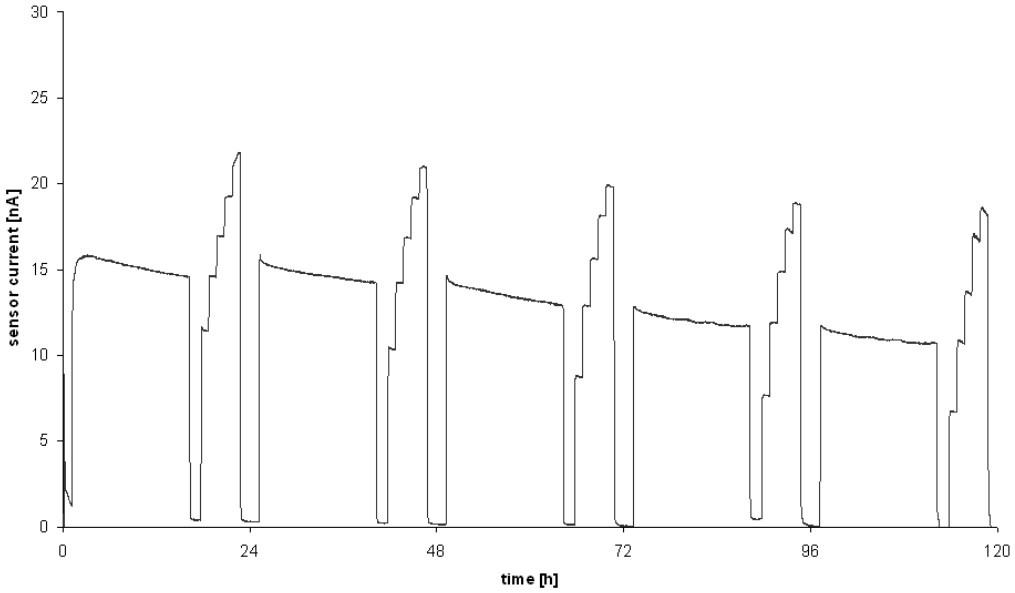

Figure 4.10: exemplary measuring result from a sensor with a p-HEMA F1/2W membrane

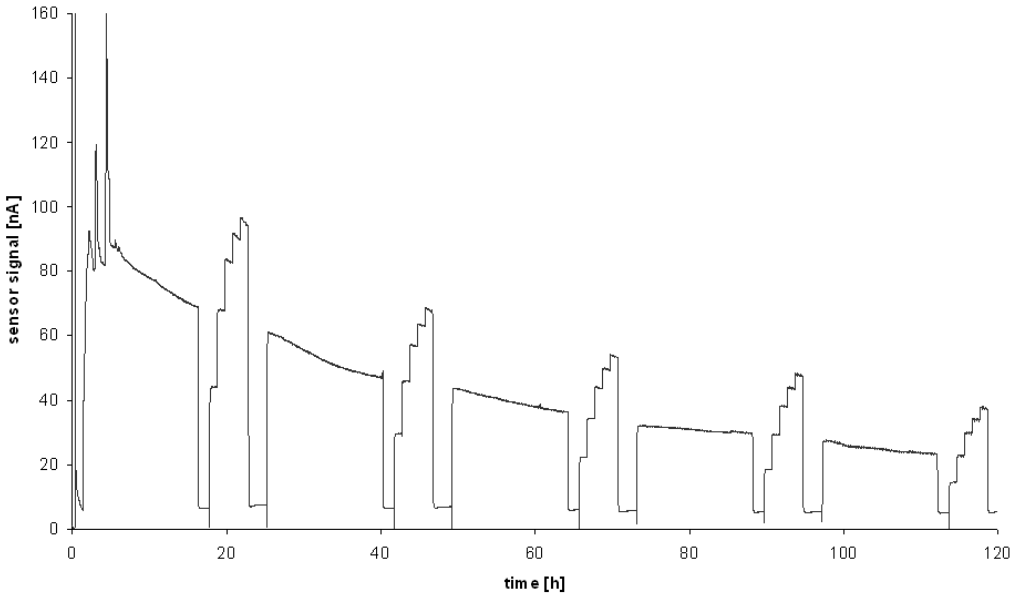

Figure 4.11: exemplary measuring result from a sensor with a p-HEMA F1/2W membrane diluted 1:1 with 2-propanol

4.3.3 PVA membrane

Poly(vinyl alcohol) is a nontoxic and flexible material with excellent film forming properties that make it a good candidate as membrane material. Furthermore, it bears many hydroxyl groups which result in a high hydrophilicity. Unfortunately, it is also a good barrier for oxygen diffusion, so it is not a perfect match.

The Poly(vinyl alcohol) used for sensor production had an average molecular weight of 85 to 124 kDa and was dissolved in ethanol to give a 5% solution. The solution was dispensed onto the working electrode and dried at room temperature. The sensors were used the next day to perform the standard measuring procedure.

As the slope and drift values of sensors with PVA membrane were quite high, which indicated poor glucose diffusion barrier– and enzyme retention properties, a second PVA was tested. Poly(vinyl alcohol-co-ethylene), a copolymer of PVA and polyethylene (PE) with reduced hydrophilic properties should result in lower slopes and better enzyme retention. The polymer ratio was 68% PVA and 32% PE respectively. A solution was prepared containing 5% PVA-co-PE in a 1:1 mixture of H_2O and 1-propanol.

Results

The expectations of the sensor results were almost met. The pure PVA membrane proved high slopes of 15.8 nA/mM, linearities of 51% and high drift values of more than 15%/d. The co-polymer with reduced hydrophilicity met the expectation to lower the slope- and raise linearity values, but the drift was still too high for an application of several days measuring time. Furthermore, the slope values decreased dramatically.

sensor design	slope [nA/mM]	lin [%]	drift [%/d]
PVA	15.8	51	-15.6
PVA-co-PE	0.9	64	-12.3

Table 4.10: sensor results derived from PVA and PVA-co-PE membranes

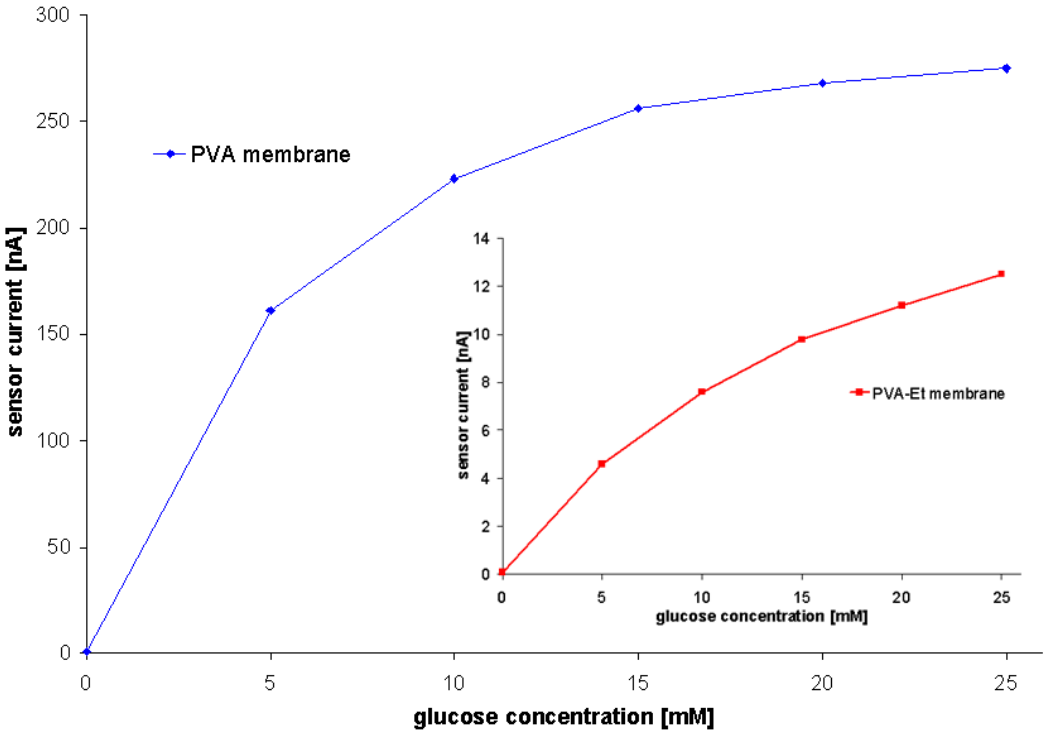

Figure 4.12: characteristics of sensors with PVA or PVA-co-PE membrane respectively

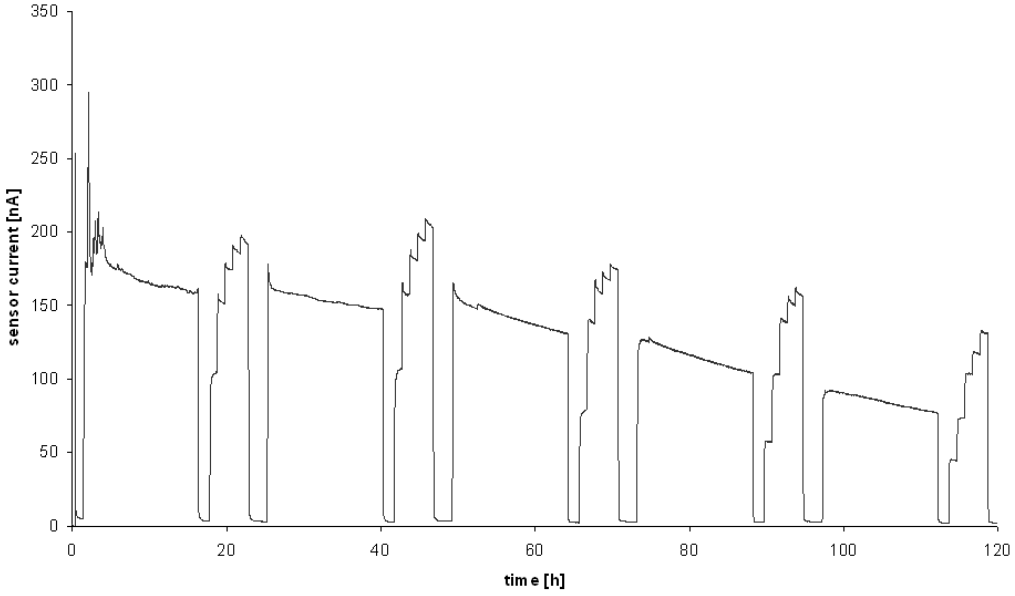

Figure 4.13: result of a sensor with PVA membrane

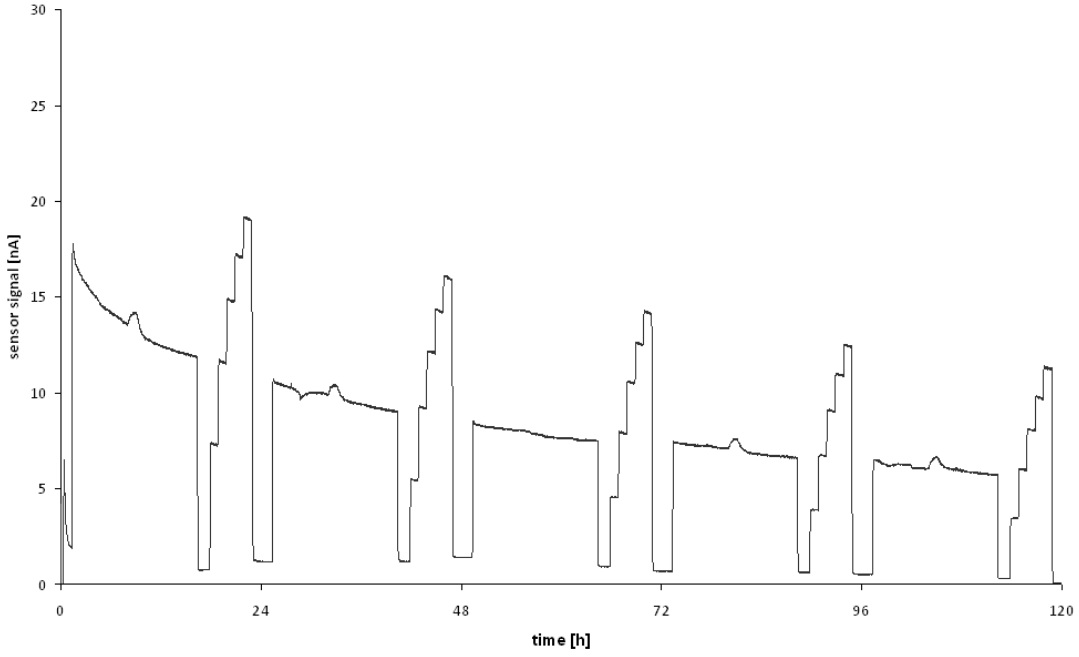

Figure 4.14: result of a sensor with PVA-co-PE membrane

4.3.4 Nafion membrane

Nafion was the first polymer published of the class of polymers with ionic properties that are called ionomers. It is a sulfonated tetrafluoroethylene based fluoropolymer-copolymer which is highly conductive to cations, permeable to water, and is able to block anionic interferents from the electrode surface, making it suitable for many membrane applications.

For sensor preparation a ready to use solution was purchased from Sigma-Aldrich containing 5% Nafion in a mixture of lower aliphatic alcohols and water. The solution was dispensed onto the working electrode and dried at room temperature overnight.

Results

Sensors with Nafion membrane resulted in a medium slope of 7.3 nA/mM, a linearity of 64%, and a drift of over 10%/day. To raise linearity and to reduce drift, a second layer of the Nafion membrane was applied which astonishingly doubled the slope value and reduced the linearity even more. An explanation may be, that by dispensing the second layer, the first layer beyond including the electrode itself was dissolved and resettled in a new structure, which was less restrictive to glucose diffusion.

sensor design	slope [nA/mM]	lin [%]	drift [%/d]
Nafion (1 layer)	7.3	64	-10.5
Nafion (2 layers)	14.1	43	-10.5

Table 4.11: sensor results derived from Nafion membranes

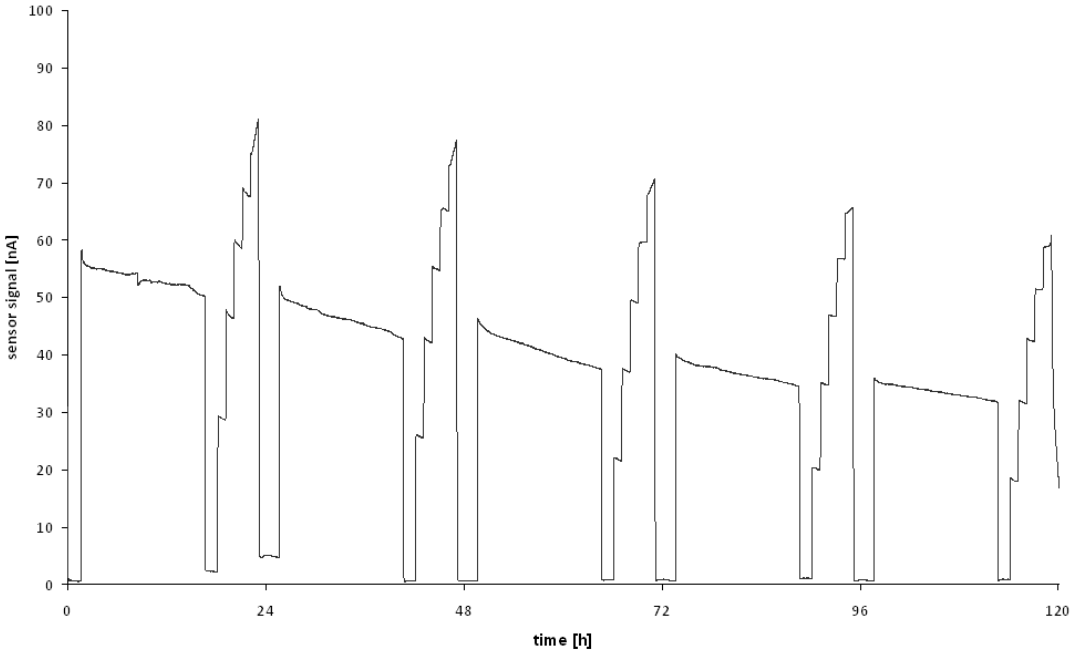

Figure 4.15: exemplary glucose profile of a sensor with one layer of Nafion

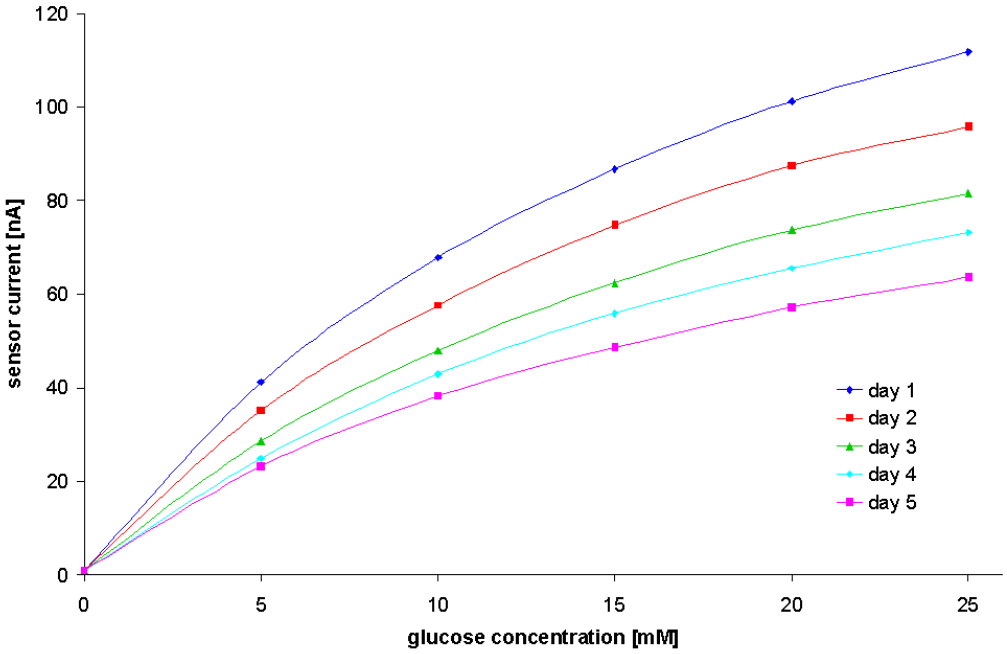

Figure 4.16: characterisitcs of sensors with one layer of Nafion

4.3.5 Poly(MPC-co-BMA)membrane

Poly(MPC-co-BMA) is an amphiphilic polymer and consists of poly(2-methacryloyloxyethyl phosphorylcholine (MPC), which is a hydrophilic biomimic, and butylmethacrylate (BMA), which is the hydrophobic counterpart in the polymer. The molar fractions of each component in poly(MPC-co-BMA) were 30% MPC and 70% BMA respectively. The lipid-attracting polymer is widely used as biocompatible surface coating for vascular applications minimizing or eliminating tissue trauma [21].

20 mg of poly(MPC-co-BMA) were dissolved in 200 μL ethanol to give a 10% solution. The results were not satisfying so a new group of sensors was coated with the doubled concentration of poly(MPC-co-BMA).

Results

Although the sensor drift could be significantly reduced by using a 20% solution of poly(MPC-co-BMA), the linearity could be increased only to a minimal level of 54%. The high sensor slopes would allow for a further increase in the concentration of the membrane solution, but the improvement of the linearity by doubling the concentration was negligible. Therefore, no further tests with higher concentrations were performed.

sensor design	slope [nA/mM]	lin [%]	drift [%/d]
Poly(MPC-co-BMA) 10% sol.	15.8	51	-15.6
Poly(MPC-co-BMA) 20% sol.	10.5	54	-6.2

Table 4.12: sensor results derived from poly(MPC-co-BMA) used in two different concentrations

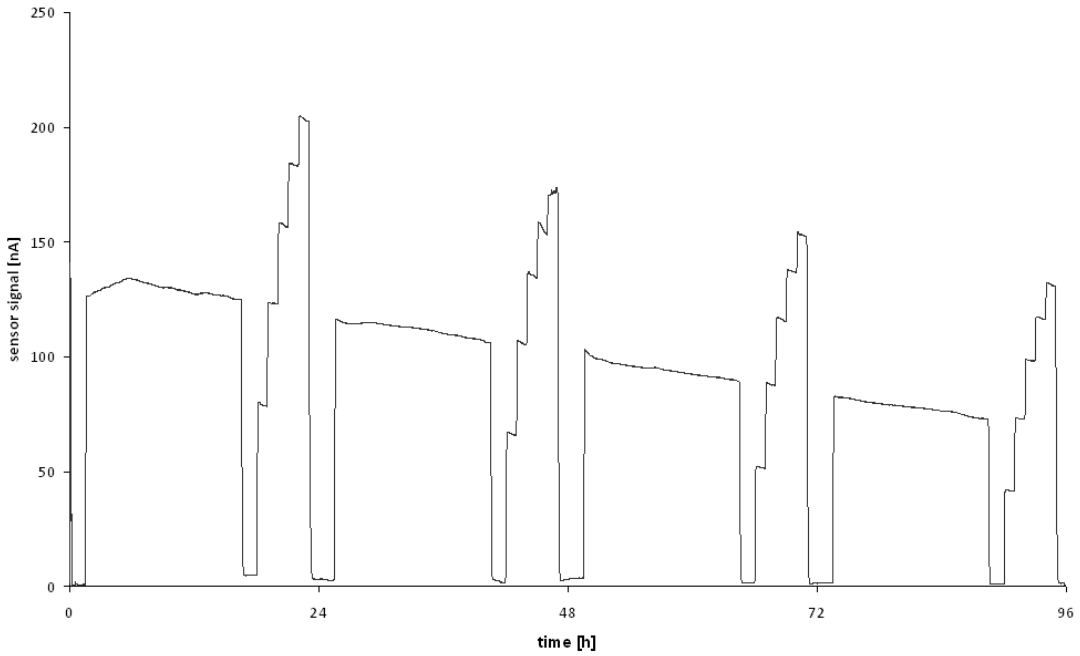

Figure 4.17: exemplary result of sensors coated with 10% MPC dispensing solution

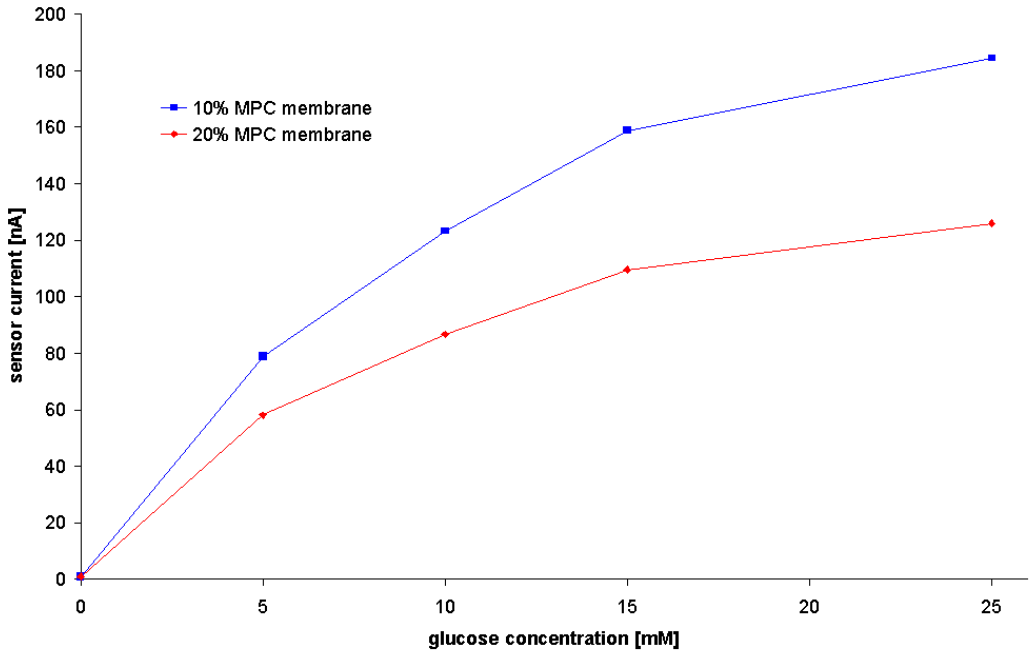

Figure 4.18: characteristics of MPC coated sensors

4.3.6 D4 and D6 hydrogel membranes

D4 and D6 were polyurethane hydrogels purchased from Tyndall-Plains-Hunter Ltd (USA). They were part of the D-series of hydrophilic polymers that were designed to take up fluids to a predetermined equilibrium level. In addition, these polymers absorb electrolytes and body fluids as well as water, thus they avoid the concentration gradients that occur when hydrophobic materials were used. The two tested materials differed in their ability to take up water. The water absorption of D4 was 100 %, the one of D6 was 415 %. The water uptake W is defined as the percentage of the mass of absorbed water to the mass of the dry polymer (see equation 4.1).

$$W = \frac{m_{wet} - m_{dry}}{m_{dry}} \cdot 100 \tag{4.1}$$

The hydrogels were dissolved in a mixture of 10% water in ethanol to give solutions containing 10% D4 and D6 respectively. The working electrode was coated by dispensing the hydrogels and then dried at room temperature for two hours.

Results

Both hydrogels were not suitable for enzyme retention on the electrode. As the sensor characteristics in table 4.3.6 prove, the enzyme was washed off the electrode very quickly.

sensor design	slope [nA/mM]	lin [%]	drift [%/d]
D4	14.8	43	-22.3
D6	13.7	48	-19.0

Table 4.13: sensor characteristics of sensors coated with D4 and D6 hydrogels

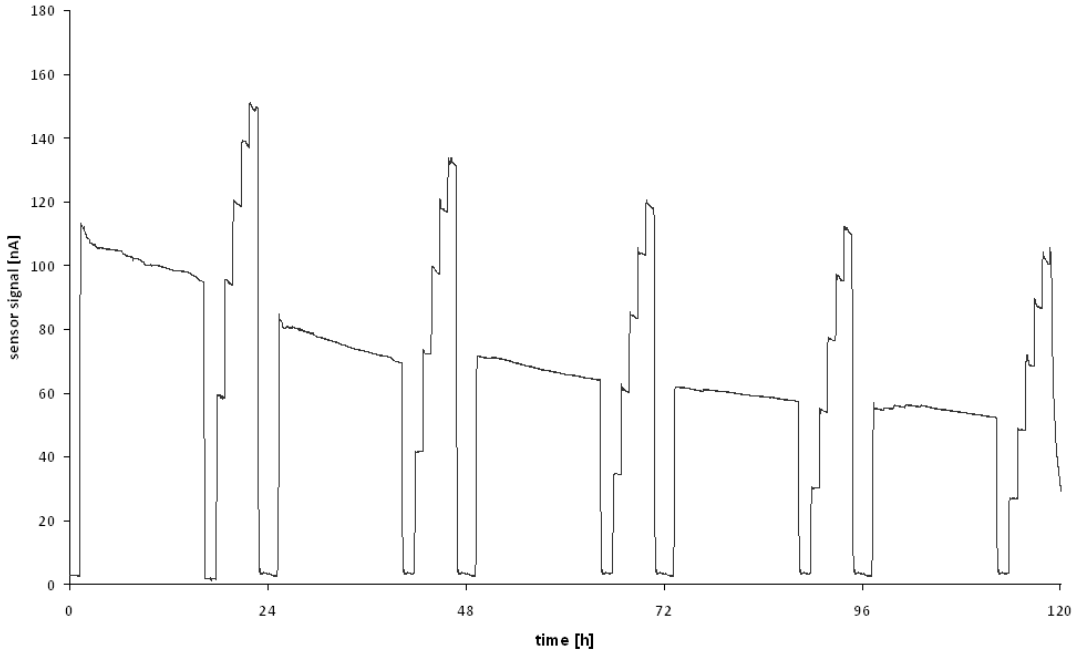

Figure 4.19: exemplary glucose profile of a sensor covered with D6 hydrogel

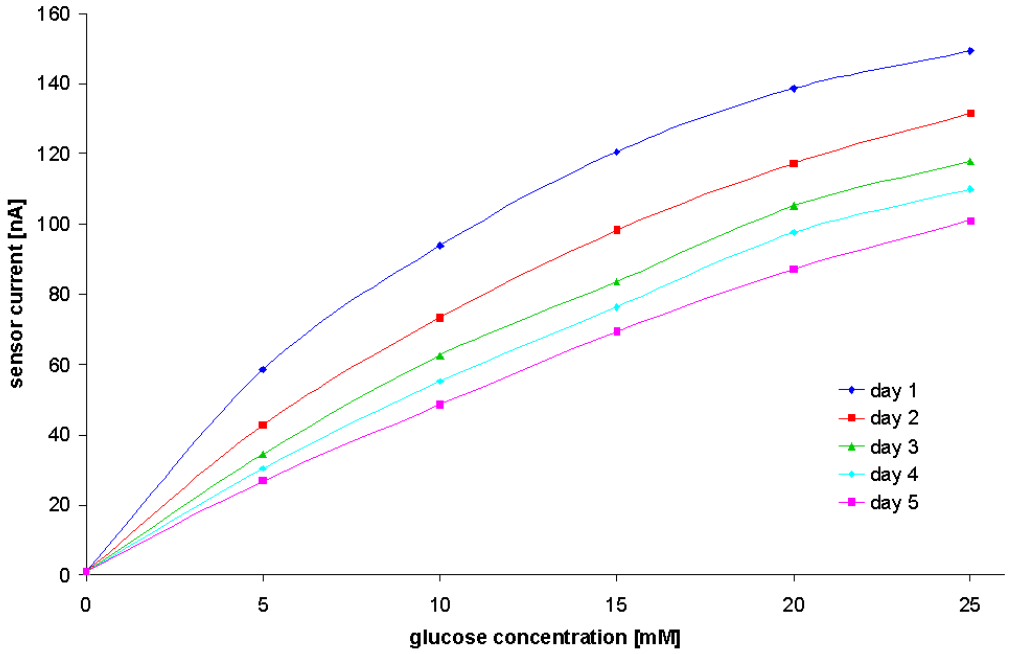

Figure 4.20: characteristics of sensors coated with D6 hydrogel

4.3.7 Polyurethane membrane

Polyurethane (PUR) is a biocompatible material used in medical grade tubings and catheters [56]. It is synthesized by step-growth polymerization of polyisocyanates and polyoles in the presence of a catalyst. If linear polymer molecules are desired diisoyanates and dioles are used, in order to get a crosslinked polymer, monomers with more than 2 functional groups are necessary. The polymer used as the cover membrane of the working electrode was polymerized with ethylenglycol and 4,4'-dicyclohexyl-methandiisocyanat, which formed the hard (hydrophobic) segment and poly(ethylen-glycol) and poly(propylenglycol) which are used as chain extenders and formed the soft (hydrophilic) segments of the polymer. The catalyst used for starting the polymerization reaction was dibutyltin-dilaurat (DBTDL) [5].

Two dispensing solutions were fabricated by dissolving the material in ethanol and tetrahydrofuran (THF), respectively, containing 5% polyurethane each. The membrane solutions were dispensed manually with a 1000 DVE dispenser (from GLT, Germany) due to the high viscosity of the derived solutions. The volume dispensed in one dispensing step is set by the duration and the magnitude of the applied air pressure. Both parameters are set to produce a droplet which securely covered the entire working electrode.

Results

The membrane derived from the ethanolic dispensing solution yielded quite reasonable sensors with a linearity of 67% and drift values of -6.2 %/day. The sensors with polyurethane membrane dispensed in THF solution showed excellent performance over 5 days. The slope of 4.4 nA/mM is easy to handle with standard electronics, the linearity of 81% is sufficient for measuring high concentrations of glucose and the positive drift of 1.1 %/day would allow for a single calibration per day.

sensor design	slope [nA/mM]	lin [%]	drift [%/d]
PUR in ethanol	9.6	67	-6.2
PUR in THF	4.4	81	+1.1

Table 4.14: influence of the membrane solvent on the sensor characteristics

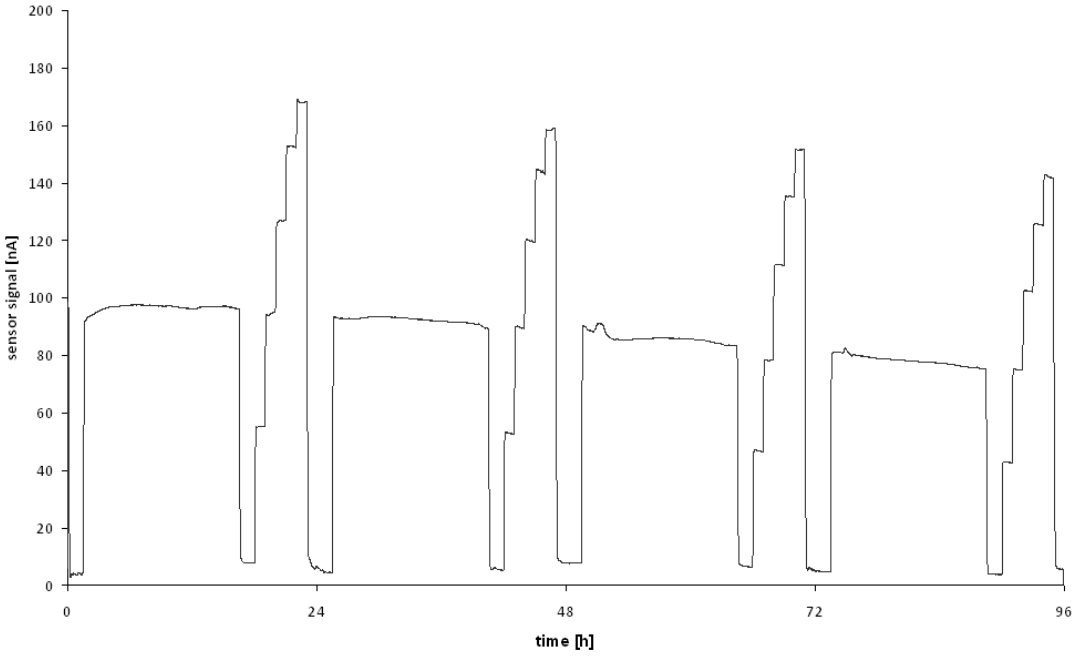

Figure 4.21: sensor with polyurethane membrane dispensed in ethanolic solution

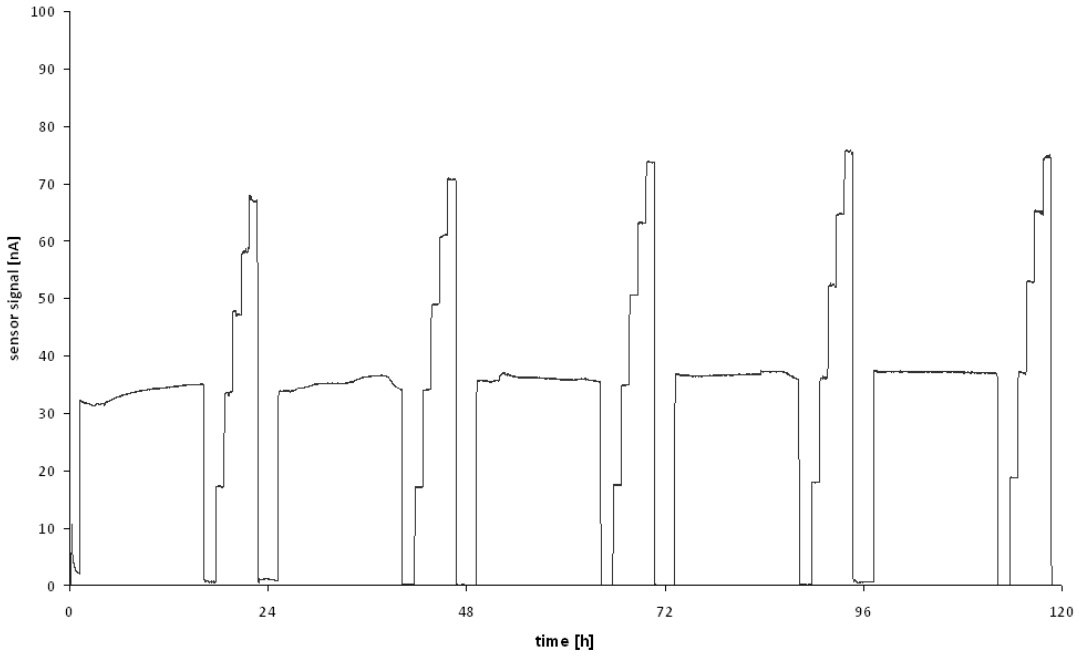

Figure 4.22: sensor with polyurethane membrane dissolved in THF

The sensor characteristics of these sensors were not completely linear (see figure 4.23), but the linear fit with a Pearson correlation coefficient of 0.99 indicated that the regression was still sufficient for the monitoring application. The change of the sensor characteristics was minimal which implied full usability of the sensors for monitoring periods of several days.

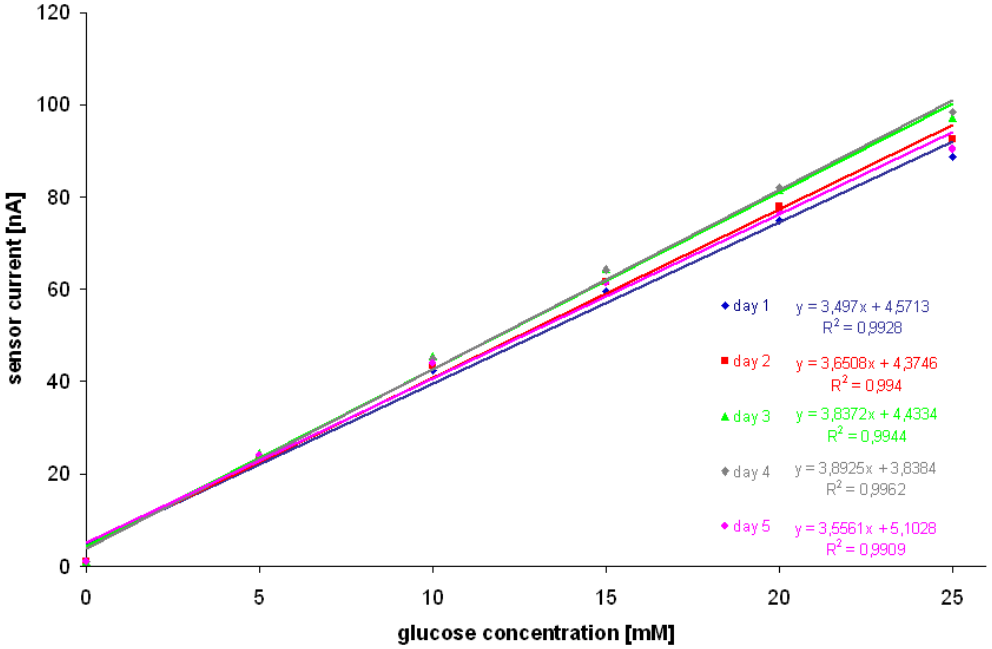

Figure 4.23: change of sensor characteristics during a 5 day in-vitro test (PUR in THF membrane)

4.3.8 Water uptake of the PUR membrane

In contrast to all materials tested as cover membrane of the working electrode of the glucose sensor, the polyurethane material gave sensors with a positive drift of the slope. An explanation may be that the water uptake of the material happens over a time period of several days, thus increasing its permeability which subsequently leads to higher sensor slopes.

The kinetics of the water uptake of the polyurethane material was tested by weighting the material during the wetting process. A tared glass slide was covered with the polymer with an approximately 10 μm thick layer by dispening the polyurethane solution containing 5 % polymer dissolved in THF. After the solvent was removed completely overnight at room temperature, the glass slide containing the dry polymer film was weighted on an analytical balance. After the weight of the film had been determined, the glass slide was put into a petrie dish filled with distilled water, and it was made certain that the polymer was completely submerged. To determine the weight of the polymer, it was removed from the water and quickly placed on and covered by filter paper to remove excess water and was then immediately placed on a tared weighing dish and weighed. The increase in weight was expressed as water uptake W, described in equation 4.2.

$$W = \frac{m_{wet} - m_{dry}}{m_{dry}} \cdot 100 \tag{4.2}$$

The measurement was performed with three samples of the polymer. The good correspondence of the results demonstrated the validity of the method to determine the wateruptake of the polymer. The results are depicted in figure 4.24.

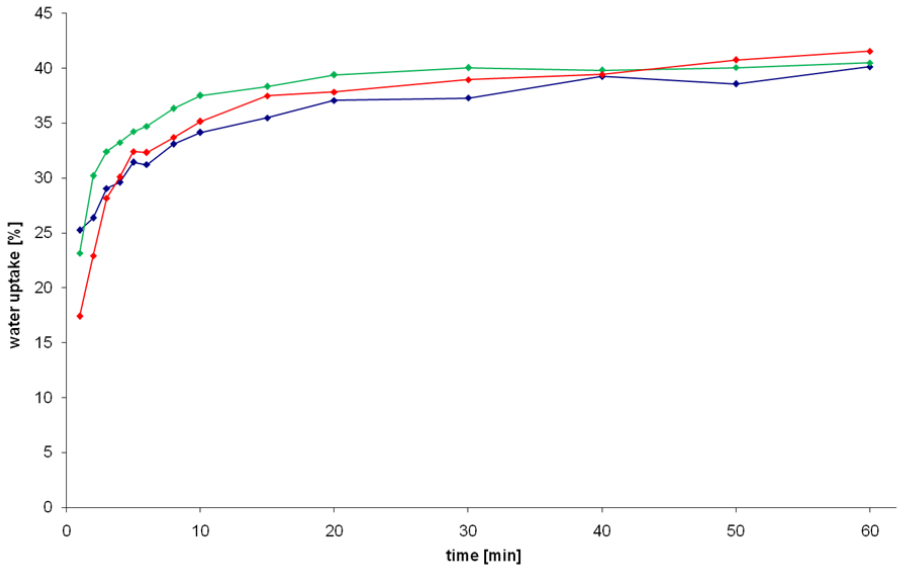

Figure 4.24: water-uptake of the polyurethane cover membrane

4.4 Cyclic voltammetry

Cyclic voltammetry was carried out in a hydrodynamic technique with a potentiostat from Gamry. The HEPES buffered saline solutions with and without glucose were pumped through the sensor at a flow rate of 300 nL/min analog to the condition during operation in the glucose monitoring device. The sensor was allowed to equilibrate after polarisation over a period of 600 seconds. Then, the potential was ramped from 150 to 700 mV (against the internal Ag/AgCl reference electrode) with a speed of 0.1 mV per second. The measurement carried out in solution without glucose proved a stable and low zero current of the sensor of about 3 nA at the working potential of 350 mV. When the potential rose above 500 mV a steep increase of the current occured due to hydrolysis of the solution (see figure 4.25). When the measurement was carried out in solution containing 5 mM glucose the sensor current rose with the potential applied. In the range of 300 - 500 mV there was only a slight rise of the current due to increase of the potential applied (see figure 4.26).

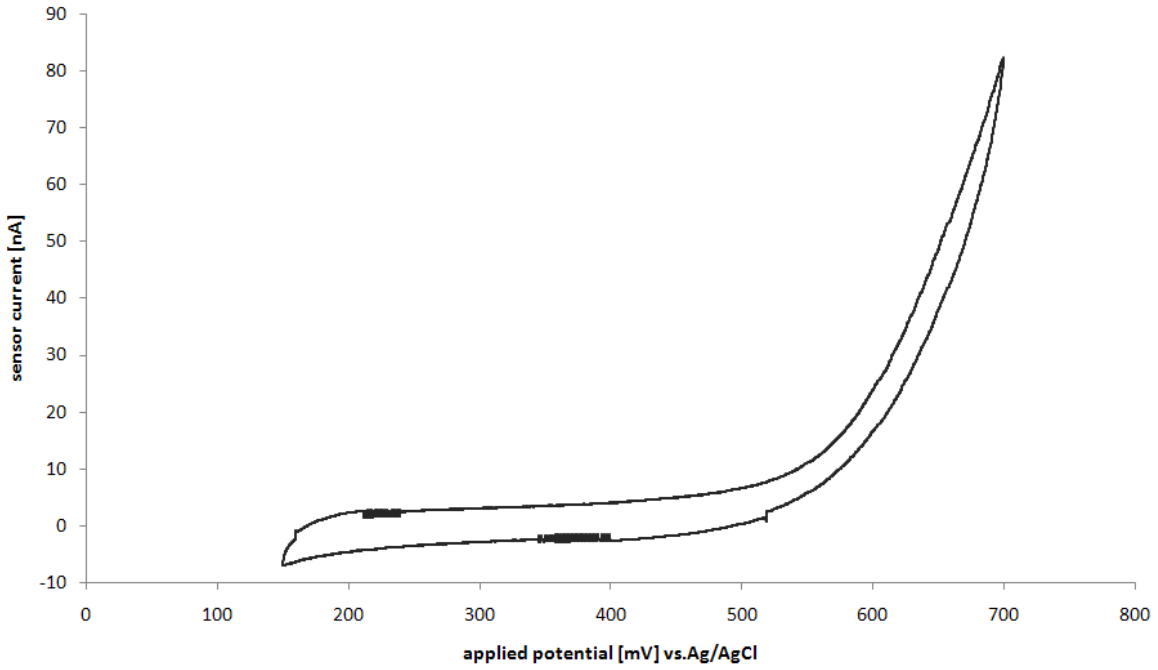

Figure 4.25: Cyclic voltammogramm of the glucose sensor in HEPES buffered saline solution

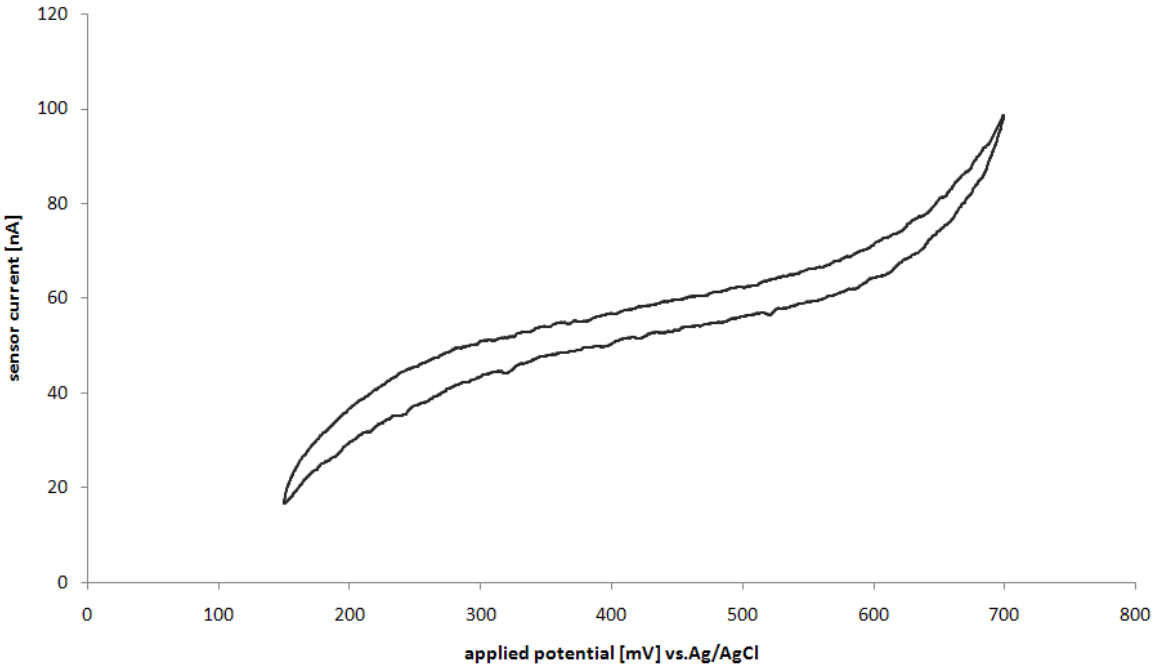

Figure 4.26: Cyclic voltammogramm of the glucose sensor in HEPES buffered saline solution containing 5 mM glucose

4.5 Interference testing

Body fluids are complex matrices with a vast number of different species dissolved or disperged, e.g. endogene substances like ions, proteins, hormones, metabolites, etc., and also exogene substances like medications. Some of them could be electrochemical active and might change the sensor current by different processes:

- The interfering substance is reduced at the surface of the electrode and adds an interferent current to the sensor signal.
- The interferent is oxidised by the hydrogen peroxide, which is generated in the enzyme reaction. By oxidation of the interferent, hydrogen peroxide is lost and the sensor signal is decreased.
- Structural homologes of glucose might also compete with the analyte for the binding sites of the enzymes. But glucose oxidase is extremely specific, thus other sugars like maltose are not oxidised by the enzyme.

To evaluate the specivity of the sensor, the sensor was tested with physiological relevant concentrations of selected electrochemical interferents following a standardized measuring programme. Three different solutions were used to perform the tests:

1. HEPES puffered physiological saline
2. HEPES puffered physiological saline with a glucose concentration of 10 mM
3. HEPES puffered physiological saline with a glucose concentration of 20 mM

Physiological concentrations of the potential interferents were added to the glucose solutions, and measured after the corresponding interferent-free solution. Each test solution was measured for a time period of two hours (see figure 4.27), which resulted in 120 data points per measured solution. The change in sensor current caused by the

selected interferent was calculated from the median values of the 2 hours measurement of the corresponding solutions with and without interferent.

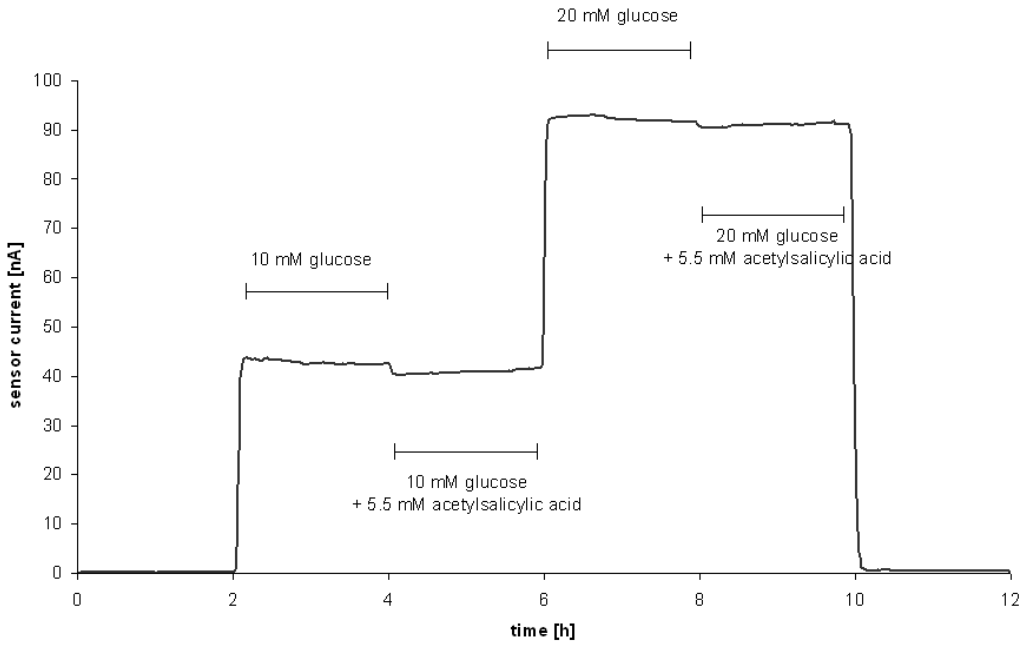

Figure 4.27: interference testing: Acetylsalicylic acid measured at two different glucose concentrations

Results

All substances tested resulted in sensor current changes less than 10 % (see table 4.5) and may well be considered insignificant in the euglycemic and hyperglycemic range. Uric acid and gentisic acid consistently cause the largest signal deviations pointing to electrochemical interferences that may become significant in the hypoglycemic range.

4.6 Testing excess quantity of enzyme

Shelf life and in-use stability is assumed to depend on the amount of enzyme activity on the working electrode. If there is too little activity left on the sensor, the binding

Interferent	test conc.	current change at 10 mM glucose	current change at 20 mM glucose
Acetylsalicylic acid	5.5 mM	–4 %	–2 %
Acetylcysteine	920 mM	3 %	1 %
Ethanol	76 mM	–1 %	0 %
K-oxalate	54 mM	5 %	4 %
Cefoxitin	2.3 mM	2 %	2 %
Uric acid	0.42 mM	–7 %	7 %
Dopamine	6.0 μM	2 %	2 %
Gentisic acid	0.12 mM	6 %	4 %

Table 4.15: Changes of current readouts for different potential interferents

sites of the enzyme will be completely occupied by the substrate molecules at higher glucose concentrations. This will subsequently lead to a decline of the sensor linearity. As there are many factors that can contribute to the deactivation of the enzyme after sensor fabrication, e.g. sterilisation, the storage period, elevated temperatures and humidity, a generous excess of enzyme activity on the sensing electrode is advantageous. To prove whether the enzyme reserve was sufficient, the GOx dispensing solution (100 mg lyophilisate in 1 mL Tween20 solution) was diluted 1:10, 1:33 and 1:100 respectively.

Results

The results of the series of measurements are listed in table 4.6. Surprisingly, the effect on sensor linearity was not consistent with the theory. A decline of linearity corresponding to the decrease of applied enzyme activity could not be observed. The sensor drift seemed also not affected by lower amounts of enzyme. The only evident effect is the decrease of the sensor slope.

sensor design	slope [nA/mM]	lin [%]	drift [%/d]
original GOx solution	6.4	67	-0.4
GOx solution dil. 1:10	2.7	62	-2.7
GOx solution dil. 1:33	1.2	64	+1.1
GOx solution dil. 1:100	0.6	75	-2.1

Table 4.16: influence of the membrane solvent on the sensor characteristics

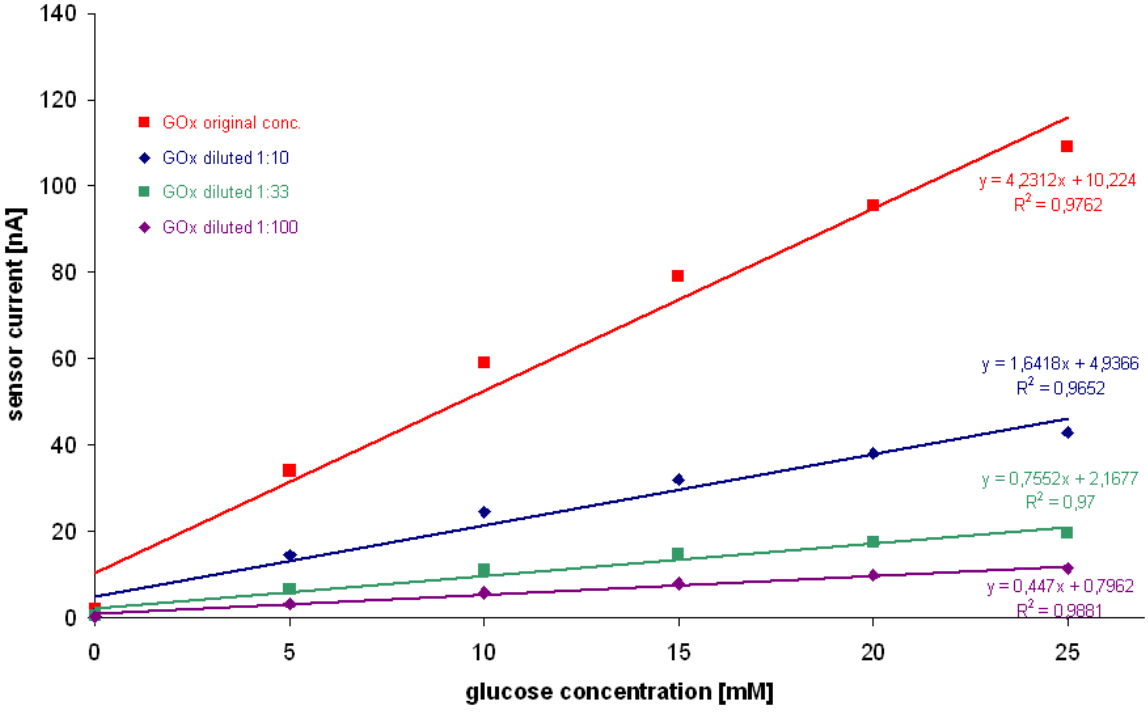

Figure 4.28: sensor characteristics of sensors with different enzyme activities

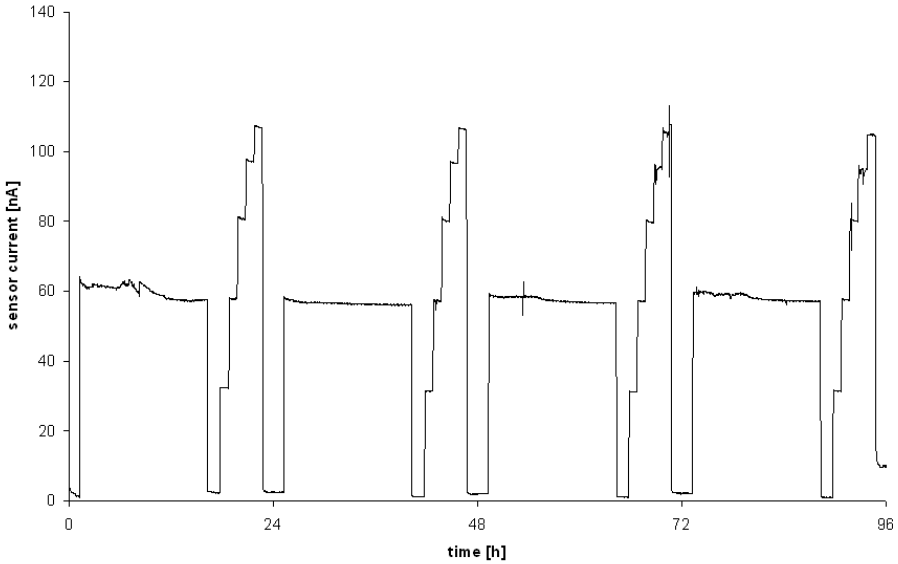

Figure 4.29: sensor result with original GOx concentration

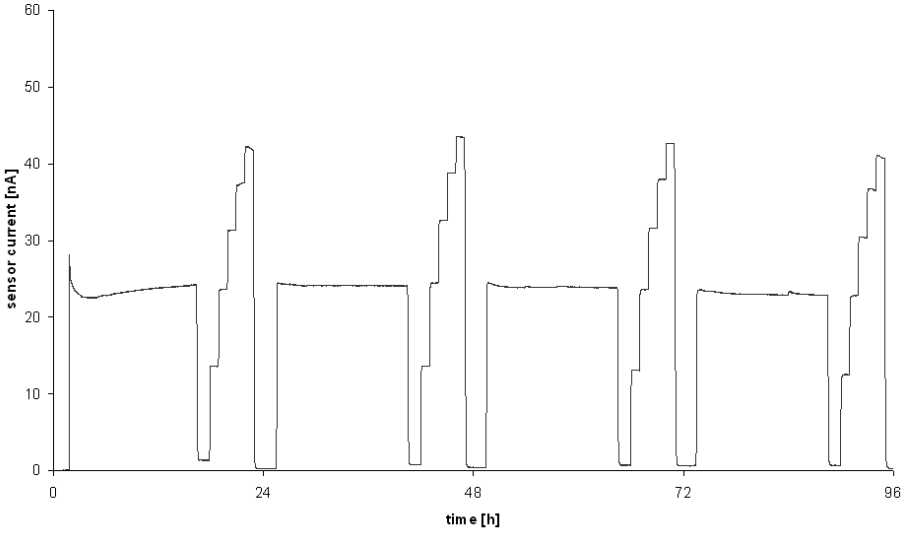

Figure 4.30: sensor result with GOx solution diluted 1:10

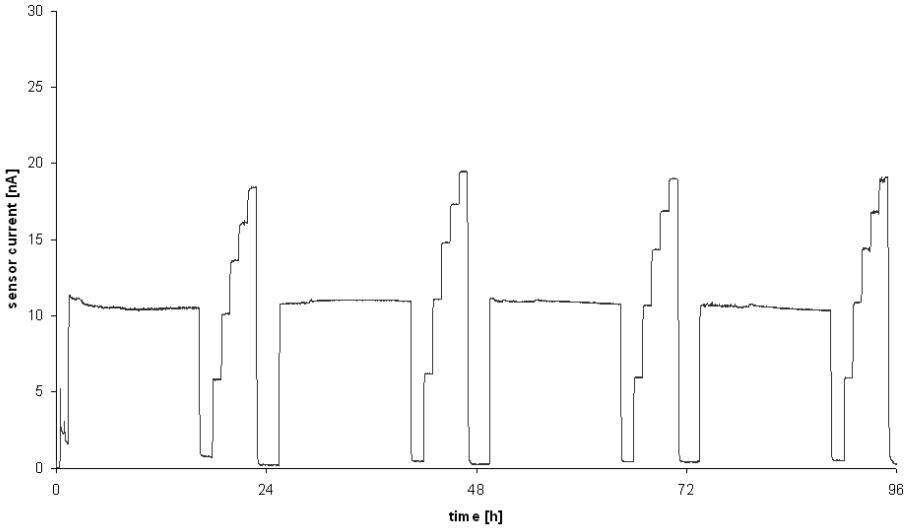

Figure 4.31: sensor result with GOx solution diluted 1:33

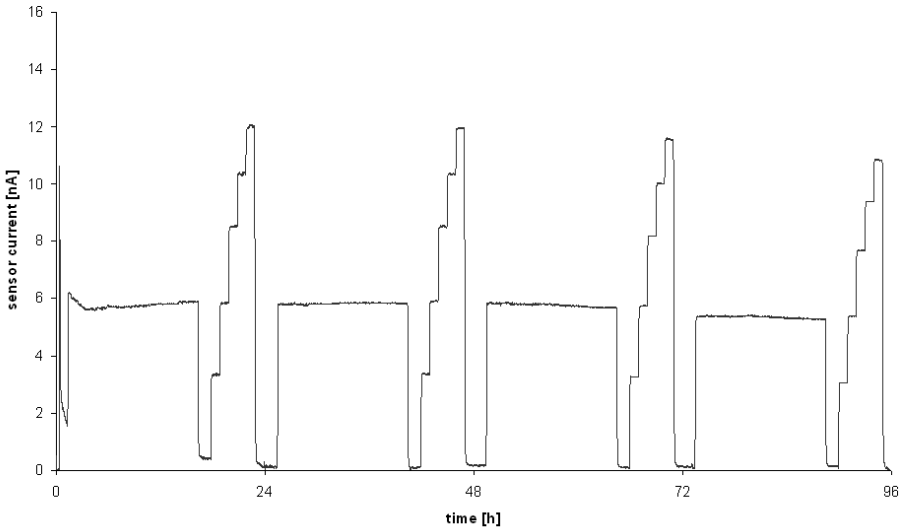

Figure 4.32: sensor result with GOx solution diluted 1:100

4.7 Oxygen dependence

The basic priniciple of amperometric glucose sensors is that the sensor current depends solely on diffusion of the analyte to the sensing electrode which in turn depends on the analyte concentration of the sample. As oxygen is consumed in the enzyme reaction by oxidising glucose to gluconolactone, the sensor current will become sensitive to oxygen levels if the available amount of oxygen decreases below the concentration necessary for the enzyme reaction. In this case, oxygen will become the limiting factor in the electrode kinetics and the sensor signals will decline and vary with the variation of the oxygen levels. As the developed glucose sensor is used in a measuring device utilising the microdialysis sampling technique, it is very unlikely that the sampled dialysate is not oxygenated sufficiently due to the fact that it is allowed to equilibrate with air surrounding the tubings connecting the catheter and the sensor. Due to the low flow-rate, it takes the dialysate approximately 30 minutes to reach the sensor.

Nevertheless, the extent to which the sensor depends on the oxygenation of the measured fluids was tested. As the porous structure of the manganese dioxide transducer allows for an oxygen recycling process within the electrode, the sensor should be minimally oxygen-dependent.

Procedure

8 sensors, including the pump and a 50 mL vial with HEPES puffered measuring solution containing 10 mM glucose, were placed in a vacuum oven. A gas mixing system was used to flush the oven with mixtures of oxygen and nitrogen containing 20.9 %, 10.5 % and 1.5 % oxygen respectively. The oxygen content was additionally checked by an oxygen sensor. Each level of oxygen was measured over a time period of 24 hours to allow for complete equilibration of the measuring system. In the end,

the air-level containing 20.9 % oxygen was repeated to cross-check for any drift of the sensors.

Results

The results were calculated as the mean values of each 24 hour measurement. As depicted in figure 4.33, only a minimal decrease of the sensor current can be seen in the 1.5 % oxygen level.

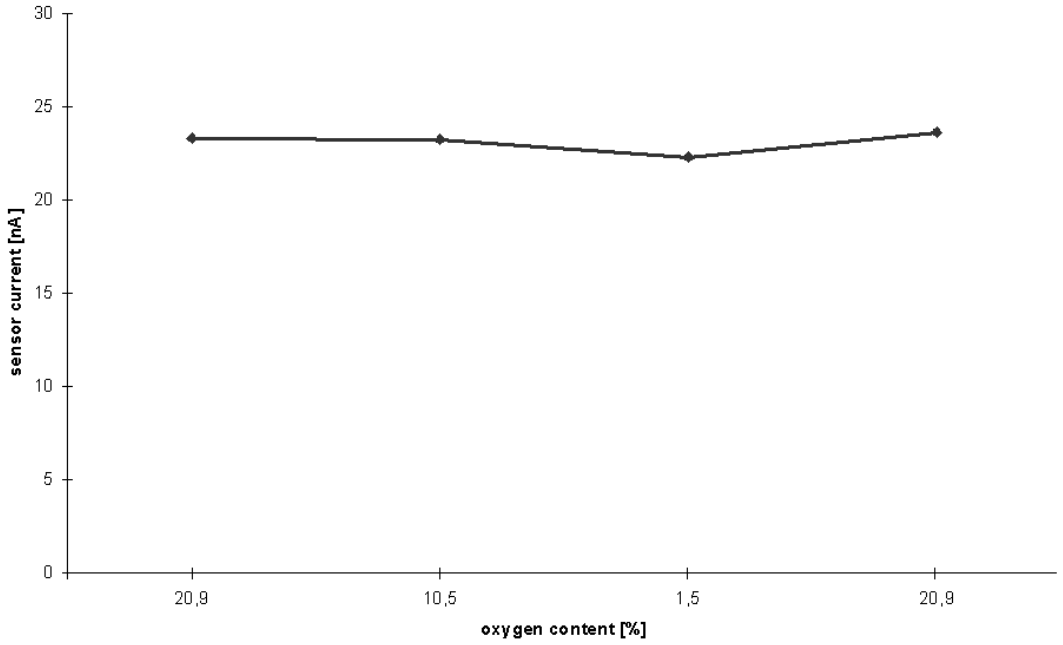

Figure 4.33: sensor signals at different oxygen levels

4.8 Sterilisation

Given that the sensor was used in a clinical research tool to perform clinical studies, there was the need to sterilise the sensor. The sterilisation process must not alter the performance of the sensor, thus a batch of 40 sensors was devided into two groups: One group had to undergo the electron beam sterilisation process with an electron

energy of 4.5 MeV and a dosis of 25 kGy, and the second group of sensors remained unsterilised as control group. 9 sensors of each group were measured with no significant difference between the two groups (see table 4.8). Furthermore, the influence of the sterilisation on the shelf-life of the sensors was investigated. No decay of the sensor slope could be observed in both sensor groups over a storage period of 18 weeks (see figure 4.34).

	slope [nA/mM]	lin [%]	drift [%/d]
control group	2.6	77	+4.1
sterilised group	2.7	76	+3.6

Table 4.17: sensor characteristics of unsterilised – and sterilised sensors

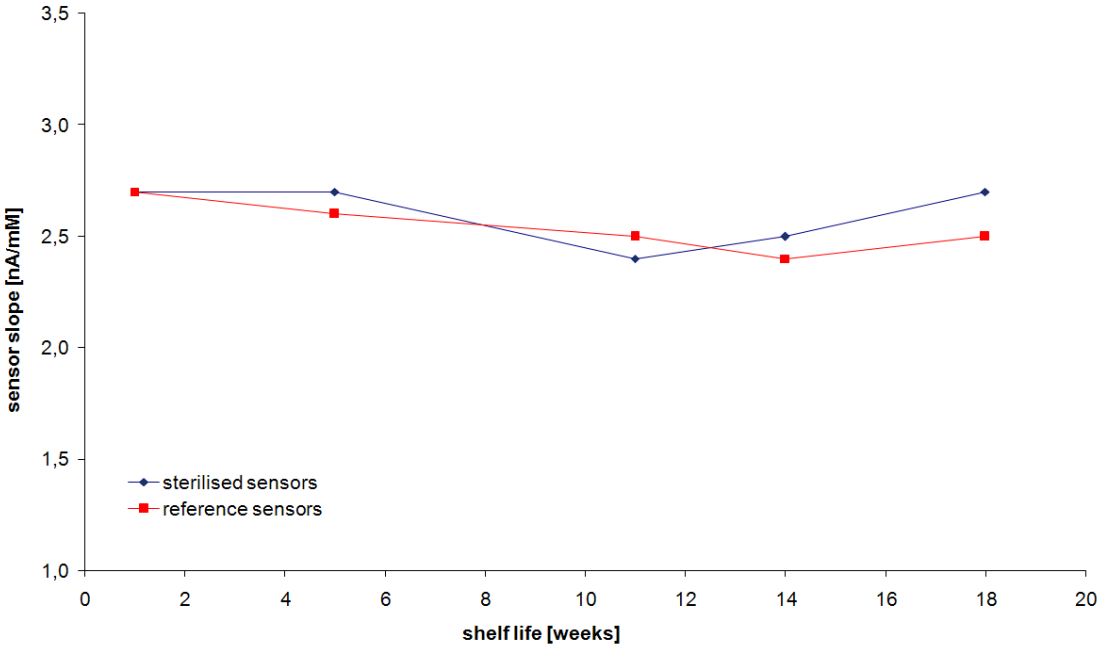

Figure 4.34: change of sensor slopes during storage of sterilised and reference sensors

5 Clinical trial

The in-vivo tests were conducted at the Institute for Diabetes Technology at the University of Ulm, Germany. Five female type 1 diabetes patients participated in this study [mean hemoglobin A1c of 7.5% (5.9 – 8.9 range), mean age of 52 years (37 – 63 range) diabetes for mean 22 years (5 – 34 range)]. Reference blood glucose was measured at least 14 times a day with an Accu-Check Compact blood glucose meter (Roche Diagnostics, Germany), while at least 10 duplicate blood glucose values were used for validation of the system performance. In each subject, two CRT systems (investigational devices called Clinical Research Tool) were placed in the abdominal subcutaneous tissue. The CRT experiments contained 86400 data points per 24 hours (one per second) over a time span of 120 h.

The system consists of an instrument (I), a disposable (II), a flow rate sensor (III), and a control PC (IV), which are connected prior to use by means of connectors (9), mounting clamps (10), and an interface cable (11) followed by closure of the shell case. The PC (IV) is connected to the instrument (I) during start-up, control of ongoing experiments, and stop of data aquisition, followed by data transfer from a data storage card (3) to the PC (IV). The glucose sensor current, flow rate, and system alarms are displayed by the instrument (I). All system parameters are available by coupling the instrument (I) and the PC (IV). The disposable (II) consists of one pouch cassette (4) and one tubing cassette (5) which are packaged separately. The microperistaltic pump (1) continuously serves to propulse the perfusion liquid via connecting tubes

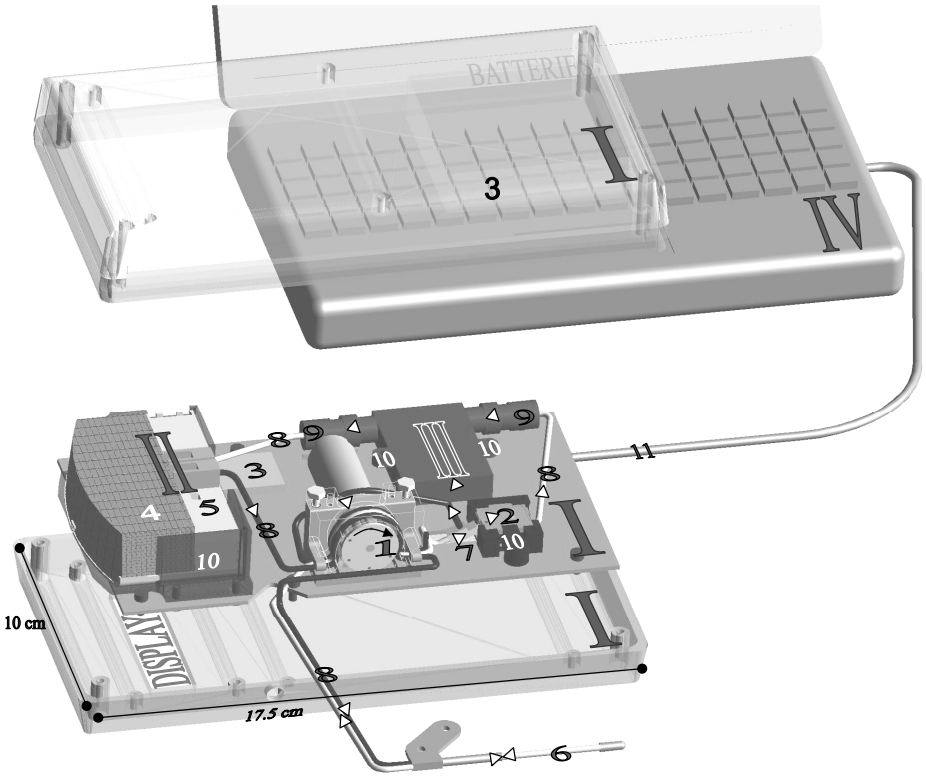

Figure 5.1: Exploded view of the CRT system

(8) thereby withdrawing the perfusion liquid from the pouch cassette (4), directing it into the microdialysis catheter (6), withdrawing the dialysate from the microdialysis catheter (6), pushing the dialysate into the bubble filter (7), degasing the dialysate, and directing it to the glucose flow through sensor (2), the flow rate sensor (III), and finally to the waste reservoir of the pouch cassette (4).

The pouch cassette and the tubing cassette of the disposable were modified cassettes of the SCGM 1 disposable [26]. The pouch cassette contains a reservoir bag with a maximum capacity of 10 mL sterile isotonic saline (147 mM NaCl) and an empty reservoir bag. The sterile tubing cassette contains a microdialysis catheter (CMA 60, CMA Microdialysis, Sweden) with a nominal cutoff of 20 kDa and a water perme-

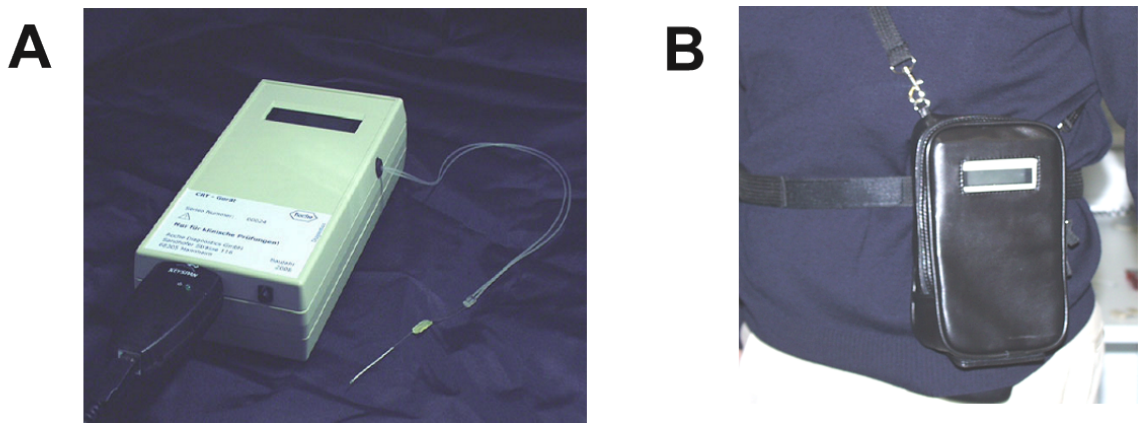

Figure 5.2: A: CRT device, B: CRT during clinical investigation

ability of 5 – 8 x 10^{-4} cm/bar/sec (T = 37°C, p = 100 mbar), a built in house assembly of a bubble filter attached to the inlet of the flow-through glucose sensor, connecting tubings, and connectors to the pouch cassette. The bubble filter features a flow-through hydrophobic hollow fiber surrounded by a chamber with reduced pressure, thus removing air from the dialysate liquid. The CRT flow rate sensor (X119177-AW, Honeywell, USA) coupled to the outlet of the flow-through glucose sensor is used to monitor the volumetric flow rate of the dialysate.

Since the flow rate sensors are reusable, they were disinfected prior each use of a CRT disposable. The pouch cassette, the tubing cassette, the flow rate sensor and the CRT instrument were connected to each other immediately prior to use. The CRT control PC served to control the instrument, to provide online access to all data acquired, and to allow communication with blood glucose meters used to perform capillary blood measurements to acquire reference glucose values.

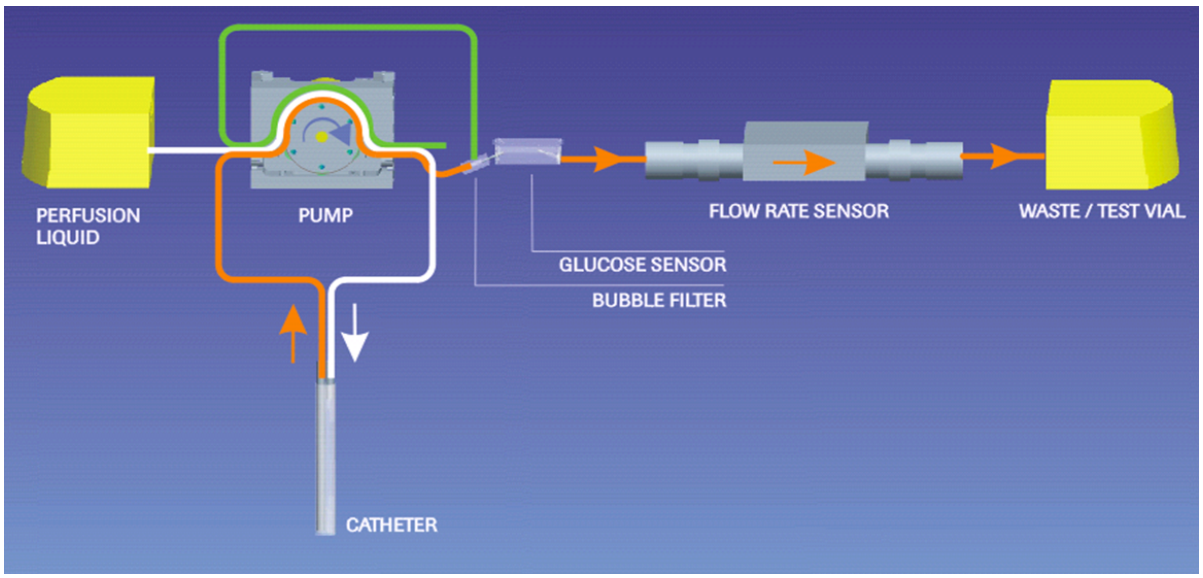

Figure 5.3: scheme of the fluidic paths of the CRT device

5.1 Data analysis

5.1.1 Correction for temperature effects

The measured sensor current $I^{\vartheta}(t')$ at the temperature $\vartheta(t')$ is normalised to the current $I'(t')$ at the reference temperature $\vartheta_0 = 25°C$ by the following equation using a temperature coefficient of 4.5 % per °C.

$$I'(t') = I^{\vartheta}(t') \cdot \left(1 - 0.045 \cdot (\vartheta(t') - \vartheta_0)\right) \tag{5.1}$$

5.1.2 Correction for fluidic lag-time

To calibrate the system, it is necessary to fit the glucose value of interstitial fluid and of capillary blood in time because there is a physical lag-time. The dialysate enters the sensor approximately 35 minutes after it was equilibrating with tissue glucose in the catheter. The glucose concentration information of the sensor is delayed by this lag-time. Therefore, the sensor readouts are shifted on the time axis for Δt minutes to

fit to the reference values.

$$I'(t) = I'(t' + \Delta t \cdot 60) \tag{5.2}$$

Figure 5.4 shows the uncorrected sensor-current $I'(t')$ versus the sensor readout $I'(t)$ corrected for the time-shift.

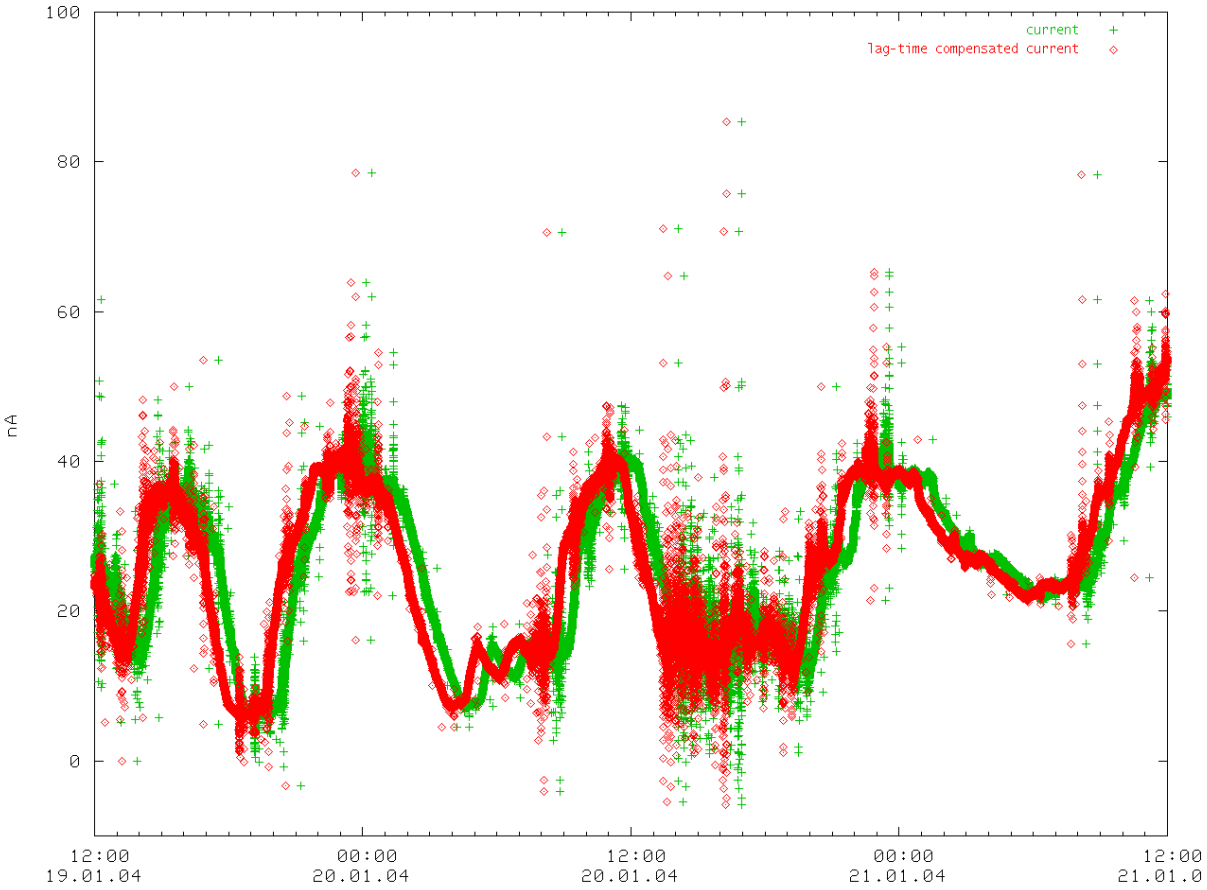

Figure 5.4: correction for the fluidic time-delay of the system response

5.1.3 Correction for sensor drift

To take into account that the sensor´s slope could decrease by P percent per day within the experiment´s duration, the decrease of the slope can be described mathe-

matically by the following equation:

$$S(t) = e^{-\kappa \cdot t} \qquad \text{with} \quad \kappa = -\frac{1}{24 \cdot 60 \cdot 60} \cdot \ln\left(1 - \frac{P}{100}\right) \tag{5.3}$$

The measured sensor current divided by $S(t)$ gives the sensor current which is corrected for the sensor-drift:

$$I(t) = \frac{I'(t)}{S(t)} \tag{5.4}$$

Figure 5.5 illustrates the correction of the slope-drift. The sensor current $I'(t)$ and the drift-compensated current $I(t)$ are shown. In this example, an exaggerated drift value of 10% per day is used for demonstration purposes.

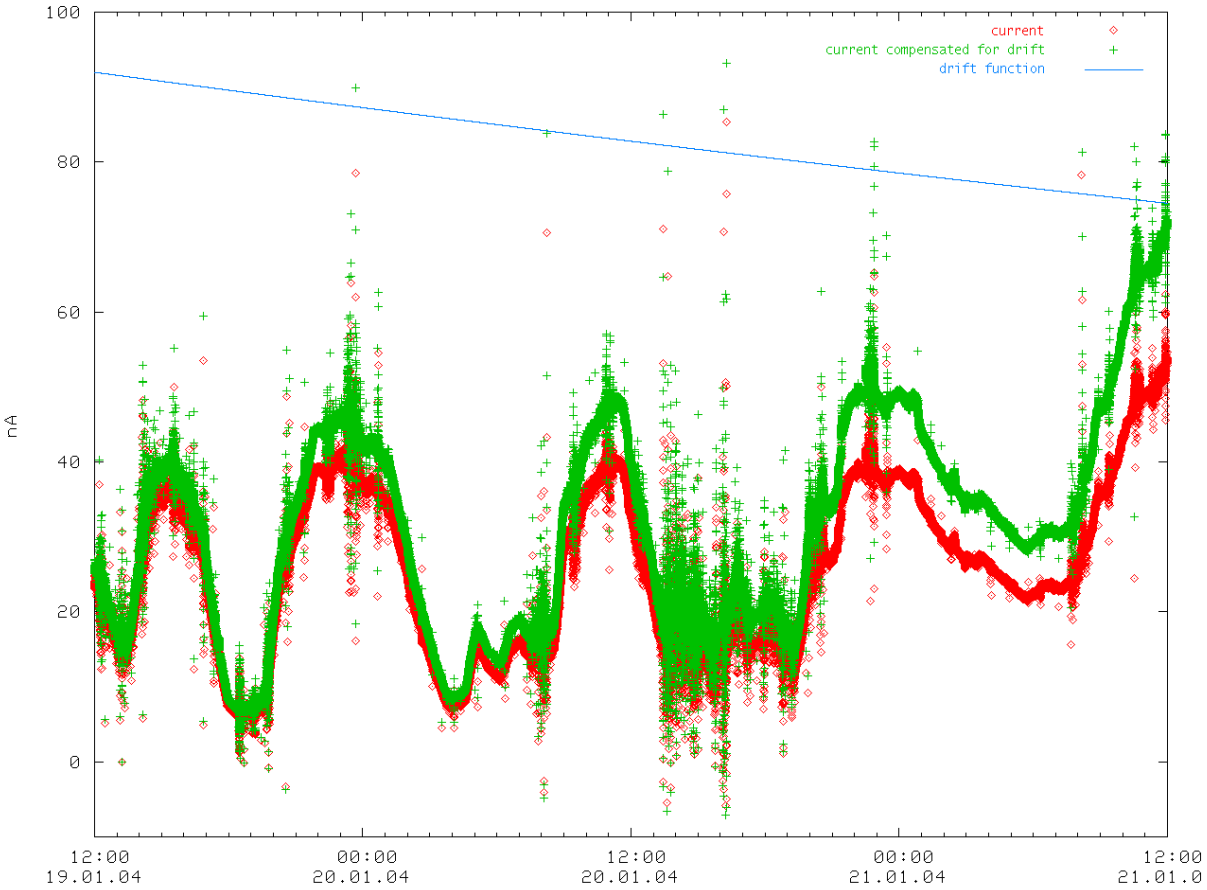

Figure 5.5: correction for the sensor drift

5.1.4 Smoothing noisy signals

A Savitzky-Golay filter is used to smooth noisy current readouts. The method essentially performs a local polynomial regression (of degree k) on a series of values (of at least k+1 points which are treated as being equally spaced in the series) to determine the smoothed value for each point. Methods are also provided for calculating the first through the fifth derivatives. The main advantage of this approach is that it tends to preserve features of the distribution such as relative maxima, minima and width, which are usually 'flattened' by other adjacent averaging techniques (like moving averages, for example).

The primary readouts of the CRT system were smoothed with a time constant of t = 5 min and a second degree regression to reduce noise in a frequency range outside feasible time constants of physiological glucose variations.

5.1.5 Reference values

Reference values are used as the arithmetic average of two distinct measurements. The average of a pair of measurements will only been taken as reference value if the deviation of the measurements to their average does not exceed 2.5%. On average, about 70% of the pairs of measurements fitted this criterium.

5.1.6 Retrospective Calibration

Using the smoothed sensor current $\tilde{I}(t)$ and the reference values taken from capillary blood glucose measurements, the current readouts can be converted to glucose concentration values $C(t)$ by linear regregression. The data of the first 24 hours is not used for calibration because there are many disurbing effects from the run-in of the catheter, the fluidic system and the sensor.

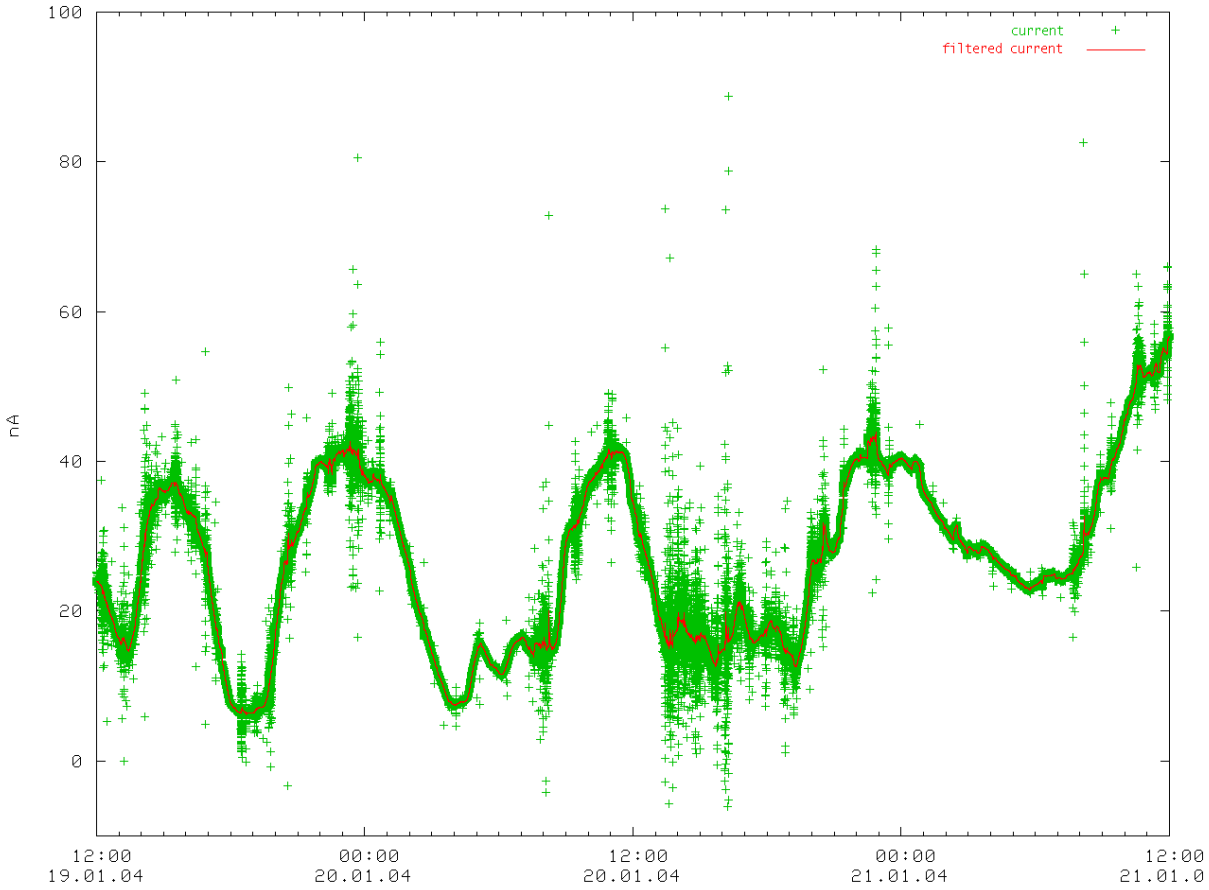

Figure 5.6: smoothing noisy signals with the Savitzky-Golay filter

$$C(t) = B \cdot (\tilde{I}(t) - I_0) \tag{5.5}$$

Equation 5.5 uses the parameters B and I_0. The value of I_0 is set 0, because only an "one-point calibration" is possible, so only one parameter can calculated.

5.1.7 Daily Calibration

Daily Calibration uses a single reference value per day to calibrate the system (the first 24 hours are as well excluded). In this case, a new B–value is calculated every 24 hours, and the I_0–value is also set 0.

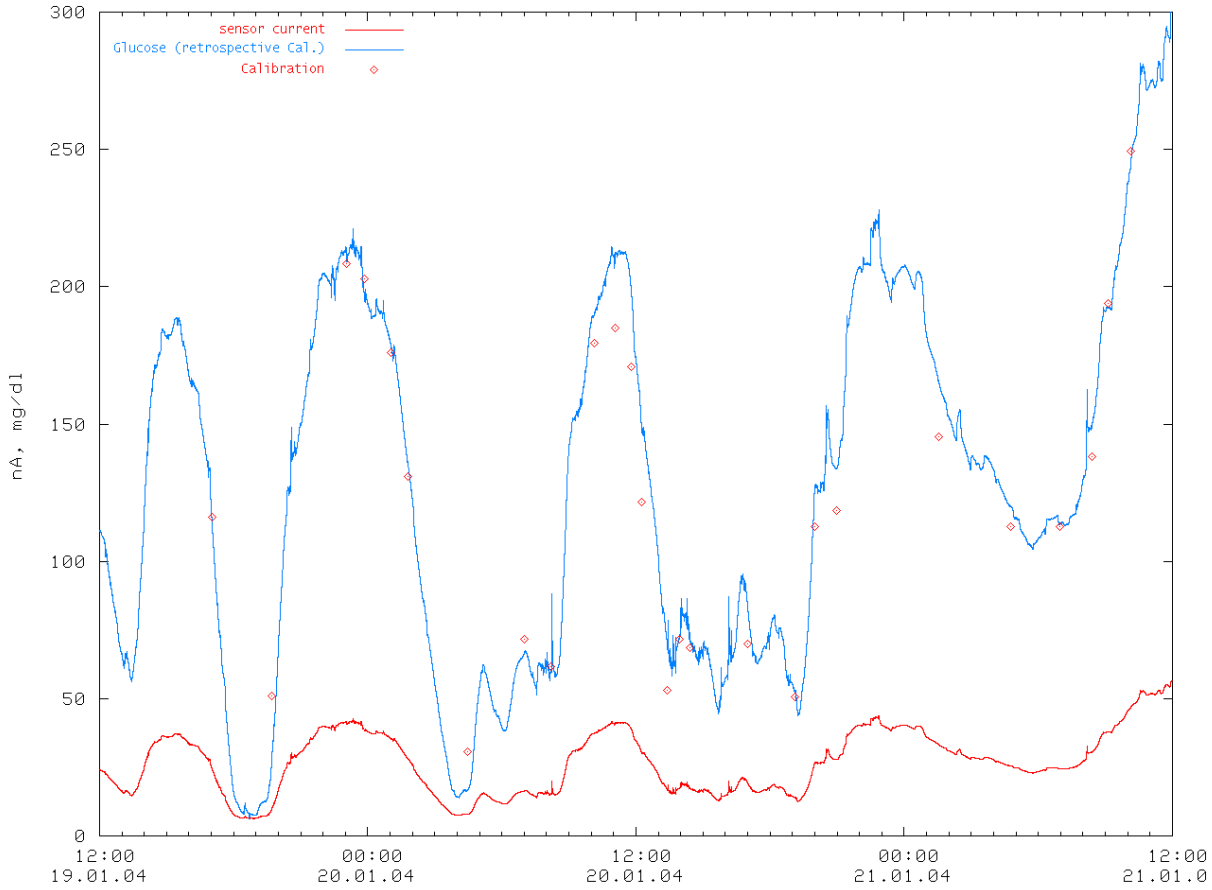

Figure 5.7: retrospective calibration using all reference values

Figure 5.8 illustrates an experiment calculated with the daily calibration procedure. Compared to the retrospective calibration, it is less suitable to evaluate the sensor performance because daily calibration depends much more on the quality of a single value and its location in the glucose profile. If the calibration point falls in a region of noisy sensor signals, the following 24 hours will be affected by the bad correlation between the reference value and the sensor current [45].

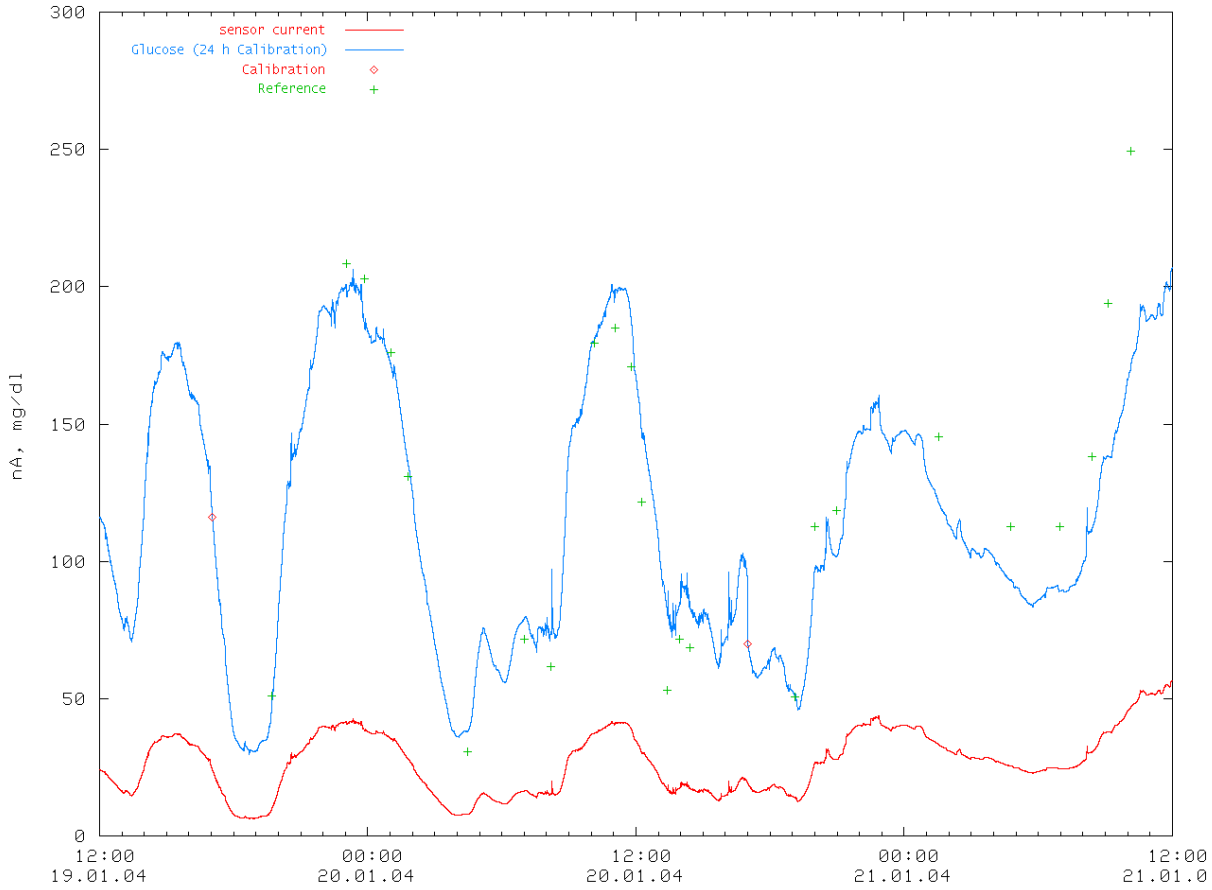

Figure 5.8: daily calibration using one reference value per day

5.2 Results

The performance of the CRT was assessed by calculating the mean absolute relative error (MARE) and the prediction error sum of squares (PRESS), error grid analysis (EGA) plots and plots of calibrated sensor signals over time in comparison with capillary blood glucose readings. Primary sensor signals were processed by eliminating a run-in time of 24 hours to rule out artefacts induced by sensor run-in and wound healing. Subsequently, sensor signals were corrected for temperature variations during the experiment and for the delay between catheter sampling time and detection time at the electrochemical glucose sensor, called the physical lag time.

$$PRESS = \sqrt{\frac{\sum_{n=1}^{N}\left(C_n - C_n^{Ref}\right)^2}{\sum_{n=1}^{N}\left(C_n^{Ref}\right)^2}} \cdot 100 \tag{5.6}$$

$$MARE = \frac{1}{N}\sum_{n=1}^{N}\frac{\left|C_n - C_n^{Ref}\right|}{C_n^{Ref}} \cdot 100 \tag{5.7}$$

Temperature compensation was based on the temperature readouts recorded and the compensation factor of 4.5 %/°C established in vitro prior to the in vivo studies. The correction for physical lag time was conducted in two different ways to investigate the effect of interexperiment mean flow rate variations on the system performance. In calibration scheme I, the average physical lag time was determined in vitro at a mean flow rate of 330 nL/min by measuring the average response time to reach 95% of the final current level after induction of a glucose concentration step of 5 mM. The determined lag time of 33 min was then utilized to correlate blood glucose reference values to the current readouts. In calibration scheme II, the physical lag time was compensated for the deviation of the mean flow rate recorded in each in vivo CRT experiment and the mean flow rate determined in vitro.

Reference values		**PRESS [%] mean (n=10)**	**MARE [%] median (n=10)**	**PRESS [%] mean (n=10)**	**MARE [%] median (n=10)**
all BG values	Cal.scheme I	12.2 ± 5.9	9.6	15.1 ± 6.4	13.6
all BG values	Cal.scheme II	12.3 ± 5.7	11.0	14.6 ± 5.6	13.6
all BG values	Δ I - II	$- 0.1 \pm 8.2$	- 1.4	0.5 ± 8.5	0.0
$\Delta t > 8$ h	Cal.Scheme I	12.4 ± 5.7	10.2	15.5 ± 6.7	14.0
$\Delta t > 8$ h	Cal.Scheme II	12.7 ± 5.5	12.0	15.2 ± 5.5	14.1
$\Delta t > 8$ h	Δ I - II	$- 0.3 \pm 7.9$	- 1.8	0.3 ± 8.6	- 0.1

Table 5.1: MARE and PRESS values for two calibration schemes

Table 5.1 shows the mean MARE and PRESS values for calibration schemes I and

II. The differences of the determined mean and median MARE and PRESS values for differently acquired physical lag times do not seem to indicate that an individual physical lag time correction is necessary for this data set. This may be due to an insignificant deviation of the mean flow rate determined in vitro and in vivo. The mean physical lag time amounts to 31.9 $\pm$ 5.6 min based on individually acquired flow rates in contrast to 33.0 $\pm$ 4.8 min based on in vitro measurements described earlier.

Experiment	**PRESS [%]**	**MARE [%]**
CRT 01	7.70	8.31
CRT 02	10.60	10.67
CRT 03	29.00	26.72
CRT 04	11.10	8.71
CRT 05	17.29	13.24
CRT 06	13.09	9.23
CRT 07	10.97	9.40
CRT 08	14.95	13.71
CRT 09	28.80	18.70
CRT 10	7.43	6.28
mean	15.09	12.50

Table 5.2: Evaluation of the accuracy of the 10 CRT systems used in the study

The agreement of reference values and continuously monitored glucose values as analyzed by a Clarke Error Grid Analysis (EGA) is given in figure 5.10 for a different number of reference values used for calibration. Figure 5.10a depicts the results, taking all blood glucose values into account, as figure 5.10b is calculated using only reference values separated by a time interval of at least 8 hours. The consideration of all reference values does not significantly affect the key features shown to demonstrate system accuracy, indicating that a smaller number of blood glucose measurements may be required in further studies. Consistent with the MARE and PRESS values given in table 5.1, the EGAs in figure 5.10 confirm an excellent measurement quality

of the CRT. 98.0% and 97.6% of all measurements were within the zones A and B respectively. In the range of 70–180 mg/dL, 99.7% and 99.8% of all measurements were in zones A and B.

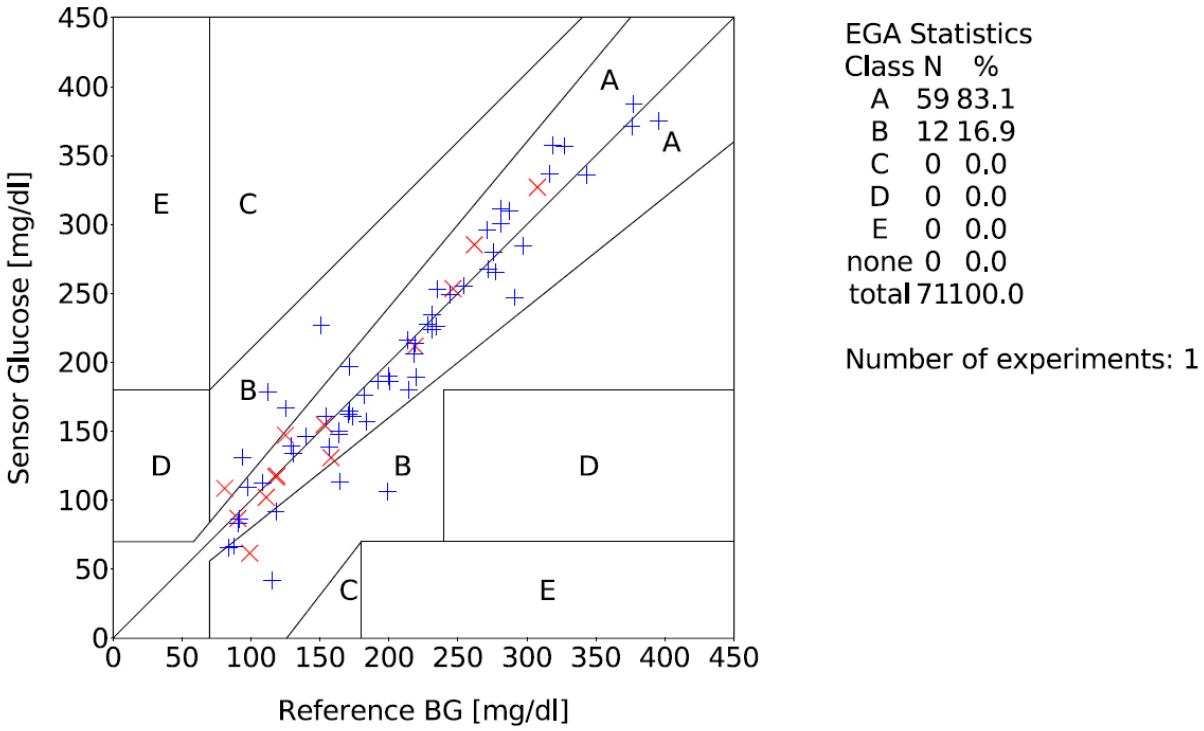

Figure 5.9: Exemplary error grid analysis of one monitoring experiment (retrospective calibration)

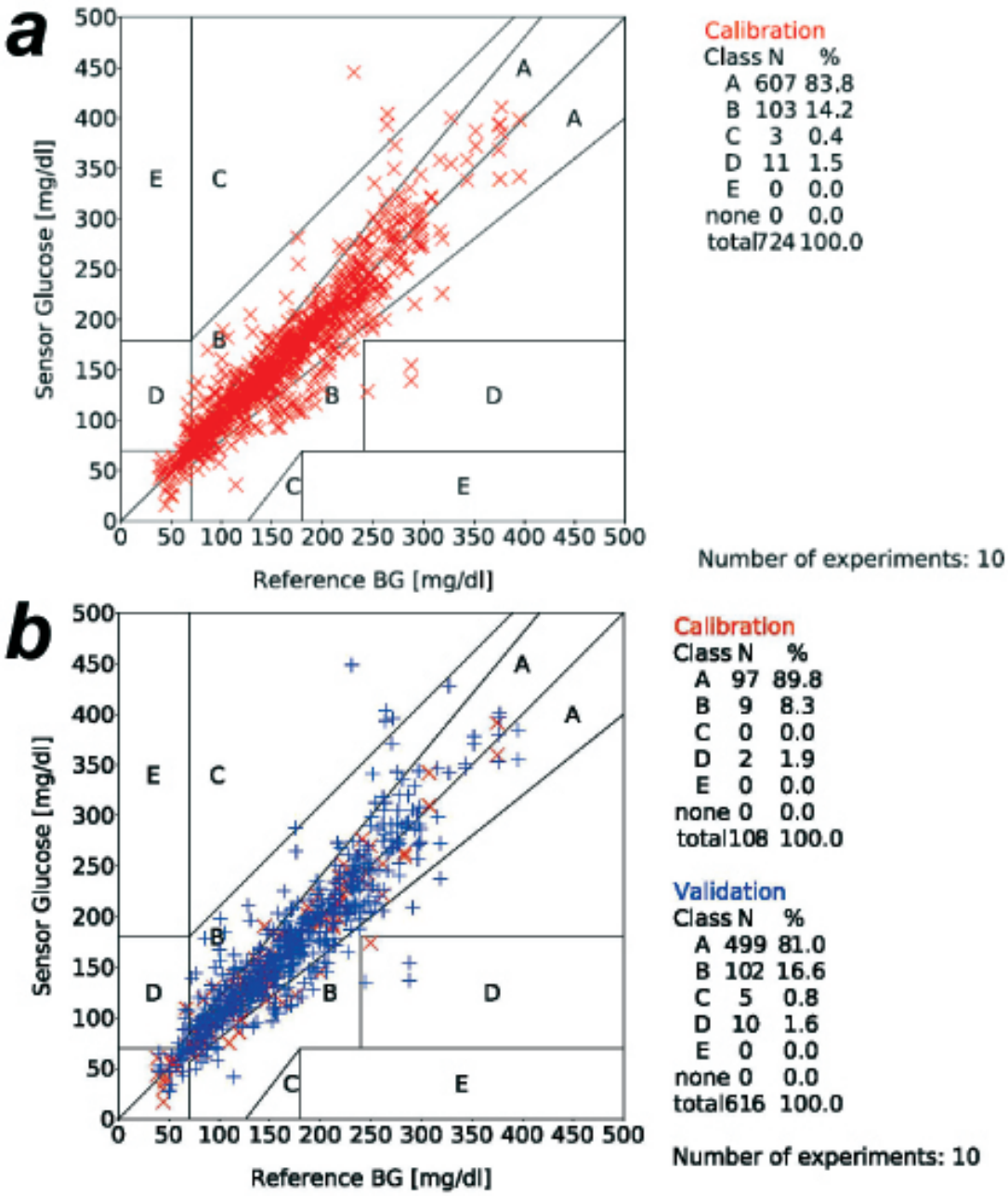

Figure 5.10: Error grid analysis of all experiments, a: calibration is calculated from all reference values, b: calibration is calculated from reference values taken every 12 hours

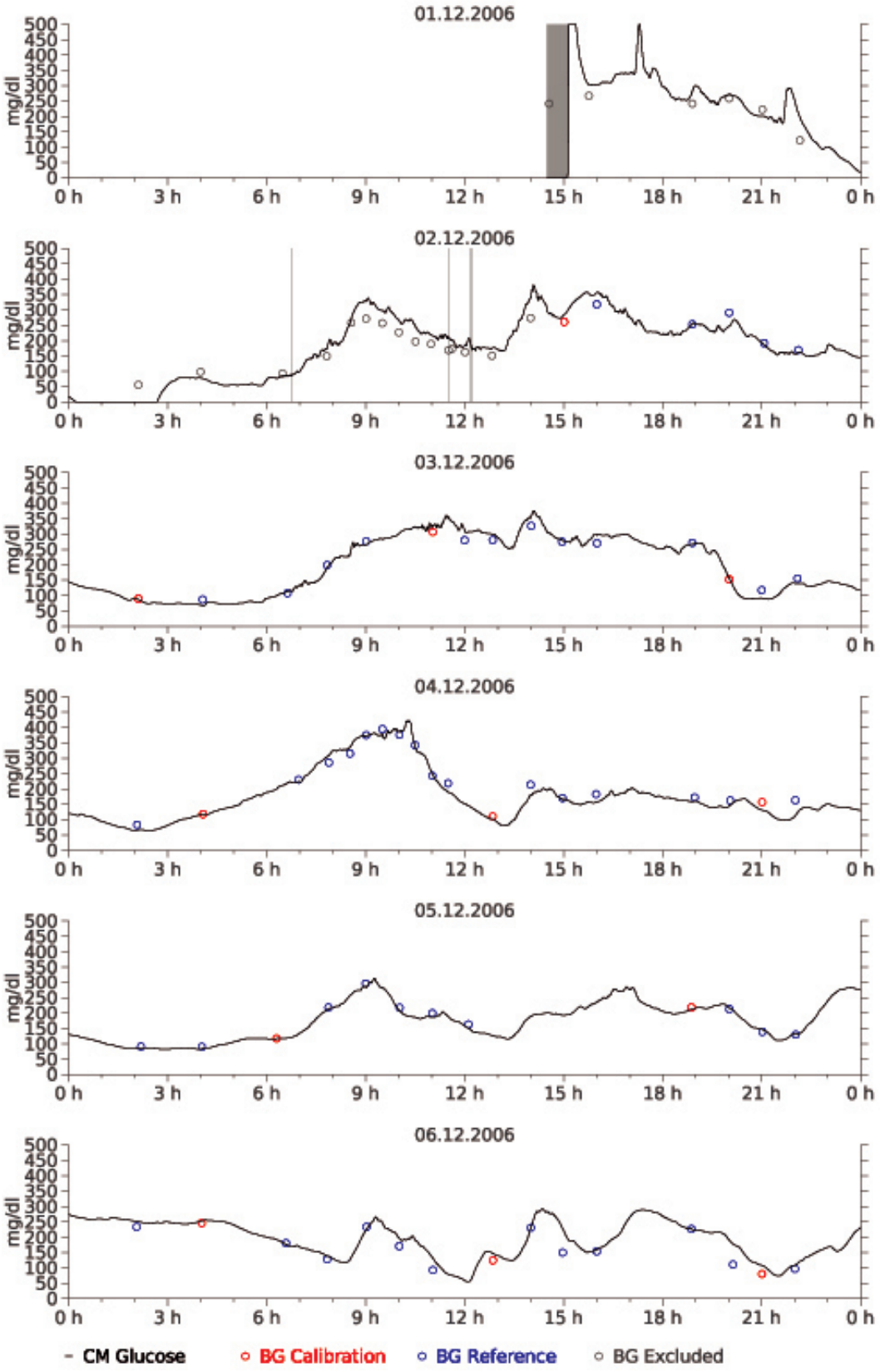

Figure 5.11: Exemplary data set of one CRT system

6 Conclusions

The results of the clinical study demonstrate an excellent performance of the glucose sensor during an ex-vivo monitoring period of at least 120 hours. Due to its unique architecture the glucose sensor performs well without electrode fouling, loss of enzyme activity and with very little slope drift over time. The sensor comprises a porous transducer made of a screen printed mixture of manganese dioxide and carbon ink which allows the oxidation of hydrogen peroxide at a low polarisation potential of 350 mV against Ag/AgCl, thus reducing the influence of electrochemically active interferents. The highly specific enzyme glucose oxidase is incorporated in the porous matrix of the transducer which prevents washing off the enzyme and results in a high hydrogen peroxide efficiency due to very short diffusion paths within the electrode. The close vicinity of enzyme and transducer promotes the oxygen recycling process which makes the sensor less dependend to the oxygen levels of the measured fluid. The cover membrane made of a polyurethane polymer applied from a 5% solution in THF proved biocompatibility and served well to prevent protein adhesion to the electrode. The water uptake of about 40 % makes it well permeable to the analyte resulting in an excellent signal/noise ratio and prevents the enzyme from leaking.

The glucose sensor is produced by three screen printing steps followed by dispensing the enzyme and the cover membrane. Both techniques are fully automated which allows for very low mass production costs. The housing of the measuring cell consists of two injection molded parts, one serving as the substrate for the application of the

electrode system and one comprising the measuring channel and fluidic connections. Both parts are snapped together in a one step process using a sealing gasket to guarantee leak free operation of the sensor. Finally, a cheap and mass producable sensor was developed for use in a monitoring device which allows for continuous glucose measurement over a time period of at least 5 days.

published paper

Ocvirk G., Hajnsek M.,Gillen R. et al.

The Clinical Research Tool: A high performance microdialysis-based system for reliably measuring interstitial fluid glucose concentration

Journal of Diabetes Science and Technology, 3(3):468-477, 2009

Bibliography

[1] Rigby G.P. Ahmed S., Vadgama P.M. Comparative assessment of chemical and γ-irradiation procedures for implantable glucose enzyme electrodes. *Biosensors and Bioelectronics*, 15:159–165, 2000.

[2] American Diabetes Association. Economic costs of diabetes in the u.s. in 2002. *Diabetes Care*, 26:917–932, 2003.

[3] American Diabetes Association. Economic costs of diabetes in the u.s. in 2007. *Diabetes Care*, 31:596–615, 2008.

[4] Schaffar B. United States Patent Application 2003/0027239: Creatinine biosensor, note = Roche Diagnostics, Graz, AT, February 2003.

[5] Shin J.H. Cha G.S., Nam H. United States Patent US6509148: Method for fabricating biosensors using hydrophilic polyurethane, January 2003. i-Sens Inc., Seoul, KR.

[6] Malhotra B.D. Chaubey A. Mediated biosensors. *Biosensors and Bioelectronics*, 17:441–456, 2002.

[7] Lyons C. Clark L.C. Electrode systems for continuous monitoring in cardiovascular surgery. *Ann NY Acad Sci*, 102:29–35, 1962.

[8] CLSI. POCT05-A, Performance metrics for continuous interstitial glucose monitoring; approved guideline. Technical report, Clinical and Laboratory Standards Institute, Dezember 2008.

[9] The Diabetes Control and Complications Trial Research Group. The effect of intensive treatment of diabetes on the development and progression of long-term complications in insulin-dependent diabetes mellitus. *New England Journal of Medicine*, 329:977–986, 1993.

[10] The Diabetes Control, Complications Trial/Epidemiology of Diabetes Interventions, and Complications (DCCT/EDIC) Study Research Group. Intensive diabetes treatment and cardiovascular disease in patients with type 1 diabetes. *New England Journal of Medicine*, 353:2643–2653, 2005.

[11] J.G. Voet D. Voet. *Biochemie*. VCH, Weinheim, 1994.

[12] Klonoff D.C. The importance of continuous glucose monitoring in diabetes. *Diabetes Technology & Therapeutics*, 2,Suppl.1:1–3, 2000.

[13] Klonoff D.C. Microdialysis of interstitial fluid for continuous glucose measurement. *Diabetes Technology & Therapeutics*, 5:539–543, 2003.

[14] Klonoff D.C. Continuous Glucose Monitoring – Roadmap for 21st century diabetes therapy. *Diabetes Care*, 28:12311239, 2005.

[15] The diabetes research in children network (DIRECNET) study group. Relative accuracy of the bd logic and freestyle blood glucose meters. *Diabetes Technology and Therapeutics*, 9:165–168, 2007.

[16] Brismar K. Ungerstedt U. Ekberg N.R., Wisniewski N. Measurement of glucose and metabolites in subcutaneous adipose tissue during hyperglycemia with microdialysis at various perfusion flow rates. *Clinica Chimica Acta*, 359:53–64, 2005.

[17] Jachimowicz A. Ernst H., Urban G. Flow monitoring in microdialysis for continuous sampling. *Proceedings of IMECE 2000: ASME MicroFluidics Symposium Nov. 5th-10th*, 2000, Orlando.

[18] Bellazzi R. et al. Design, methods and evaluation directions of a multi-access service for the management of diabetes mellitus patients. *Diabetes Technology & Therapeutics*, 5:621–629, 2003.

[19] Bungay P.M. et al. Microdialysis of dopamine interpreted with quantitative model incorporating probe implantation trauma. *Journal of Neurochemistry*, 86:932–946, 2003.

[20] Chaurasia C.S. et al. Aaps-fda workshop white paper: Microdialysis principles, application, and regulatory perspectives. *Pharmaceutical Research*, 24:1014–1025, 2007.

[21] Ho S.P. et al. Frictional properties of poly(mpc-co-bma) phospholipid polymer for catheter applications. *Biomaterials*, 24:5121–5129, 2003.

[22] Kapitza C. et al. Continuous Glucose Monitoring: Reliable Measurements for up to 4 Days with the SCGM1 System. *Diabetes Technology & Therapeutics*, 5:609–614, 2003.

[23] Nathan D.M. et al. Intensive diabetes treatment and cardiovascular disease in patients with type 1 diabetes. *New England Journal of Medicine*, 353:2643–2653, 2005.

[24] Reinauer H. et al. Laboratory diagnosis and monitoring of diabetes mellitus. Technical report, 2002.

[25] Ritter C. et al. Multiparameter miniaturised sensor arrays for multiple use. *Sensors and Actuators B*, 76:220–225, 2001.

[26] Schoemaker M. et al. The SCGM1 System: Subcutaneous Continuous Glucose Monitoring Based on Microdialysis Technique. *Diabetes Technology & Therapeutics*, 5:599–608, 2003.

[27] Th. Von Woedtke et al. Sterilization of enzyme glucose sensors: problems and concepts. *Biosensors and Bioelectronics*, 17:373–382, 2002.

[28] Thevenot D.R. et al. Electrochemical biosensors: Recommended definitions and classification. *Pure Appl.Chem.*, 71:2333–2348, 1999.

[29] Wientjes K.J.C. et al. Effects of Microdialysis Catheter Insertion into the Subcutaneous Adipose Tissue Assessed by the SCGM1 System. *Diabetes Technology & Therapeutics*, 5:615–620, 2003.

[30] Wisniewski N. et al. Decreased analyte transport through implanted membranes: Differentiation of biofouling from tissue effects. *Journal of Biomedical Materials Research*, 57:513–521, 2001.

[31] International Diabetes Federation. Diabetes atlas, second edition, 2003.

[32] International Diabetes Federation. Diabetes atlas, third edition, 2007.

[33] Centers for Disease Control and Prevention. National diabetes fact sheet: general information and national estimates on diabetes in the united states, 2003.

[34] Mastrototaro J.J. et al. Gross T.M. Performance evaluation of the minimed continuous glucose monitoring system during patient home use. *Diabetes Technology & Therapeutics*, 2:49–56, 2000.

[35] UK Prospective Diabetes Study (UKPDS) Group. Intensive blood-glucose control with sulphonylureas or insulin compared with conventional treatment and

risk of complications in patients with type 2 diabetes (ukpds 33). *Lancet*, 352:837–853, 1998.

[36] Wring S.A. Hart J.P. Screen-printed voltammetric and amperometric electrochemical sensors for decentralized testing. *Electroanalysis*, 6:617–624, 1994.

[37] Heinemann L. Lodwig V. Heise T., Koschinsky T. Hypoglycemia warning signal and glucose sensors: Requirements and concepts. *Diabetes Technology & Therapeutics*, 5:563–571, 2003.

[38] Mastrototaro J.J. The minimed continuous glucose monitoring system. *Diabetes Technology & Therapeutics*, 2,Suppl.1:13–18, 2000.

[39] Robert J.J. Continuous monitoring of blood glucose. *Hormone Research*, 57,Suppl.1:81–84, 2002.

[40] Skyler J.S. The economic burden of diabetes and the benefits of improved glycemic control: The potential role of a continuous glucose monitoring system. *Diabetes Technology & Therapeutics*, 2,Suppl.1:7–12, 2000.

[41] Chen K.C. Effects of tissue trauma on the characteristics of microdialysis zero-net-flux method sampling neurotransmitters. *Journal of Theoretical Biology*, 238:863–881, 2006.

[42] Vadgama P. Kyröläinen M., Håkanson H. Minimal-fouling enzyme electrode for continuous flow measurement of whole blood lactate. *Biosensors and Bioelectronics*, 12:1073–1081, 1997.

[43] Heinemann L. Continuous glucose monitoring by means of the microdialysis technique: Underlying fundamental aspects. *Diabetes Technology & Therapeutics*, 5:545–561, 2003.

[44] Mcleod K.J. Lesperance L.M., Spektor A. Calibration of the continuous glucose monitoring system for transient glucose monitoring. *Diabetes Technology and Therapeutics*, 9:183–190, 2007.

[45] Heinemann L. Lodwig V. Continuous glucose monitoring with glucose sensors: Calibration and assessment criteria. *Diabetes Technology & Therapeutics*, 5:573–587, 2003.

[46] Hajnsek M. Miniaturisierung eines H_2O_2 Sensors und Überführung in einen Glukose Biosensor. Diploma thesis, TU Graz, 2000.

[47] Marsoner H. Offenbacher H. European Patent EP0603154: Amperometric enzyme electrode, August 1998. AVL List GmbH, Graz, AT.

[48] Gründler P. *Chemische Sensoren, eine Einführung für Naturwissenschaftler und Ingenieure*. Springer, Berlin, 2004.

[49] Heller A. Quinn C.P., Pathak C.P. Photo-crosslinked copolymers of 2-hydroxyethyl methacrylate, poly(ethylene glycol) tetra-acrylate and ethylene dimethacrylate for improving biocompatibility of biosensors. *Biomaterials*, 16:389–396, 1995.

[50] Vadgama P.M. Reddy S.M. Ion exchanger modified pvc membranes - selectivity studies and response amplification of oxalate and lactate enzyme electrodes. *Biosensors and Bioelectronics*, 12:1003–1012, 1997.

[51] Smoller B.R. Roe J.N. Bloodless glucose measurements. *Crit Rev Ther Drug Carrier Syst*, 15:199–241, 1998.

[52] Schoonen A.J.M. Schmidt F.J., Sluiter W. Glucose concentration in subcutaneous extracellular space. *Diabetes Care*, 16:695–700, 1993.

[53] Wientjes K.J.C. Schoonen A.J.M. A model for transport of glucose in adipose tissue to a microdialysis probe. *Diabetes Technology & Therapeutics*, 5:589–598, 2003.

[54] Roche Applied Science. Datasheet: glucose oxidase from aspergillus niger, 2007.

[55] Despopoulos A. Silbernagel S. *Taschenbuch der Physiologie*. Thieme, Stuttgart, 2004.

[56] Cooper S.L. Coury A.J. Takahara A., Okkema A.Z. Effect of surface hydrophilicity on ex vivo blood compatibility of segmented polyurethanes. *Biomaterials*, 12:324–334, 1991.

[57] Pizziconi V.B. Towe B.C. A microflow amperometric glucose biosensor. *Biosensors and Bioelectronics*, 12:893–899, 1997.

[58] Lintott J. Turner M. How to select a sterilisation process. *Medical Device Technology*, 22:33–34, December 2001.

[59] Michael A.C. Yang H., Peters J.L. Effects of mass transfer and uptake kinetics on in vivo microdialysis of dopamine. *Journal of Neurochemistry*, 71:684–692, 1998.